**Forschungszentrum Karlsruhe**
in der Helmholtz-Gemeinschaft

**Wissenschaftliche Berichte**
FZKA 6960

# Magnetically Driven Micro Ball Valve Fabricated by Multilayer Adhesive Film Bonding

**C. Fu, R. Truckenmueller,**
**Z. Rummler, W. K. Schomburg**

**Institut für Mikrostrukturtechnik**

**Januar 2004**

**Forschungszentrum Karlsruhe**

in der Helmholtz-Gemeinschaft

Wissenschaftliche Berichte

FZKA 6960

# Magnetically Driven Micro Ball Valve Fabricated by Multilayer Adhesive Film Bonding

Chien-Chung Fu[(*)], R. Truckenmueller, Z. Rummler, W. K. Schomburg

Institut für Mikrostrukturtechnik

[(*)]Von der Fakultät für Maschinenbau der Universität Karlsruhe (TH)

genehmigte Dissertation

Forschungszentrum Karlsruhe GmbH, Karlsruhe

2004

**Impressum der Print-Ausgabe:**

**Als Manuskript gedruckt**
**Für diesen Bericht behalten wir uns alle Rechte vor**

**Forschungszentrum Karlsruhe GmbH**
**Postfach 3640, 76021 Karlsruhe**

**Mitglied der Hermann von Helmholtz-Gemeinschaft**
**Deutscher Forschungszentren (HGF)**

**ISSN 0947-8620**

# Magnetically Driven Micro Ball Valve Fabricated by Multilayer Adhesive Film Bonding

Zur Erlangung des akademischen Grads eines

**Doktors der Ingenieurwissenschaften**

An der Fakultät für Maschinenbau der

Universität Karlsruhe (TH)

genehmigte

**Dissertation**

von

Chien-Chung Fu

aus Taiwan

Tag der mündlichen Prüfung: 19. Nov. 2003

Hauptreferent: Prof. Dr. V. Saile

Korreferent: Prof. Dr. R. Zengerle

# Abstract

**Title: Magnetically Driven Micro Ball Valve Fabricated by Multilayer Adhesive Film Bonding**

A multilayer adhesive film bonding process was developed and a magnetically driven micro ball valve was designed and fabricated as a demonstrator using this new bonding method.

The new bonding process uses adhesive films as bonding mediums. This bonding method can be applied to bond polymer housings, membrane and other different materials. The Taguchi method was used to find the proper process parameters to get enough bonding strength. The deformation of punched microstructures during each process step was analyzed in a statistical way. The sealing properties were tested with nitrogen and water solution. The compatibility with the AMANDA process was demonstrated by bonding separated membranes on polymer housings.

The micro ball valve consists of three PSU and three FeNiCr layers, which are bonded together in one step with five punched adhesive films. The PSU layers were produced by hot embossing. Micro mechanical milling was employed to fabricate the molds needed. Laser cutting technology was selected to pattern FeNiCr layers demonstrating rapid prototyping. A small series production of approximately 50 micro ball valves was successfully realized in the laboratory.

The valve can operate in two modes. One is an on-off switching mode and the other is a proportional mode. In the on-off switching mode, the valve switches the outlet pressure at two distinguished levels. The maximum switchable differential pressure of this valve is 200 kPa. The switch frequency was up to 30 Hz. In the proportional mode, controlling the ball position can regulate the outlet pressure. The magnetic force of the coil balances the forces of the flow and the weight of the ball. In this mode, the valve can steer the output pressure continuously in a range between 0 to 110 kPa, when the input pressure is 200 kPa. Inclination effects caused by the gravitation force were also investigated. The valve was found to be suitable for use at all inclination angles. The average leakage was measured to be approximately 0.3% of the flow through the open valve.

# Kurzfassung

**Titel: Ein magnetisch gesteuertes Mikrokugelventil hergestellt durch das Verbindungsverfahren mehrschichtiger Klebfolien**

Ein Verbindungsprozess mit mehrschichtigen, klebfähigen Filmen wurde entwickelt, und ein magnetisch gesteuertes Mikrokugelventil wurde entworfen und mit diesem neuen Verbindungsprozess als Demonstrator hergestellt.

Der neue Verbindungsprozess benutzt Klebfolien als Verbindungsmedium. Diese Methode kann für das Verbinden von Gehäuse und Membranen aus Polymeren und verschiedener anderer Materialien verwendet werden. Die Taguchi Methode wurde eingesetzt, um geeignete Prozessparameter für ausreichende Verbindungstärke zu finden. Die Verformung von gestanzten Mikrostrukturen in jedem Prozessschritt wurde statistisch analysiert. Die Versiegelungseigenschaften wurden mit Stickstoff und Wasserlösungen getestet. Die Kompatibilität mit dem AMANDA Prozess wurde durch das Verbinden separater Membranen auf polymere Gehäuse demonstriert.

Das Mikrokugelventil besteht aus drei PSU und drei FeNiCr Folien, welche in einem Schritt mit fünf gestanzten Klebfolien zusammen verbunden wurden. Die PSU Folien wurden durch das Heissprägen hergestellt. Das mikromechanische Fräsen wurde für die Herstellung der Formeinsätze eingesetzt. Das Laserschneideverfahren wurde ausgewählt, um die Strukturierung von FeNiCr Folien als Rapid Prototyping zu demonstrieren. Eine Kleinserienproduktion von ca. 50 Mikrokugelventilen wurde erfolgreich im Labor realisiert.

Das Ventil kann in zwei unterschiedlichen Modi operieren. Der erste Modus ist ein on-off Umschaltmodus, der andere ein proportionaler Modus. Im on-off Modus schaltet das Ventil den Ausgangsdruck auf zwei unterschiedliche Niveaus. Der maximal schaltbare Differenzdruck von diesem Ventil beträgt 200 kPa. Die Schaltfrequenz betrug bis zu 30 Hz. Im proportionalen Modus kann der Ausgangsdruck durch die Kugelposition reguliert werden. Die magnetische Kraft von der Spule gleicht die Fluss- und Gewichtskräfte der Kugel aus. In diesem Modus kann das Ventil den Ausgangsdruck im Bereich von 0 - 100 kPa stufenlos steuern, wenn der Eingangsdruck 200 kPa beträgt. Die durch die Schwerkraft verursachten Neigungseffekte sind ebenfalls untersucht. Die Untersuchung zeigt, dass das Ventil für alle Neigungswinkel geeignet ist. Die durchschnittliche Leckage betrug ca. 0.3% der Strömung durch das offene Ventil.

# Directory

Page

# 0 Preface

Micro system technology has been developed for more than 20 years. New technologies, new processes and fancy ideas for products have been continuously created. From bulk micro machining and surface micro machining to the LIGA process researchers and engineers have tried their best to apply micro system technologies to make the components as small as possible. In many cases, the cost of fabrication is not considered as a crucial issue. There is a common consensus in this field that due to the possibilities of batch processes and mass production, the cost of each component could be so low that it could be neglected as in the field of semiconductors.

However, expensive apparatus and equipments are usually needed to produce micro systems. Therefore, although many industrial partners indeed have much interest to step into this promising and dazzling technology field, in real situations they are in many cases hindered by a high investment threshold. At this moment, in order to broaden the range of micro system products on the market, as a micro system engineer, one of the most important tasks is to find a cost efficient and low threshold way to help more industrial partners stepping into and making profits from the this technology.

Therefore, it was the objective of this work to find a fabrication process that allows to produce micro components at low cost and reasonable investment. Such a process should enable small and medium size companies to earn their money even with small-scale production series.

To achieve this strategic task, two main guidelines were followed throughout the whole work. One is *"Outsourcing"*. It means that the advantages and merits of the parts supply companies are employed by us. Their mass production abilities and their process optimizations to get low cost, mass producible, market standard elements are used to build up our products and minimize the unnecessary expensive production steps. This will lead to the reduction of investment threshold of our industrial partners. In this work, the moving element and the driving part were outsourced, which are usually fabricated either by very difficult processes or by very expensive facilities in the cases of other active micro valves. [Robe94][Goll96] [Kohl00][Rogg01][Kais00].

The second is *"Process Simplification".* In this dissertation, alignment aids were used throughout the entire fabrication. The product can be manufactured and assembled without any difficult optical alignments, which are usually needed in fabrication of other micro systems. In addition, a new bonding method was developed that allows assembling and bonding micro fluidic components in one step including three-dimensional micro flow channels. The new bonding method is not only easier to process, but also facilitates the design of polymer housings. No adhesive chamber systems have to be added and considered during the housing design.

A new, easy, and cost efficient fabrication process for micro components was demonstrated in this dissertation, which is suitable for batch and mass production with advantages of short design time, fast manufacturing and flexibility without expensive facilities which are in many

cases difficult to be afforded by a new and small or medium-sized company. As a demonstrator, a micro ball valve was developed and fabricated by this method with reasonable characteristics.

In order to provide a view on existing technologies important for this work, chapter 1 describes briefly the AMANDA process, reviews and compares different micro valves inside and outside of our institute introducing their basic mechanisms and characteristics. Then the motivations are described, why a new bonding technology needed to be developed and why the micro ball valve with a magnetic drive was chosen as a demonstrator.

Chapter 2 describes how the micro ball valve was constructed. The micro ball valve was designed from an original idea and then through the considerations of minimum actuating forces. To determine the basic dimensions of the valve, the actuating magnetic forces were estimated and computed by finite element simulations under different conditions.

A new process using 3M VHB acrylate adhesive films was developed and described in chapter 3. This alternative bonding method can be applied to bond polymer housings, membrane and other different materials. The chapter describes the properties of the adhesive films and the process steps at first. Then the Taguchi method was used to find the proper process parameters to get enough bonding strength. Punched microstructures deformation through the process was analyzed in statistical way. The sealing properties were tested both with nitrogen and water solution. The compatibility with the AMANDA process was demonstrated by bonding separated membranes on polymer housings.

Following the design and construction considerations described in chapter 2, chapter 4 describes how the micro ball valves were fabricated and realized. The micro ball valve was made from three PSU and three FeNiCr layers. They were bonded together using five punched adhesive films in one step. To fabricate the hot-embossing molds for polymer housings, micro mechanical milling was employed. To obtain different surface roughness requirements, two kinds of fabrication methods, diamond ultra milling and tungsten carbide micro milling, were used. Critical microstructure contours were improved by tool diameter compensations and path modifications. The ball chamber layer was separated into two parts in the mold to reduce the demolding force. With the aids of a multi step demolding method and a high adhesive counter plate with trenched grooves on it, the ball chamber layers with a thickness of 1.6 mm each were successfully demolded. Laser cutting technology was selected to pattern FeNiCr layers demonstrating the rapid prototyping production. Combing with punched adhesive films and the new developed bonding method, a small series production of approximately 50 micro ball valves was successfully realized in our laboratory.

Chapter 5 reports on the characteristics of the valve. The valve can operate in two modes. One is on-off switching mode and the other is a proportional mode. In the on-off switching mode, the valve switches the outlet pressure at two distinguished levels. The maximum switchable differential pressure of this valve is 200 kPa. The switching frequency was up to 30 Hz. In the proportional mode, controlling the ball position can regulate the outlet pressure. The magnetic force of the coil balances the forces of the flow and the weight of the ball. In this mode, the valve can steer the outlet pressure continuously in a range between 0 to 110 kPa with the input pressure of 200 kPa. Inclination effects caused by gravitation influence on

the free moving ball are also investigated in this chapter. The valve was found to be suitable for use at all inclination angles. The average leakage of the closed valve was measured to be approximately 0.3% of the flow through the open valve.

# 1 Existing technologies

To get an overall view of the existing technologies, this chapter describes at first the AMANDA process, which has been developed at Forschungszentrum Karlsruhe for many years with many applications especially in micro fluidic components. Then, different micro valves are reviewed and compared; their basic mechanisms and characteristics are introduced. Then it will be explained why a new bonding technology was developed and why a micro ball valve with a magnetic drive was chosen as an application demonstrator.

## 1.1 The AMANDA process

The AMANDA process has been developed since the beginning of the 1990s. The process is a combination of three individual fabrication steps. Its name AMANDA is a German acronym "**A**bformung, Oberflächen**m**ikro-mech**an**ik un**d** Membr**a**nübertragung", which means molding, surface micro machining and membrane transfer [Scho96]. This process is distinguished by the fact that a large number of low-cost polymer micro components can be fabricated in batches and the process is suitable for mass production. In addition, because of the molding process, micro components can be made from versatile materials and make use of the different special properties of polymer materials. Products like micro pumps [Büst94], micro valves [Fahr95] [Goll96] [Goll97] [Kais00] [Rogg02], micro sensors [Mart98] [Wulf01] [Diit02] and a micro degasser [Rumm00] have been successfully developed by this method in the past years.

### Molding

The molded parts can be produced mainly by two kinds of methods: Injection molding and hot-embossing. The comparison and the advantages and disadvantages of the two molding processes were described in the references [Heck98] [Hane00]. According to the precision requirements of the microstructures, the mold can be fabricated by different processes like LIGA, thick film resist photolithography (SU-8), silicon direct deep RIE, or ultra diamond mechanical milling. The materials used for molding can be adapted to the special needs of the application. Typical thermoplastic materials used are PMMA, POM, PSU, PEEK, PVDF, PA, COC, LCP and PC. More information can be found in the references [Heck00] [Heck99] [Heck98].

### Surface micro machining and diaphragm transfer

In AMANDA, surface micro machining is mainly used to fabricate membranes, which are usually put between housings. The membrane is used as movable elements with actuating circuits or mechanical function layers with sensing elements in the micro components. The membrane is fabricated on an 80 – 100 nm low-adhesion layer made from Au that allows the membrane to be separated from the silicon wafer. The material of the membrane can be made from polymers such as polyimide or metals such as titanium according to the requirements. Thermal actuating coils [Büst94], temperature sensing elements [Ditt02], and strain gauge systems [Wulf01], can be built up on the membrane as functional parts by standard surface micro machining methods.

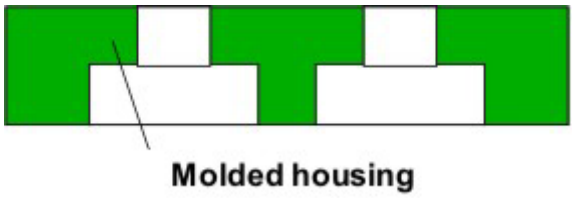


(a)

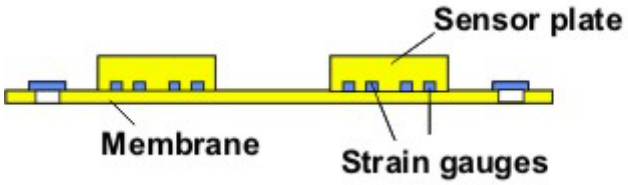


(b)

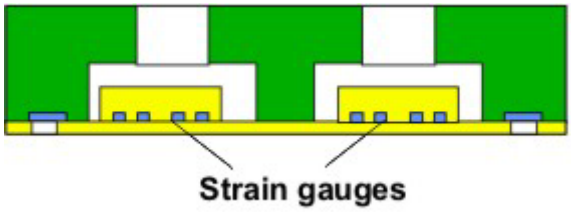


(c)

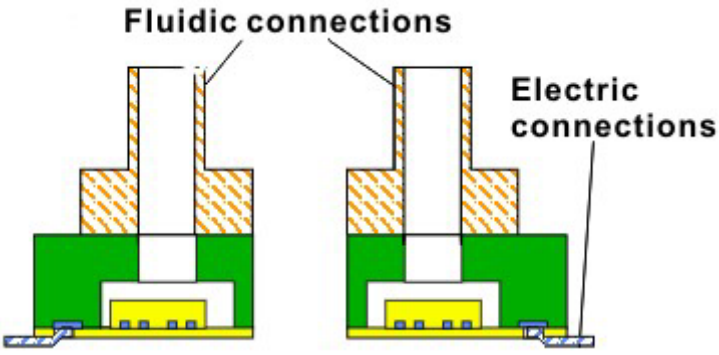


(d)

**Fig. 1.1.1 The AMANDA Process.**

**(a) The molded housing with microstructures produced by hot-embossing process.**
**(b) Membrane with functional elements made by surface micro machining.**
**(c) Combination of a micro structured membrane and a polymer housing.**
**(d) Micro components with fluidic and electric connections after dicing. [Wulf01]**

## 1.2 The chamber adhesive bonding process

To separate the functional membrane from the silicon wafer, a special bonding method has been developed [Maas96][Fu02]. The molded polymer housing is adhesively bonded to the membrane stretched over the silicon wafer (Fig 1.2.1). Adhesive is injected into a chamber system (Fig. 1.2.2), which directs the glue to the desired positions.

The chamber system comprises adhesive chambers and function chambers. The adhesive chambers are injected with the adhesive and the function chambers are used as functional cavities of the micro components (Fig. 1.2.2). The two types of chambers are separated by partitions (Fig. 1.2.1 and Fig. 1.2.2), which prevent the adhesive from entering into the functional cavities.

The gap between the partition and the membrane (Fig. 1.2.1), which is typically a result of surface roughness and small faults in the housing, is permeated by adhesive in the bonding process. In this way, the adhesive can seal the functional cavities, which is in most cases necessary for micro-components, such as micro fluidic devices. An overall yield in devices of up to 80 percent has been achieved with this method in the labs of the Forschungszentrum in small series production of micro valves and flow sensors.

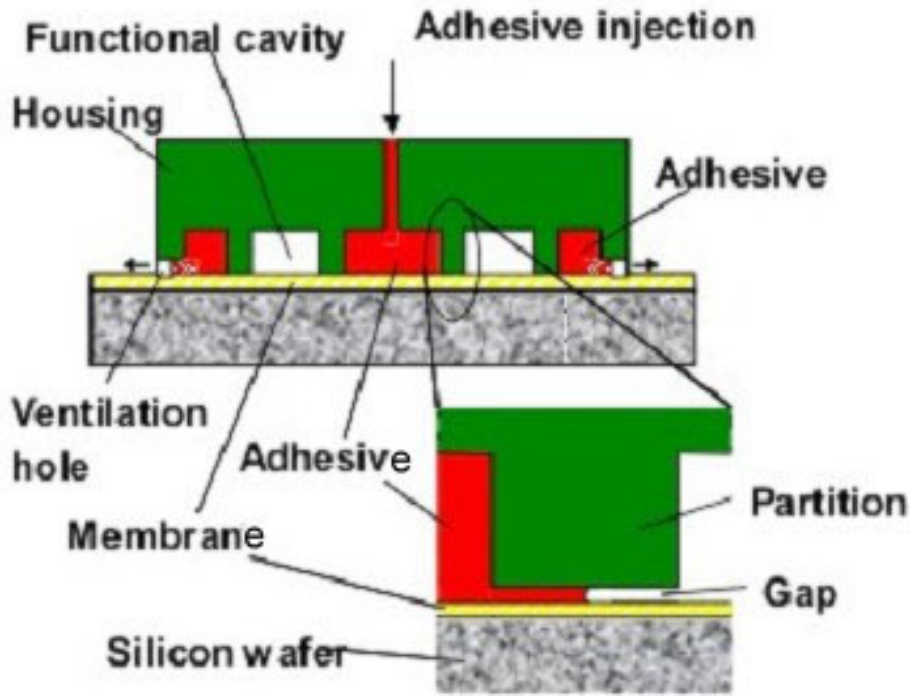


**Fig. 1.2.1: The chamber adhesive bonding process. A polymer housing is adhesively bonded to a membrane stretched over a silicon wafer. Adhesive is injected into a chamber system that directs the glue to the desired positions. [Fu02]**

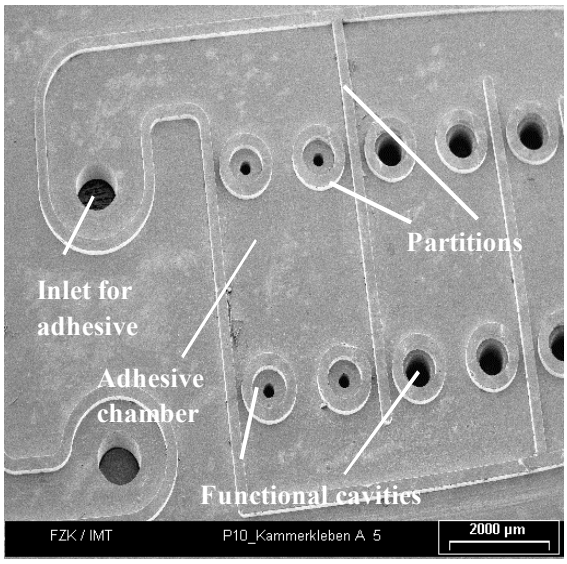


**Fig. 1.2.2: SEM of a polymer housing showing a chamber system for adhesive bonding, including adhesive chambers, functional cavities and adhesive inlets. [Fu02]**

However, the design of the chamber system has to make sure that the functional cavities are not filled with adhesive (Figure 1.2.3). Some attempts have been made to analysis the adhesive flow behavior and to predict the optimized design of the chamber system dimensions [Fu02]. Nevertheless, this bonding method is not considered as an easy and straightforward process, although high yield rate has been realized. For such a high yield rate, the process has to be executed by a well-trained technician on a specific designed apparatus very carefully. Besides, alignment between the membrane and the polymer housing has to be achieved optically through a microscope, so opaque material is very difficult to bond by this process [Kais00].

A new and easier bonding method is, therefore, desired. The new bonding process should have batch and mass production capability. It should be compatible to the AMANDA process and can bond most of the materials used by AMANDA components. Easy alignment and multilayer bonding ability will be a great plus. In this dissertation, a new bonding method was therefore, developed named the multilayer adhesive film bonding. For more details about this process, please see chapter 3.

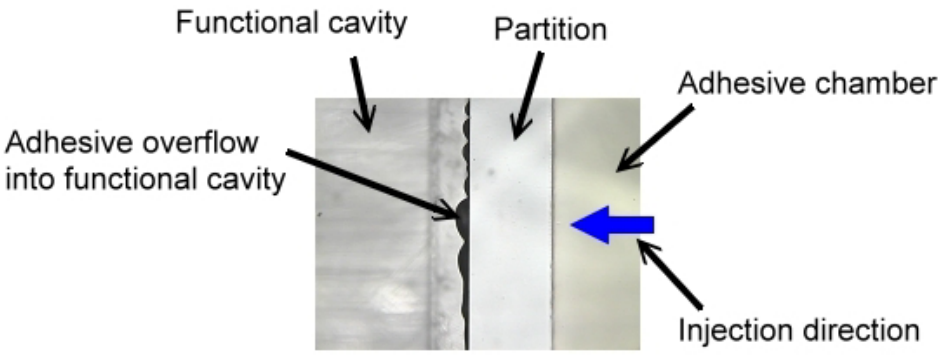


**Fig. 1.2.3: An example of adhesive overflow into the functional cavity.**

## 1.3 Active micro valves

In the past years, active micro valves using different kinds of working principles have been investigated by different research groups [Krus99]. They usually use a membrane or boss as valve shutter that is driven by thermally induced [Goll96], electrostatic [Robe94], piezoelectric [Rogg01], shape memory alloy [Kohl00], or magnetic [Kais00] forces to open or close the valve.

In general, the driving mechanisms of micro valves can be classified into the following catalogues [Kais00]:

***1.Electrostatic***

Electrostatic valves are outstanding due to their low energy consumption. The energy is only needed when the valve switches. However, the Coulomb force decreases dramatically with the distance between electrodes. Valve strokes over 10 µm are very difficult to realize by this method [Bran92] [Bosh93] [Goll97] [Huff93] [Wagn96].

***2.Piezoelectric***

With piezo ceramics, large driving force can be achieved. The energy is also only needed when the valve switches as in the case of the electrostatic actuators. Because the deformation of this actuator is very small, it is difficult to realize a large valve stroke. Large driving voltage around hundreds of volts is an undesired factor for micro system applications, however, it is usually needed for piezo ceramics. Because the thermal expansion coefficient of piezo ceramic is much smaller than that of polymer, If polymer housings are used to construct a piezo micro valve, the behavior could be easily influenced by the temperature [Esah89] [Rogg00] [Ross95] [Shoj91].

***3.Thermal driven***

Three thermal driven mechanisms are mainly used in the micro systems: thermapneumatics [Fahr94] [Goll96] [Zdeb94], bi-metal and shape memory alloy [Ditt98] [Goebe99] [Skro97]. Essential disadvantages of thermal actuators are their long cycle time and low power efficiency.

***4.Electromagnetic***

The magnetic force is thought to show a high energy density as a driving mechanism in the micro system field [Wagn90][Wagn91]. There are two principles to apply a magnetic force. One of them is the Lorenz law. It was once used as driving mechanism for a micro valve fabricated by the AMANDA process [Kais00]. Electric current was input to a linear circuit made from gold on a polyimide membrane with a predefined direction, a magnetic field was built by a permanent magnet external. The membrane can be driven up and down by switching of the input current directions.

## 1.4 The Demonstrator --- the magnetically driven micro ball valve

To demonstrate the new bonding method, a micro valve was developed and fabricated. In this demonstrator, iron balls were used to be the movable parts of the micro valve. The electromagnetic transcendent force induced by a commercially available magnetic coil is used as the driving mechanism. This approach has several significant advantages as listed below.

**Iron balls as movable parts**

No suspension:

A freestanding iron ball without suspension excludes mechanical internal stress and the danger of lifetime reduction owing to material fatigue. No extra power is needed to overcome the spring force of a suspension [Krus99]. A suspension membrane used in other micro valves usually has to be designed and produced very carefully. Many physical and chemical properties have to be considered. For example, water absorption and temperature variations will usually influence the mechanical properties of a polymer membrane or boss. For brittle membranes used in silicon micro machining, mechanical stress compensation has be considered. This usually results in a sandwich structure and complicates the fabrication processes.

Outsourcing:

As mentioned in the preface, the movable part and the driving elements are usually fabricated either by very difficult processes or by very expensive facilities in the cases of other micro valves. This results in high investments, long fabrication and design time and low yield. If instead, these parts are bought at the market, the advantages and merits of the supply companies will contribute to the success. Their mass production abilities and process optimizations will help us to achieve low costs and eliminate expensive process steps, which will lead to the reduction of the investment threshold of our potential industry partners.

**The driving mechanism**

To actuate a free-floating moving part, however, no directional current can be input, therefore, Lorentz law cannot be applied in our case. By switching and tuning the electric current input to a magnetic coil, an induced force can be generated by the gradient of the magnetic field. The force can be used to drive the ball and control the ball movement. A commercial available coil with a soft magnetic core is used to generate the desired magnetic field around the ball. A valve stroke of more than 200 μm has been achieved. The details of construction and fabrication considerations will be introduced in chapter 2 and chapter 4.

# 2 Design

This chapter describes how the micro ball valve was constructed. The micro ball valve was designed from an original idea and then through the considerations of minimum actuating forces and fabrication feasibility. To determine the basic dimensions of the valve, the actuating magnetic forces were estimated and computed by the finite element simulations under different conditions.

### 2.1 How the micro valve works ---- an original idea

A first idea of the micro ball valve was constructed for a feasible study of a special application. To describe the mechanism of the micro ball valve, figure 2.1.1 is illustrated as follows. The micro valve is driven by a magnetic coil. An over-pressure fluid is filled and maintained in a vessel. Through the center of the magnetic coil, the fluid flows into a ball chamber. In the ball chamber, there is an iron ball. Lifting force of the fluid rises up the ball and seal a valve seat on the top of the ball chamber. For example, in the figure 2.1.1, the ball B seals the valve seat 2B. The over-pressure is then transmitted through the ball chamber to the actuator interface in the figure (the red arrow), to drive an actuator for the special application. If an sufficient input current is given to the coil, for example, in the case of valve A, the induced magnetic force pulls the ball A down against the fluid pressure difference and seals the valve seat 1A. The pressure in the ball chamber is then reduced from the actuator interface through the ventilation channel (the green arrow). The action of the actuator on the actuator interface is therefore released.

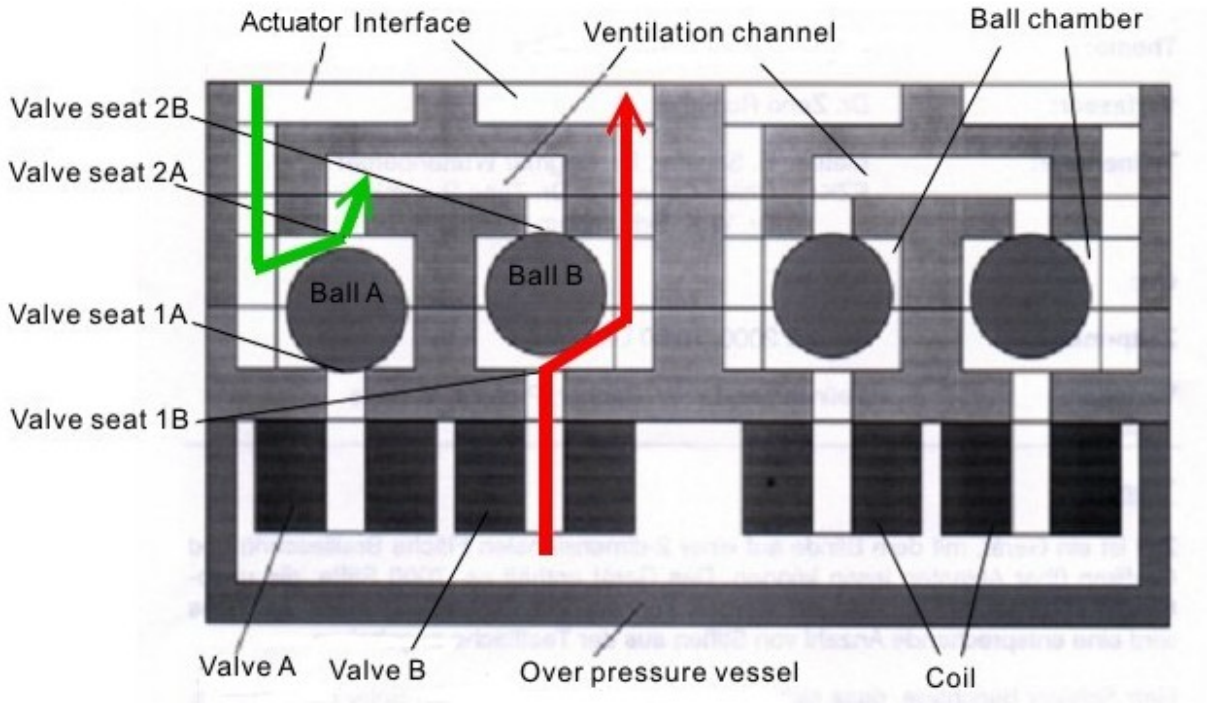


**Fig. 2.1.1 The first idea of the micro ball valves. The red arrow shows the flow direction when no current is input to the coil, while the green with sufficient input current.**

## 2.2 The minimum force needed to pull the ball

In order to estimate the minimum force needed, the movement of the ball has to be considered in three phases. One is when the ball is on the top of the ball chamber and seals the valve seat 2 as the ball B in the figure 2.1.1. In this state, there is no dynamic flow in the ball chamber, because in the application, a pressure sensor is attached to the actuator interface as shown in the figure 2.4.4. Therefore, to pull the ball down from valve seat 2B, the magnetic force needed can be computed statically through the equation:

$$F_1 = \pi r^2 P - W_{ball}$$

(Equation 2.2.1)

Where r is the radius of the valve seat 2B, P is the pressure difference between the ventilation channel and the over-pressure vessel, and $W_{ball}$ is the ball weight. To avoid blocking by contamination or particles in the fluid, the radius of the valve seats is chosen to be 150 µm. When the ventilation channel is connected to the atmosphere, the over-pressure will be the operational pressure of this valve. It was chosen to be 200 kPa for the application. After computing, the value of the first term in the equation 2.2.1 is 0.014 N. The weight of the ball is a function of its diameter. The gravitational force of the iron ball with a diameter of 3 mm is 0.0011 N. By subtraction, the force needed to pull the ball down from the valve seat 2B is obtained. It is computed to be 0.013 N in this status.

The second phase is when the ball is pulled down from the valve seat 2B and before it seals the valve seat 1B (figure 2.1.1). In this phase, the valve seat 2B is open, the ball chamber is connected to the ventilation channel and the fluid starts to flow. The force needed to pull the ball down can be computed through the equation:

$$F_2 = F_{lift} - W_{ball}$$

(Equation 2.2.2)

where $F_{lift}$ is the lifting force of the dynamic flow in the ball chamber. This force can be roughly estimated by the equation [Whit86]:

$$F_{lift} = 0.5 * C_D * \rho V^2 A$$

(Equation 2.2.3)

$C_D$ is a function of Reynolds number. The empirical value can be looked up in the reference [Whit86]. A $C_D$ value of 0.8 is suitable for our case. $\rho$ is the fluid density. A standard density of nitrogen of 1.162 Kg/$m^3$ is used here. V is the velocity of the fluid around the ball, which is measured to be 34.2 m/s under an over-pressure of 200 kPa. A is the cross section area of the ball. For a ball with a diameter of 3 mm, A is 7.1E-6 $m^3$. After computing, the estimated value of $F_{lift}$ can be obtained to be 0.0038 N. After subtraction by $W_{ball}$, the force needed to pull the ball down in this phase ($F_2$) is obtained. It is computed to be 0.00274 N. It is smaller than $F_1$.

The last phase is when the ball seals the valve seat 1 as the ball A shown in the figure 2.1.1. The needed force is used to overcome the pressure difference between the ball chamber and the over-pressure. Because the ball chamber is connected to the ventilation channel in this phase, $F_3$ can be computed just as in the first phase.

$$F_3 = F_1$$

(Equation 2.2.4)

Therefore, to ensure that the ball can be pulled down from the valve seat 2 and seal the valve seat 1, the magnetic force generated by the ball-coil system has to be larger than $F_1$.

## 2.3 Evaluation of the magnetic forces under different conditions

The only magnetic force, which has to be evaluated, is the force that is generated when the ball lies at the position of valve seat 2B, because the magnetic force is inversely proportional to the square of the distance between the iron ball and the top of the coil. When the force mentioned above is larger than $F_1$, it can ensure that the generated force at other positions will be also larger than the minimum actuating force needed.

The Ansys[tm] Emag module was used to simulate the generated forces under different conditions. An Ansys program based on the scripting language APDL (Ansys parametric design language) was developed to simulate the ball-coil system. Figure 2.3.1 shows an example of the construction of the simulated system. The number of coil windings, core magnetic permeable coefficients, input current, and the ball diameter were set to be variable in the program. The distance between the bottom of the ball and the top of the coil was set to be 350 µm. The coil length was changeable in the program and set to be proportional to the number of coil windings. The coil width was set to be the same as the ball diameter.

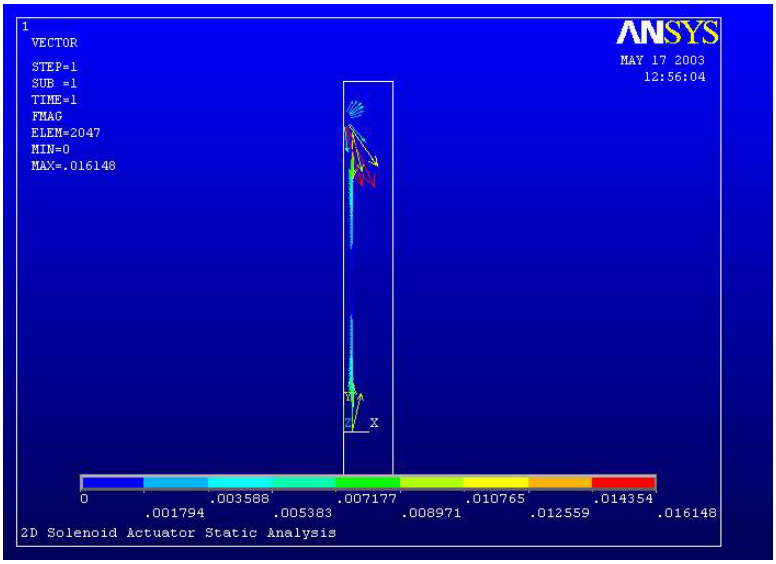


**Fig. 2.3.1 A construction of the ball-coil system for Ansys simulations using the PLANE 53 (2D 8-node magnetic solid) elements in the axis symmetric mode.**

There are a lot of different situations with parameter combinations. In order to describe the features and properties of such a system, only some results are illustrated in the following sub-sections. The number of the coil windings, input current, diameter of the ball, and the magnetic permeability of core related to the generated magnetic force with selected fixed values were shown here.

**Number of coil windings**

Figure 2.3.2 shows the generated force simulated as a function of the number of coil windings. The higher the number of coil windings is, the larger the generated force will be. However, the coil windings can be increased only finitely, because more windings will result in a larger coil size.

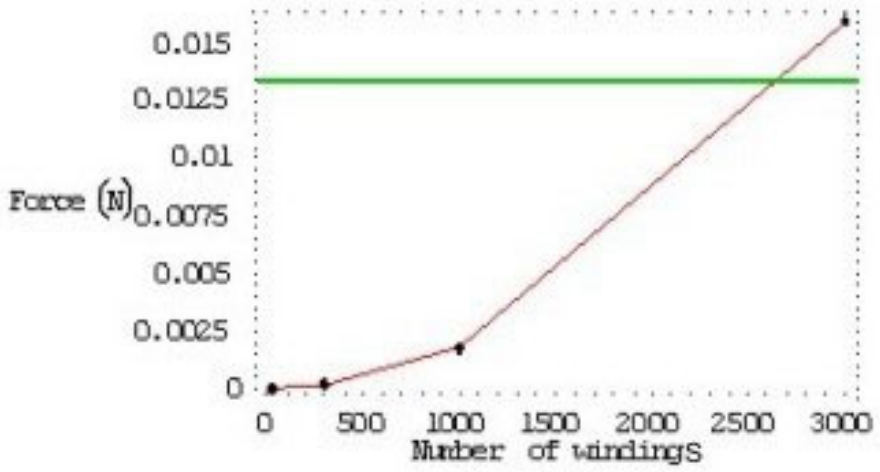


**Fig. 2.3.2 The magnetic force generated from the ball-coil system as a function of the number of the coil windings. In this figure, the ball diameter was set to be 3 mm. The input current was set to be 300 mA. The core permeability was set to be 5000. The green line is the minimum force needed.**

**Input current**

The magnetic force generated is proportional to the square of the input current as shown in the figure 2.3.3. However, in practical applications the input current can be increased only to a certain limit. The coil we used with 3000 windings has a resistance of 70 Ω. This leads to a proper input current that should not exceed 300 mA.

**The diameter of the ball**

The generated force is induced from the space gradient of the magnetic field generated by the coil. Therefore, the larger the ball size is, the larger is the force the system can generate. Figure 2.3.4 shows the calculated force as a function of the ball diameter. The input current was set to be 300mA, the number of winding was 3000, with a ferromagnetic core of permeability 5000.

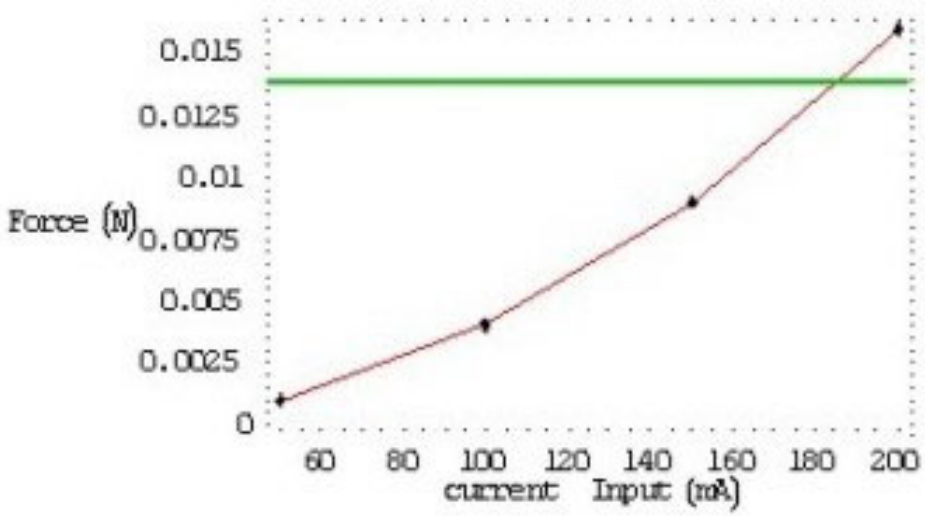


**Fig. 2.3.3** **The magnetic force generated from the ball-coil system is a function of the input current. In this figure, the ball diameter was set to be 3 mm. The number of coil windings was 3000. The core permeability was set to be 5000. The green line is the minimum force needed.**

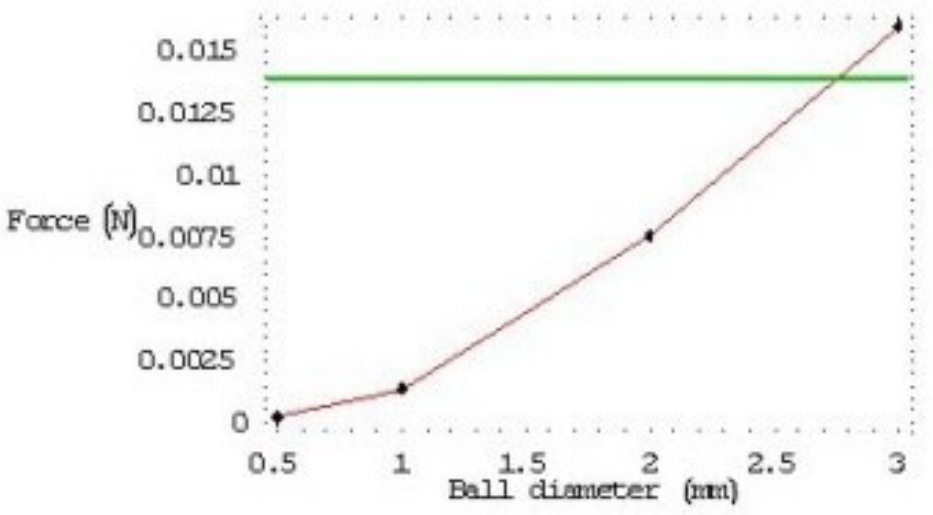


**Fig. 2.3.4** **The magnetic force generated from the ball-coil system is a function of the ball diameter. In this figure, the input current was set to be 300 mA. The number of coil windings was 3000. The core permeability was set to be 5000. The green line is the minimum force needed.**

### Ferromagnetic core

Figure 2.3.5 shows the influence of the ferromagnetic core. The generated force is strongly intensified by the ferromagnetic core. In Figure 2.3.5, simulations used an input current of 300 mA, a ball diameter of 3 mm and 3000 coil windings. The generated force was not sufficient to pull the ball down in the absence of the ferromagnetic core (specific magnetic permeability = 1). Therefore, it is necessary to add a ferromagnetic core in the valve construction. In order to guide the over-pressured fluid into the ball chamber in the presence of ferromagnetic core, a three-dimensional bypass flow channel is needed as showed in Figure 2.4.1. A ferromagnetic core with a specific magnetic permeability of 5000 is suitable for this application. The soft ferromagnetic cores can be supplied by the company Vacuum Schmelz [Vacu98]. A specific magnetic permeability higher than 5000 would not give further significant contribution to the generated force.

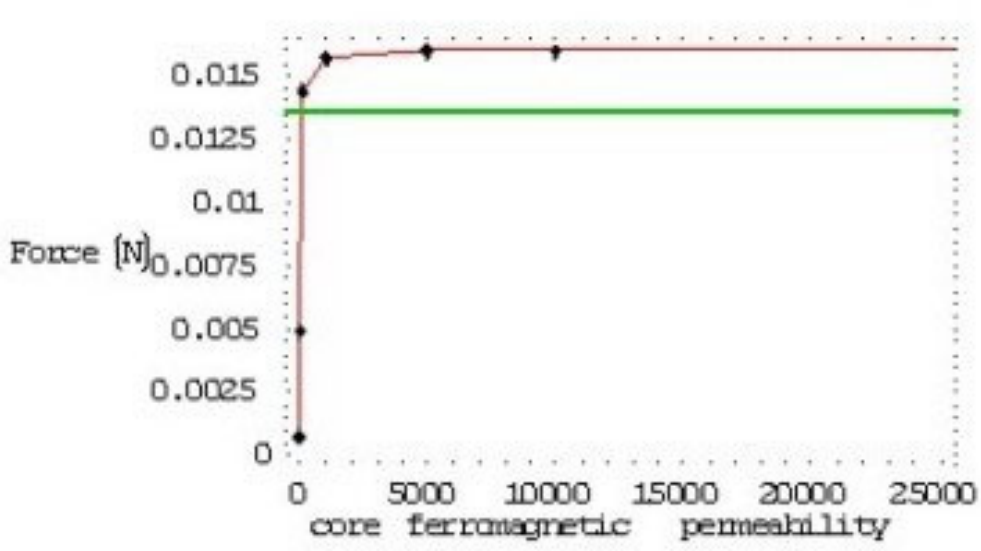


**Fig. 2.3.5 The magnetic force generated from the ball-coil system as a function of the permeability of the ferromagnetic core. In this figure, the input current was set to 300 mA. The number of coil windings was 3000. The ball diameter was 3 mm. The green line marks the minimum force needed for the valve.**

### Short summary of the simulation evaluation

1. The more windings the coil has, the larger is the force generated. (F is about proportional to $N^2$)
2. The input current has to be large enough to ensure the functionality, but not over 300 mA. (F is about proportional to $I^2$)
3. The ball has to be large enough. (F is about proportional to $d^2$)
4. A ferromagnetic core is required.
5. A by-pass three-dimensional flow channel is needed.

## 2.4 Construction of the micro ball valve

This section describes the construction and dimensions of the micro ball valve. The micro valve consists of three polymer and three metal layers.

### Top layer

The first polymer layer is the top layer with a valve seat (valve seat 2). It was designed to be 0.50 mm thick. The diameter of the valve seat was set to be 300 µm (figure 2.4.1). An opening with a diameter of 2 mm was designed for the actuator interface, which will be used to connect a pressure sensor in the characteristics measurement in chapter 5.

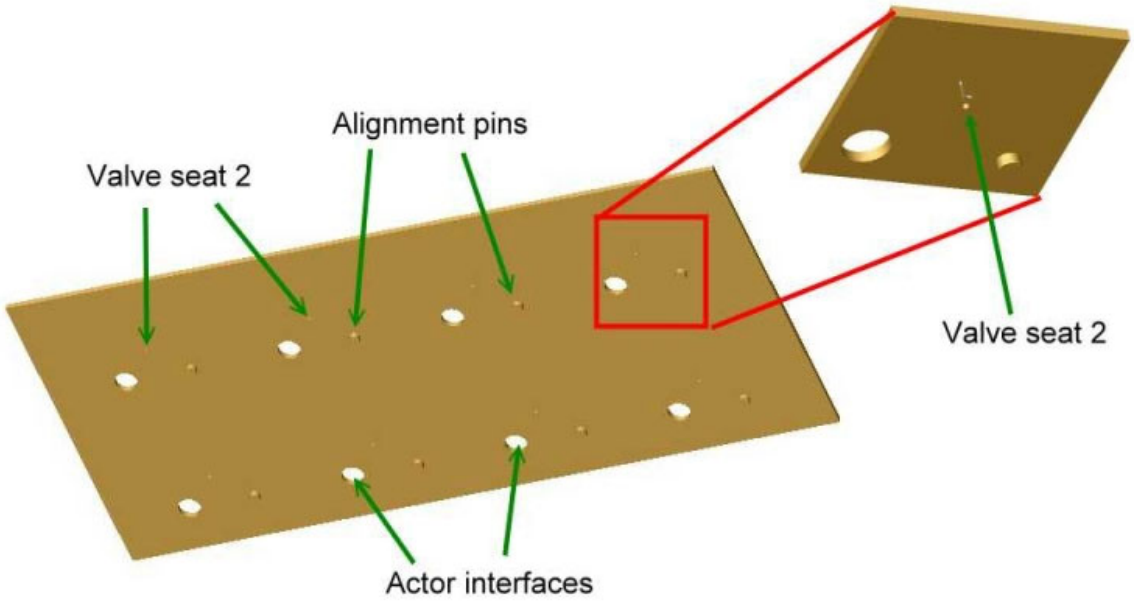


**Fig. 2.4.1 The construction of the top layer. It was 0.50 mm thick and contained valve seats with a diameter of 300 µm, alignment pins and actuator interfaces with a diameter of 2 mm.**

### Ball chamber layers

The next two polymer layers are ball chamber layers. These two layers formed a ball chamber with a height of 3.2 mm. The connection channel was designed to be 1 mm wide. It guided the fluid flow from the ball chamber to the actuator interface in the top layer (Figure2.4.2).

### Metal layers

Three metal layers formed a three-dimensional flow channel that allowed to keep the space under the ball to be free for the ferromagnetic core. The sandwich-like flow channel was designed to be 1 mm wide and 100 µm thick (Figure 2.4.3). The opening of the top metal layer formed the valve seat 1 with a diameter of 300 µm. The opening of the bottom metal layer was used as a fluid inlet with a diameter of 1 mm.

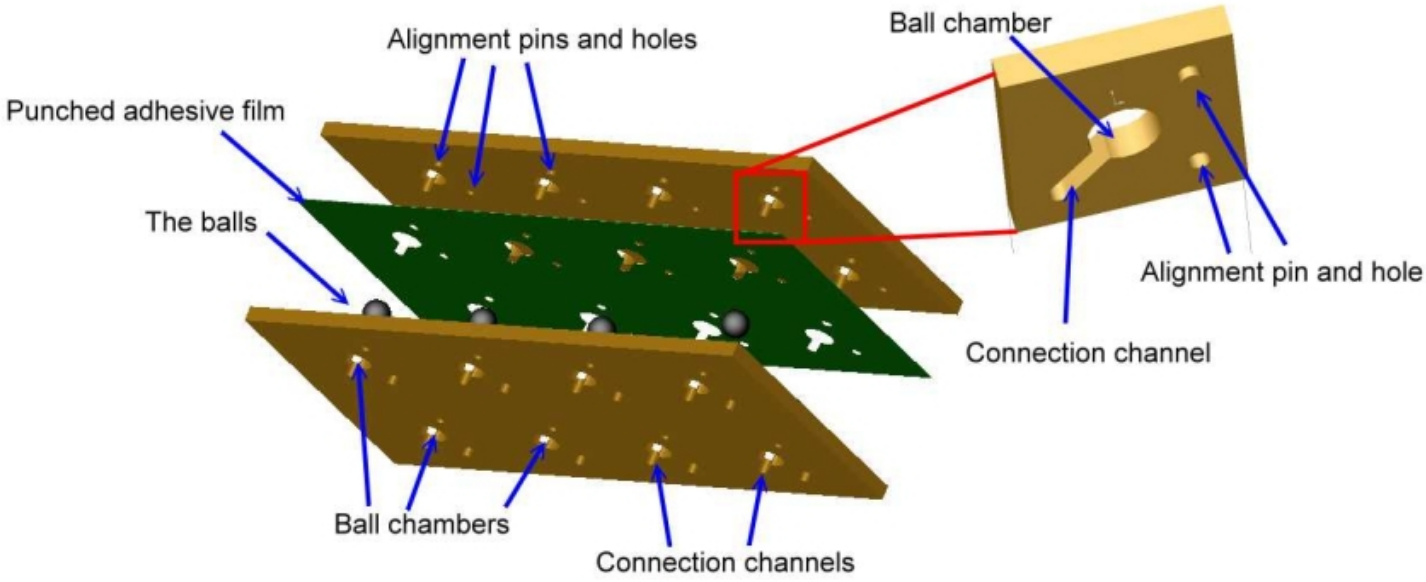


**Fig. 2.4.2** **The ball chamber layers. The picture shows iron balls and a punched adhesive film in between. The thickness was set to be 1.60 mm each. The layer contained ball chambers, connection channels and alignment pins and holes.**

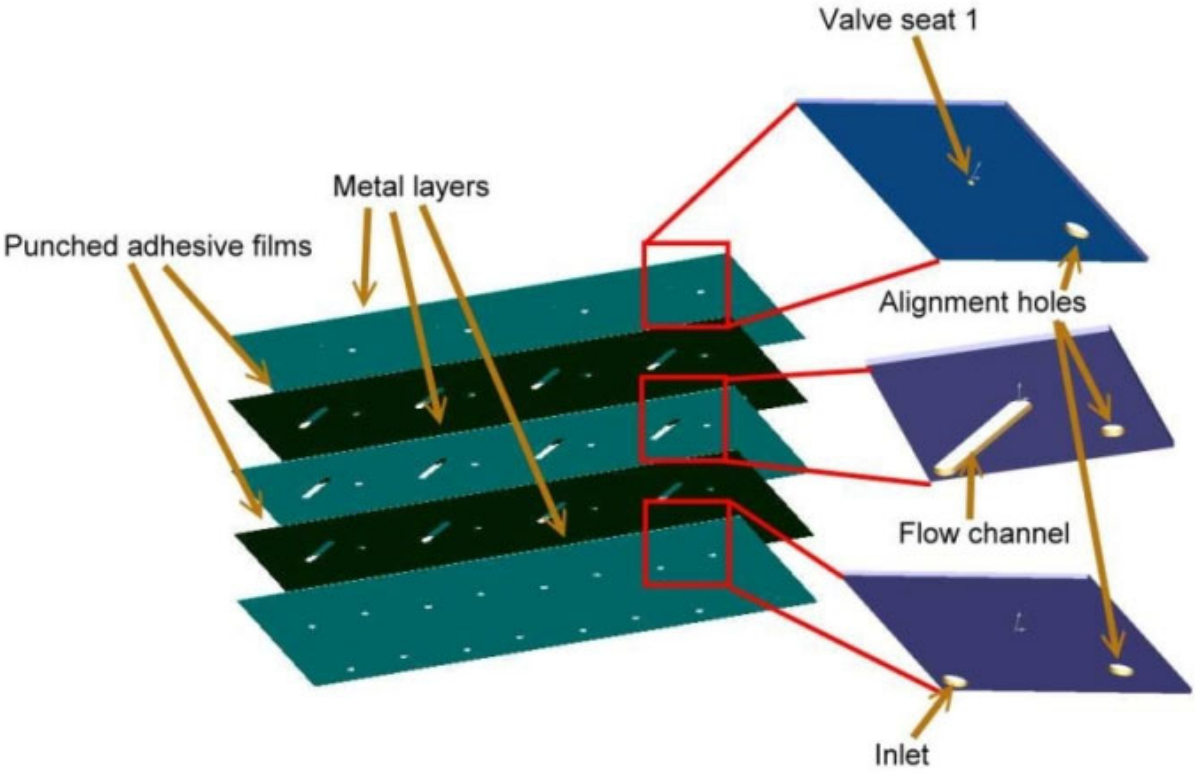


**Fig. 2.4.3** **The three metal layers. The picture shows the three metal layers and two punched adhesive films in between. Their thickness was 90, 100, and 90 µm, respectively. The layers contained valve seats with a diameter of 300 µm, flow channels, inlet holes and alignment holes.**

### Coil, core and the ball

A commercial coil with a length of 10 mm, diameter of 8 mm and 3000 windings was used, which was supplied by Era Electronik GmbH. Combined with a soft magnetic core the coil can drive the ball according to the simulation results in section 2.3. The three dimensional channel in the metal layers was used to guide the fluid bypassing the soft magnetic core into the ball chamber. Iron balls with a diameter of 3 mm were used, which were supplied by the company Britannia Waelzlager & Industrietechnik GmbH. A pressure sensor is connected to the outlet / actuator interface in order to detect the actions of the valve.

Figure 2.4.4 shows the total construction of the ball valve. The valve seat 2 is connected to the atmosphere in this design as ventilation. The outlet is connected to a pressure sensor. Fluid is driven by an over-pressure from the inlet. It enters into the bypass flow channel formed by the metal layers, then passes the valve seat 1 and flows into the ball chamber (the red arrow). When no power is supplied to the coil, the pressure difference between the inlet and the valve seat 2 lifts the ball up and seals the valve seat 2. The inlet pressure is then transmitted through the outlet to the pressure sensor. When a sufficient current is applied to the coil, the magnetic force pulls the ball down sealing the valve seat 1. The outlet pressure is then reduced to the ambient pressure by ventilation through the valve seat 2. The measurement results of the characteristics of the valve are described in chapter 5.

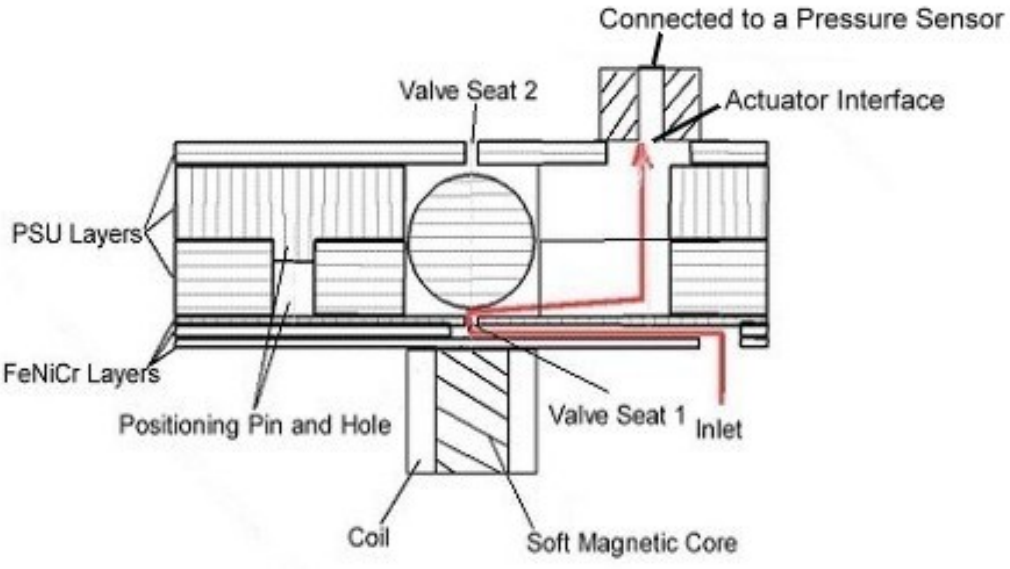


**Fig. 2.4.4 Construction of the micro ball valve. The gas flowed from the inlet through the three-dimensional flow channel formed by FeNiCr layers to the ball chamber. The outlet was connected to a pressure sensor to obtain the pressure signal.**

# 3 Adhesive Film Bonding Process

The development of a new bonding process using 3M VHB acrylate adhesive films is described in this chapter. This bonding method can be applied to bond polymer housings, membrane and other different material, for example, metal. This chapter describes the properties of the adhesive films and the operational steps. Taguchi method was used to find the proper process parameters to get enough bonding strength. The deformation of the punched microstructures through each process step was analyzed in a statistic way. Sealing properties were verified using the mediums of nitrogen and water. AMANDA process compatibility was demonstrated through bonding separated membranes on polymer housings.

## 3.1 The properties of the selected adhesive film

The selected acylate adhesive film 3M VHB 9460P is transparent with a thickness of 50 µm. One of the remarkable features of this adhesive film is its temperature resistance. It can operate under a temperature of 150 ℃ for long time, and for short time even up to 260 ℃. The material of the adhesive film is continuous visco-elastic. The bonded area is free from internal stress. It can be used as vibration damping of the applied devices as well. The acrylat material is closed-celled; sealing property is therefore insured (see section 3.4) [3M96]. The films can bond with different high surface energy materials. Applicable materials include metal, ceramic and polymer, for example, aluminum, steel, glass, $Si_3N_4$, hard-PVC, ABS, and PMMA …etc. Table 3.1.1 summarizes the general properties of the adhesive film.

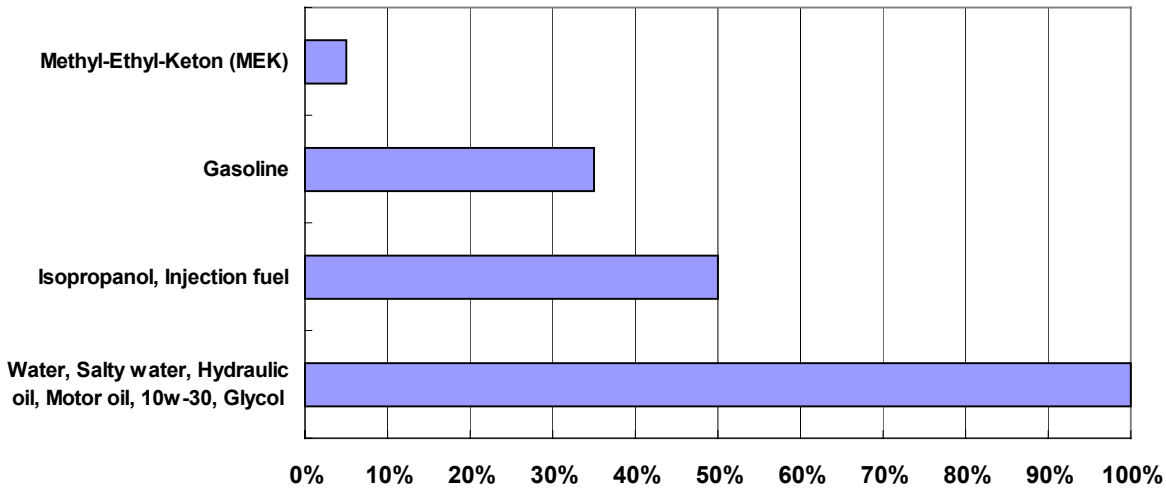


**Figure 3.1.1 The chemical withstandness test of the adhesive film. The values are the ratio of the rest peeling off force to the nominal value after the bonded parts merged in the test medium for 72 hours at the temperature of 25 ℃ [3M 96]**

To know for what kind of products and mediums this adhesive film is applicable. A chemical withstandness against Methyl-Ethyl-Keton (MEK), gasoline, isopropanol, water, salty water, motor oil, glycol...etc was examined by 3M. (Figure 3.1.1) The test uses stainless steel and

aluminum films bonded by the adhesive film. The bonded parts were put in the media mentioned above for 72 hours at room temperature and then its bonding force was measured. The results showed that the adhesive film withstands very well against water, salty water, oil, and glycol...etc.

**Table 3.1.1 The general properties of the 3M VHB adhesive film. [3M96]**

| | |
|---|---|
| Adhesive film | 3M VBH 9460 |
| Main material | Acrylat |
| Color | Transparent |
| Protect cover | Paper |
| Temperature withstandness (°C)<br>Long term<br>Short term | <br>150<br>260 |
| Nominal tensile strength (kPa)* | 690 |
| Nominal shear strength (kPa)** | 55 |
| Nominal peel off force (N/m)*** | 1200 |
| Electrical isolation resistance (MΩ/6.25 $cm^2$) | $10^6$ |
| Electrical discharge resistance (Volt) | 1000 |
| Process exhaust ****<br>Total Mass Loss (%)<br>Volatile Condensable Material (%) | <br>0.85<br>0.00 |
| Applicable adherent material<br>(High energy surface material) | High grade steel, Glas / Expoxy, Enamel, Ceramic, Phenolharze, Nickel Steel, ABS, PC, Al, Electro-platted Steel, hard-PVC... |

*Al-Al, tensile strength test, bonded area 6.45 $cm^2$, room temperature, at a pull speed of 50mm/min.

** Steel-Steel dynamic shear strength test, bonded area 6.45 $cm^2$, room temperature, 12.7mm/min.

*** Steel-Steel, 180° peel off, room temperature, 300 mm/min.

**** NASA Reference Publication June1984 „Out-gassing Data for Selecting Spacecraft Material.

## 3.2 The process

### Preparing the parts

To achieve a better adhesion, a clean, and fat and particle free surface of the adherents is necessary to be prepared at the first step. Isopropanol / water (50/50) was used as cleaning medium. By rinsing the parts in an ultrasonic bath and then wiping carefully on the surface to be bonded with the cleaning medium, the required cleanness can be achieved.

The adhesive film was delivered in rolls with a protection paper on one side. The paper was coated with a low surface energy (low adhesion) material. To protect the adhesive film during the punching process, another protection paper was used to cover the film double-sided (Figure 3.2.3 (a)). In these two papers, one side has weaker adhesion to the film, while the other

other side adheres stronger. To keep the punched microstructures as undeformed as possible during the peeling off from the protect paper, it has to be noticed which side of the protect papers is the weaker adhesion side. This side was peeled off and brought to the dried and cleaned surface on the adherent. With a small force, the adhesive film was gently laminated onto it. This allows the adhesive film to distribute homogeneously on the surface to be bonded and avoids the formation of air bubbles. A lamination tool (Figure 3.2.1) can be used to achieve this, but it can only be applied with a very small pressure in order to avoid damaging the punched microstructures.

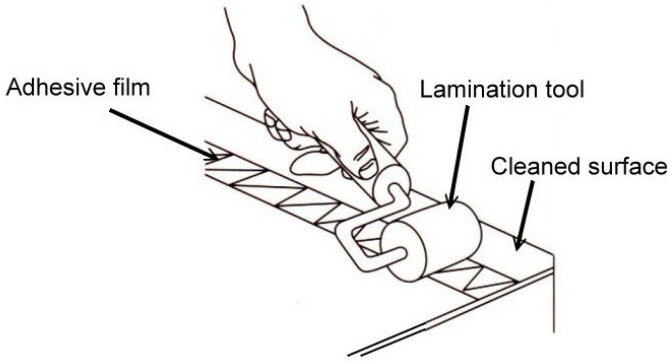


**Fig. 3.2.1 Application of the adhesive film on the cleaned adherent surface. A lamination tool can be used to improve the distribution homogeneousness of the adhesive film.**

After this, the second protect paper was peeled off. When the adhesive film has been distributed homogeneously on the PSU part, by peeling off the second protective paper, less damaging on the punched microstructures was observed in this step than that during the first peeling off step. (Figure 3.2.3) Further deformation analysis induced from the peeling off steps is described in section 3.3.

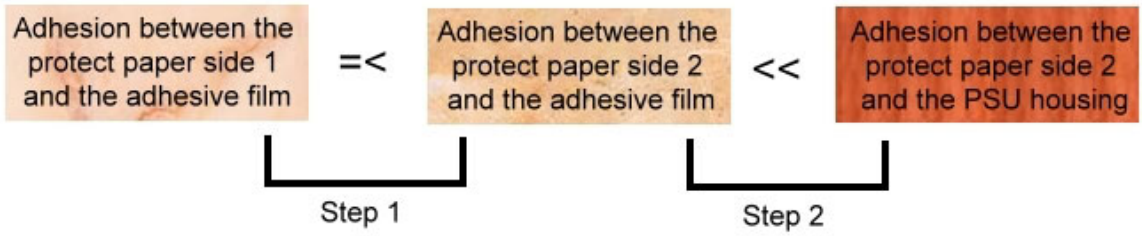


**Fig. 3.2.2 The adhesion strength between different materials is compared. Darker color means higher adhesion strength. The protect papers are coated with low surface energy material. The adhesion between the PSU housing and the adhesive film is much stronger than the adhesion between the protect paper and the adhesive. In the peeling off process, in order to keep the punched microstructures undeformed, the step 1 is more critical than the step 2.**

The last step is to bring the second PSU part onto the uncovered adhesive film surface. With the aid of the alignment pins and holes designed in chapter 2 and chapter 4, this step turned out to be very easy. It can be processed without any help of an optical microscope. The whole parts preparing process except the surface cleaning can be executed within a couple of minutes. (Figure 3.2.3)

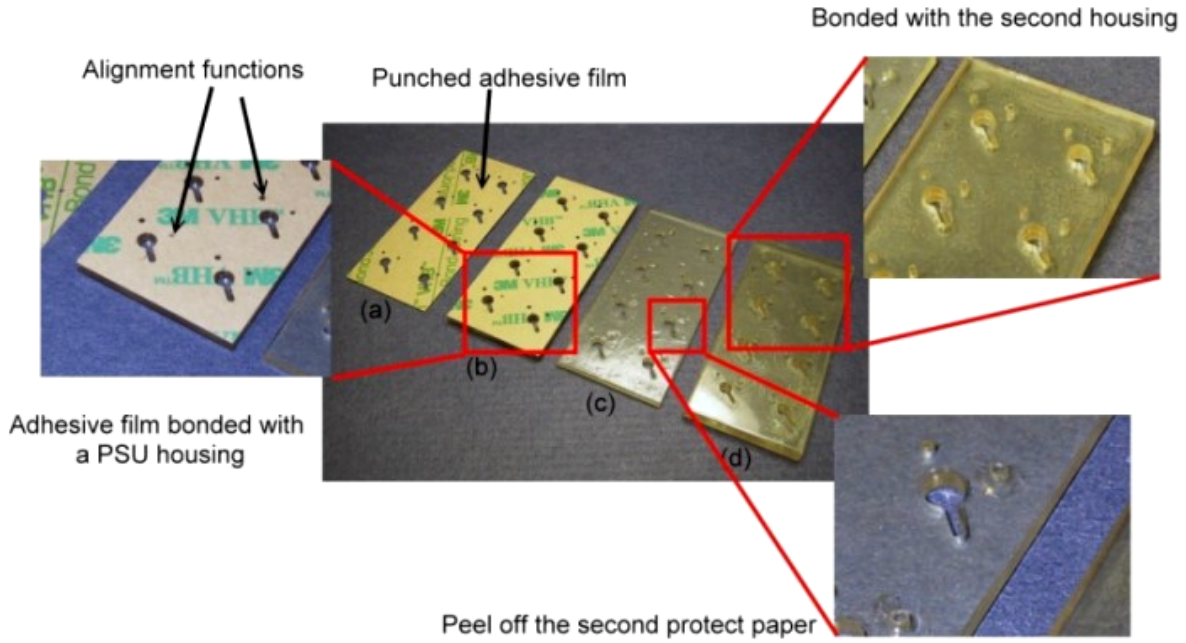


**Fig. 3.2.3. Parts preparation. (a) Punch the adhesive film. (b) Bond onto a PSU housing surface. (c) Peel off the second protection paper. (d) Bring the second housing on.**

In the case of multiple layers, the steps mentioned above are repeated without significant differences.

### Curing

Heating, press forces, and vacuum are conditions needed for the curing process. A hot-embossing machine was adapted to offer these conditions and to perform this manufacturing step (figure 3.2.4).

Vacuum environment can minimize the rest air bubbles between the bonded layers. It can improve not only the quality of the bonding but also the appearances of the bonded surface. Silicon rubber was used as sealing o-rings. They were used for sealing a vacuum chamber between the two press plates. The lower plate was designed as a fixture made from brass plate with a set of well-arranged holes. The arrangement of the holes was corresponding to the alignment pins and holes of the micro ball valves. This embedded alignment function on the press plate further facilitated the curing process.

The curing process starts with the evacuation of the vacuum chamber. A vacuum of 10 Pa was applied for the curing process.

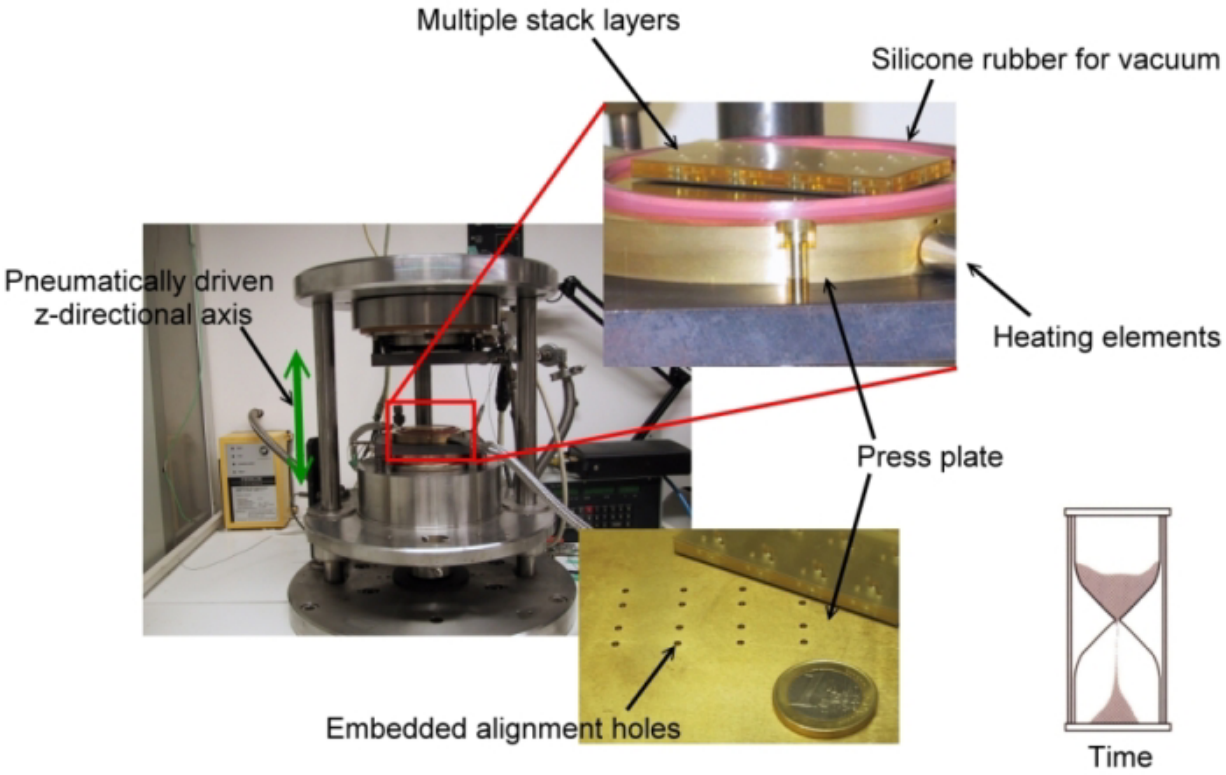


**Fig. 3.2.4 A hot-embossing machine was adapted as the curing tool. The three main manipulation parameters are press force, process temperature, and curing time. The press plate was equipped with embedded alignment holes. Silicone rubber was used as a vacuum sealing to minimize air bubbles between the bonded layers.**

There are two working modes of the pneumatically driven z-axis of the hot-embossing machine. One is the constant press mode. The other is the regulated tracking mode. In the constant press mode, the press force is held constant. While in the regulated tracking mode, the z directional position is controlled during the process. For the curing of our adhesive film bonding, the constant force mode has to be selected, because during the curing process, the adhesive films will expand a little bit, if the tracking mode would be selected, the automatic control of the machine would induce undesired large force, which would damage the sensitive punched microstructures.

To obtain the highest bonding strength, parameters used in the curing process have to be properly chosen. In order to obtain the proper process parameters, we built standard test samples to measure the bonding strength.

### 3.3 Bonding strength

To evaluate the bonding strength, the standard process DIN 53288 was applied, which is usually used to measure the bonding tensile strength of adhesives. Cylinders with a circular bonding area of 20 mm in diameter were used. The testing samples were made from PSU. The adhesive film was bonded at first between the two PSU cylinders. After curing using the selected process parameters, the sample was then tested on a standard tensile test machine cf. figure 3.3.1.

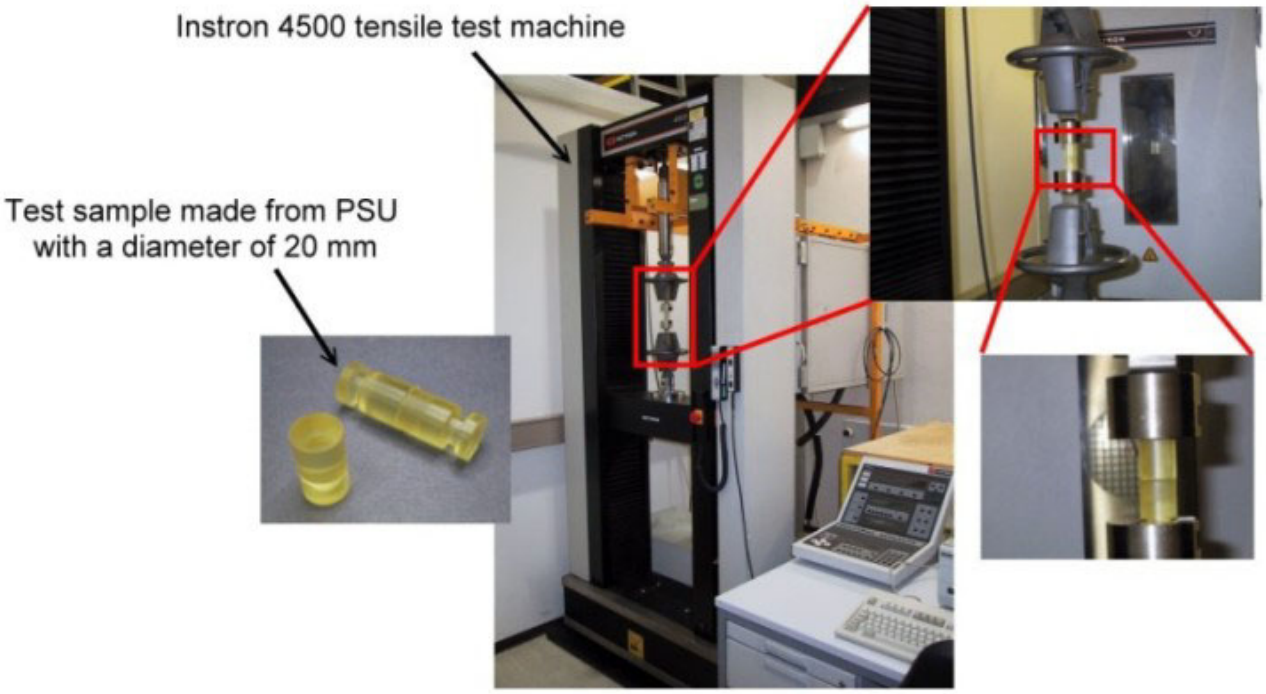


**Fig. 3.3.1 Bonding strength of the adhesive films was verified on the Instron 4500 tensile strength test machine according to the standard process DIN53288. The test samples were made from PSU with a circular area with a diameter of 20 mm.**

To find the proper process parameters and to minimize the number of required experiments, the Taguchi experiment design method was applied, which allows the researcher to use less experiments to handle properties of a process influenced by different factors and to find out the optimal solutions [Roy 01]. Three levels of each of the parameters, press pressure, temperature and process time were selected to investigate the process cf. table 3.3.1. A L9 table is suitable for this analysis. (Table 3.3.2) E is a redundant parameter. Instead of 27 different cases for three three-level factors in this process, only 9 experiments were needed to be used to analyze the curing process. For more information about the terminology definitions / explanations of the Taguchi method, please read the remark at the end of this chapter.

In this case, the bonding strength is a property of “Larger is Better”. It means we would like to find a set of process parameters to let the produced bonding strength as large as possible. For every selected process parameter in the L9 table, two experiments were made. The SN (signal to noise ratio) valve equation for a property of “Larger is Better” is

$$SN = -10 * \log(0.5 * (\frac{1}{y_1^2} + \frac{1}{y_2^2}))$$

(Equation 3.3.1)

The results are shown in the table 3.3.3. To get a more concise and clear vision, each SN valve was subtracted by a number of 45. Assistant table was obtained by summation of the SN (-45) valves of the related factor levels. (Table 3.3.4) Figure 3.3.2 shows the influence of the process parameters by the different factor levels. From the figure, the optimal parameters can be selected. In this case, the larger press pressure, higher temperature and longer process time will lead to higher bonding strength. The optimal parameters A3, B3, C3 was therefore selected. From the figure, press pressure (A) changes from 0 to 200 kPa showed larger influences on the bonding strength than the changes of curing temperature from 15 to 65°C and of the process time (C) from 20 to 60 minutes. The average bonding strength of 652 kPa was then measured by the experiment using parameter 200kPa press pressure, 65°C and one hour process time.

**Table 3.3.1 The experiment factors and its levels used in the Taguchi method**

| Factor | Level | | |
|---|---|---|---|
| | 1 | 2 | 3 |
| A: Press pressure (kPa) | 0 | 100 | 200 |
| B: Temperature (°C) | 15 | 40 | 65 |
| C: Curing time (min) | 20 | 40 | 60 |

**Table 3.3.2 Experiment design with 3 three-level factors (A L9 orthogonal table)**

| Experiment | Factors | | | |
|---|---|---|---|---|
| | A | B | C | E |
| 1 | 1 | 1 | 1 | 1 |
| 2 | 1 | 2 | 2 | 2 |
| 3 | 1 | 3 | 3 | 3 |
| 4 | 2 | 1 | 2 | 3 |
| 5 | 2 | 2 | 3 | 2 |
| 6 | 2 | 3 | 1 | 1 |
| 7 | 3 | 1 | 3 | 2 |
| 8 | 3 | 2 | 1 | 3 |
| 9 | 3 | 3 | 2 | 1 |

**Table 3.3.3 The experiment results**

| Experiments | **A** | **B** | **C** | E | **Bonding strength (kPa)** | | **SN** | **SN (-45)** |
|---|---|---|---|---|---|---|---|---|
| | | | | | $y_1$ | $y_2$ | | |
| 1 | 1 | 1 | 1 | 1 | 217.0 | 236.4 | 47.08 | 2.08 |
| 2 | 1 | 2 | 2 | 2 | 285.4 | 301.6 | 49.34 | 4.34 |

| | | | | | | | | |
|---|---|---|---|---|---|---|---|---|
| 3 | 1 | 3 | 3 | 3 | 376.7 | 379.3 | 51.55 | 6.55 |
| 4 | 2 | 1 | 2 | 3 | 331.2 | 347.2 | 50.60 | 5.60 |
| 5 | 2 | 2 | 3 | 2 | 431.3 | 446.3 | 52.84 | 7.84 |
| 6 | 2 | 3 | 1 | 1 | 392.8 | 394.0 | 51.90 | 6.90 |
| 7 | 3 | 1 | 3 | 2 | 488.4 | 507.6 | 53.94 | 8.94 |
| 8 | 3 | 2 | 1 | 3 | 444.7 | 452.1 | 53.03 | 8.03 |
| 9 | 3 | 3 | 2 | 1 | 568.1 | 587.9 | 55.23 | 10.23 |

**Table 3.3.4 Assistant table (SN (-45))**

| | | | | | |
|---|---|---|---|---|---|
| A1 | 12.98 | B1 | 16.63 | C1 | 17.01 |
| A2 | 20.34 | B2 | 20.22 | C2 | 20.18 |
| A3 | 27.21 | B3 | 23.68 | C3 | 23.33 |

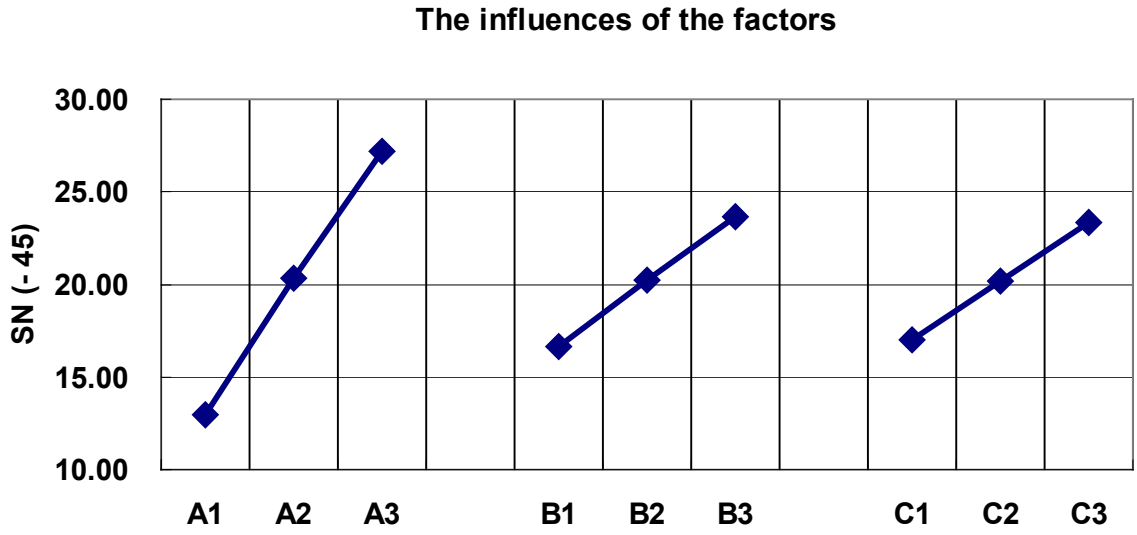


**Fig. 3.3.2 The influences on the bonding strength by the different levels of the process parameters. To get a higher bonding strength, process parameters A3, B3, C3 were selected. Press pressure (A) changes from 0 to 200 kPa have larger influences on the bonding strength than the changes of curing temperature from 15 to 65 ˚C or of the process time (C) from 20 to 60 minutes.**

### 3.4 Deformation analysis of the punched microstructures

The deformation of the punched microstructures was investigated through the whole bonding process. The deformations were measured after punching, peeling off and joining and curing.

#### Deformation through punching process

Because of their material property, the punched protect papers have many mechanical burrs. It is very difficult to observe the exact structure dimensions. To evaluate the accuracy of the microstructures the punching process can achieve, a PSU film with a thickness of 150 µm was applied, punched and measured. (Figure 3.4.1) The flow channel structure was used as the evaluation standard. The designed specification of the channel width is larger than 1.20 mm. Figure 3.4.2 shows a typical example of measured results of the eight structures on a PSU film using a microscope. The other measured results are listed in Appendix 1. Figure 3.4.3 shows the statistic results of 56 Channel widths on seven punched films. The average dimension of the measured punched flow channels is 1.306 mm and the standard deviation is 0.006 mm.

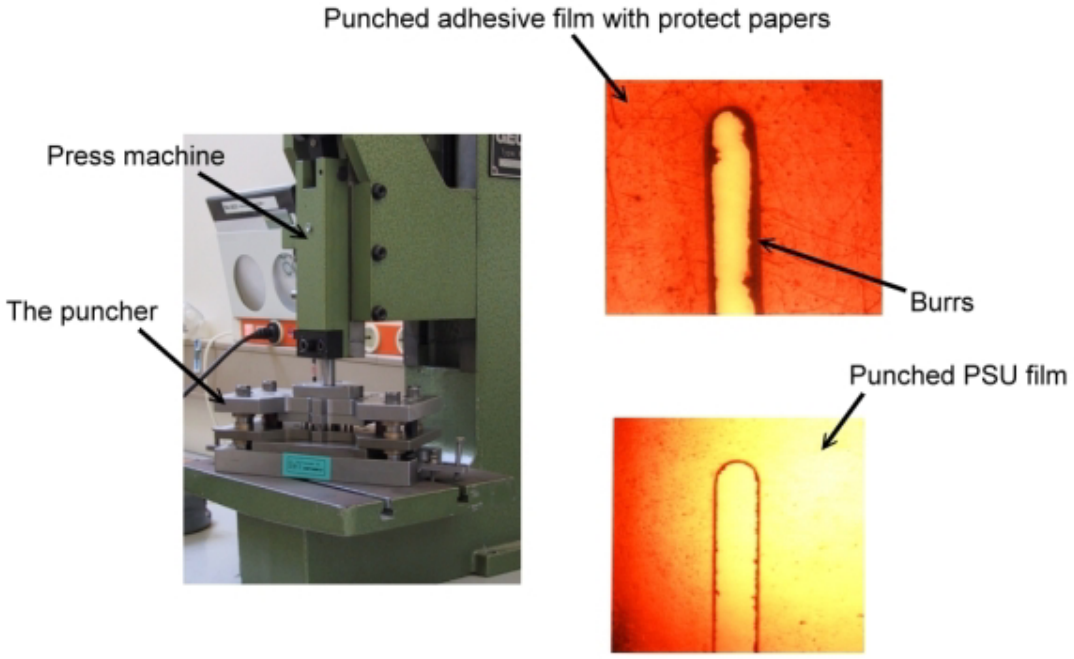


**Fig. 3.4.1 The puncher mounted on a manual press machine. Punched microstructures showed many burrs on the adhesive film protection paper such that it is difficult to observe the exact dimensions. Punched PSU films have less burrs. Therefore, they were used as the standard mediums to evaluate the microstructure accuracy the punching step can achieve.**

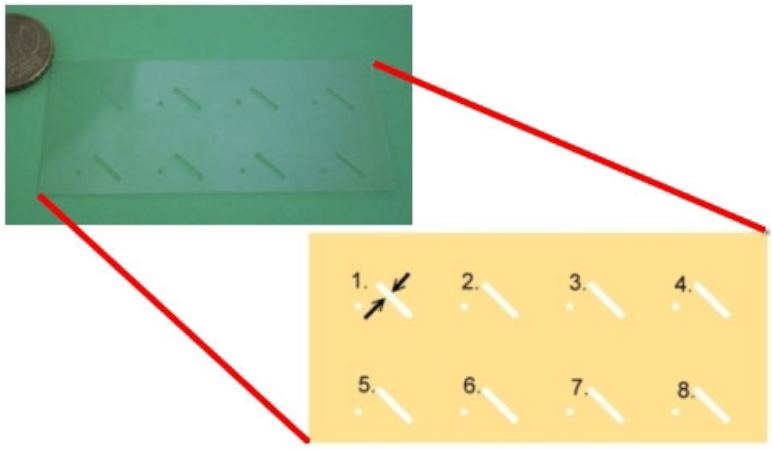


| No. | 1. | 2. | 3. | 4. | 5. | 6. | 7. | 8. |
|---|---|---|---|---|---|---|---|---|
| Width (mm) | 1.316 | 1.304 | 1.301 | 1.313 | 1.304 | 1.305 | 1.301 | 1.307 |

**Fig. 3.4.2** An example of measurement results of eight flow channel structures on a punched PSU film.

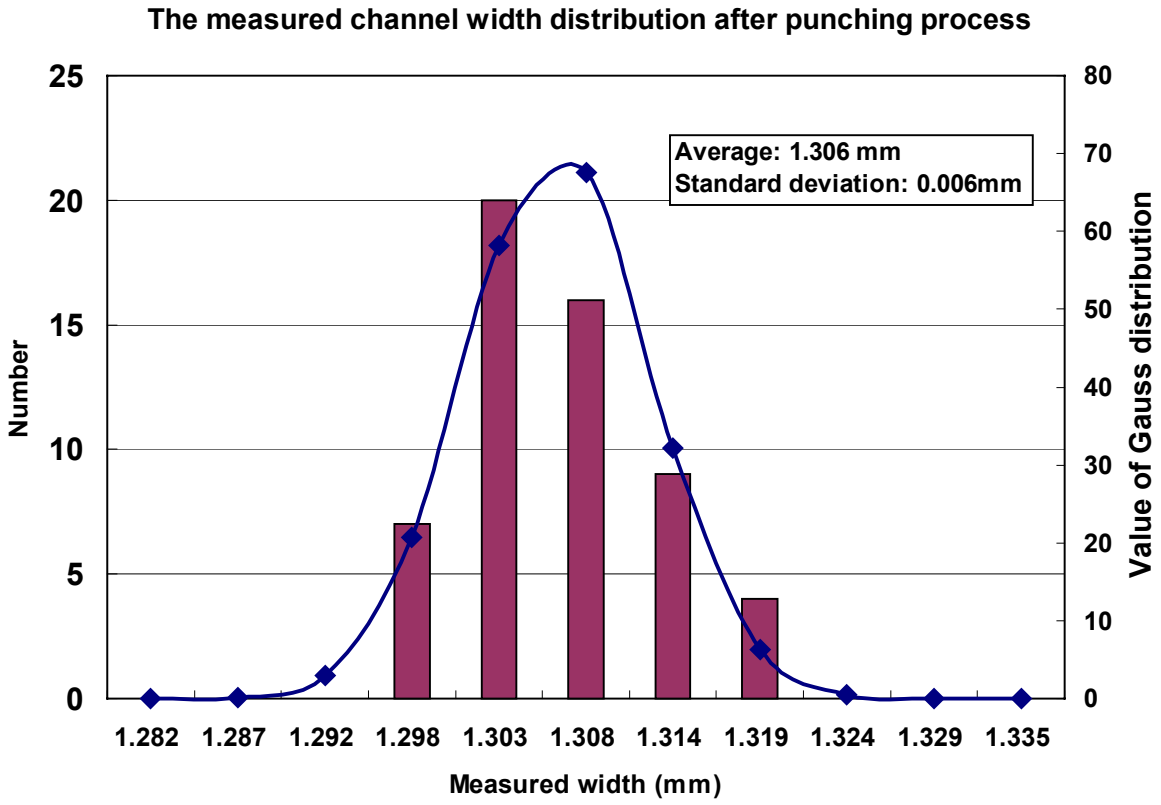


**Fig. 3.4.3** The statistical result of measured 56 channel widths on seven PSU films after the punching process. The standard deviation of the measured results was 0.006 mm. The average value was 1.306 mm. The blue line shows the corresponding Gauss distribution.

**Deformation of the microstructures on the adhesive films through parts preparing**

In order to evaluate the deformation of microstructures on the adhesive films through parts preparing, adhesive films were punched and brought in between two 150 µm PSU films. The PSU films used here were not punched. Although there were burrs on the protection papers, no burrs was observed on the punched adhesive films, because the material of the adhesive film is not fiber structured.

The PSU is transparent enough to obverse the dimension of the punched microstructures on the adhesive film. The step was processed manually at room temperature. Figure 3.4.4 shows a typical measurement result of a sample. The other measured results are listed in Appendix 1. Figure 3.4.5 shows the statistical result of 56 data. The average dimension measured was 1.472 mm and the standard deviation was 0.069 mm.

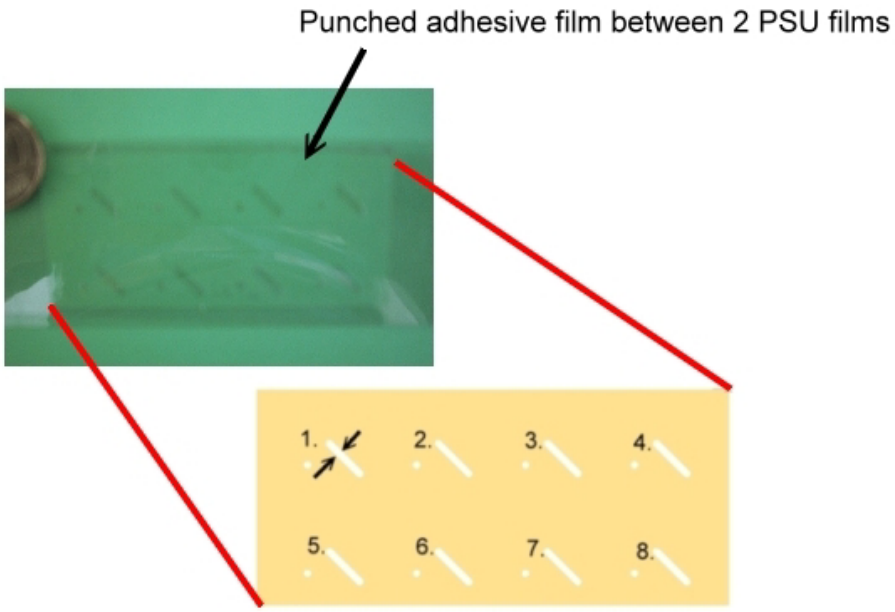


| No. | 1. | 2. | 3. | 4. | 5. | 6. | 7. | 8. |
|---|---|---|---|---|---|---|---|---|
| Width (mm) | 1.47 | 1.46 | 1.54 | 1.43 | 1.37 | 1.42 | 1.52 | 1.44 |

**Fig.3.4.4 A typical measurement result of punched microstructures on an adhesive film after parts preparing step. The punched adhesive film was brought in between the two PSU films with a thickness 150 µm. The other measured results are listed in Appendix 1.**

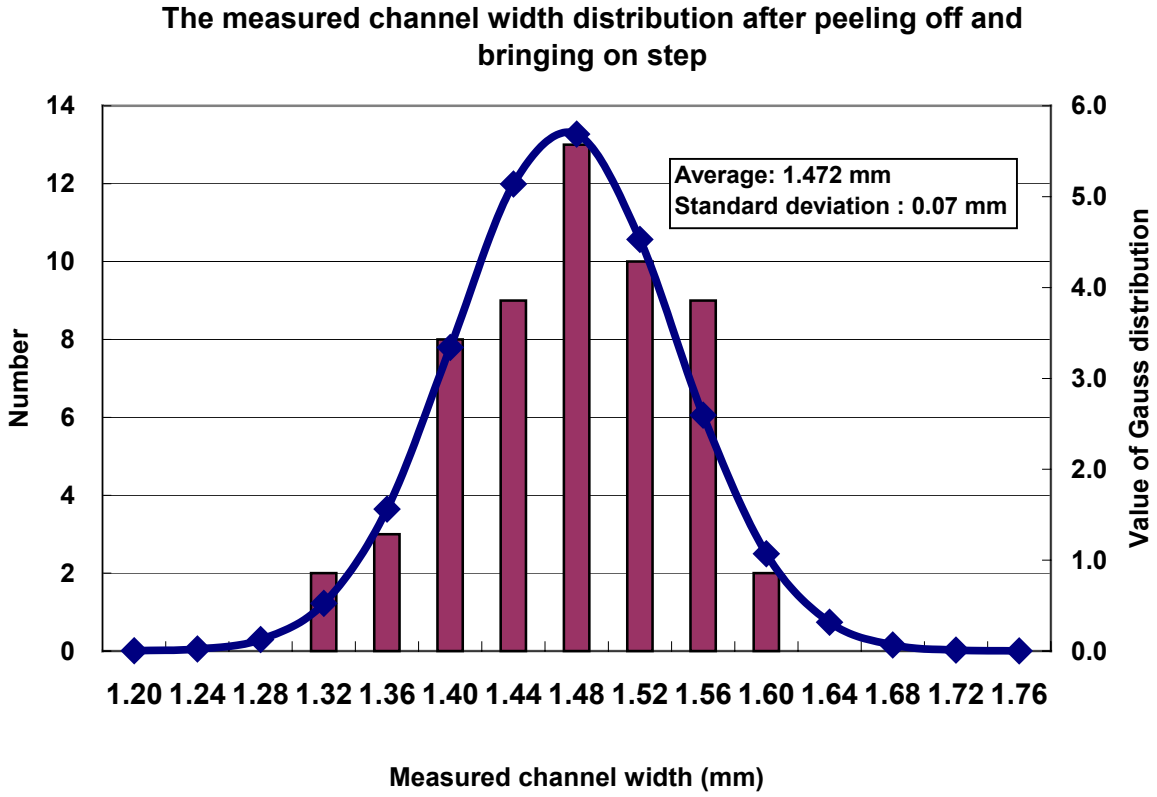


**Fig. 3.4.5** **The statistical result of measured 56 channel widths on seven adhesive film samples after parts preparing step. The standard deviation of the measured results was 0.07 mm. The blue line shows the corresponding Gauss distribution.**

### Deformation through curing

The deformation of the microstructures on the adhesive film through curing was evaluated and analyzed under different process parameters using Taguchi method. Punched adhesive films were bonded between two 150 µm PSU films using the same experimental factors and levels as in the bonding strength test. (Table 3.2.1 and Table 3.2.2)

The punched adhesive film flows towards the inner side during curing. The channel dimension after curing is therefore smaller than that before the curing process without exception. The deviations were computed by subtractions of the measured data after the process from the data before the process. The measured deformations showed large imhomogeneities that were attributed to differences of temperature distribution on the machine during the curing process. Therefore, only the four inner channel widths on each sample were used which were placed near the center of the heating plate and showed less imhomogeneities.

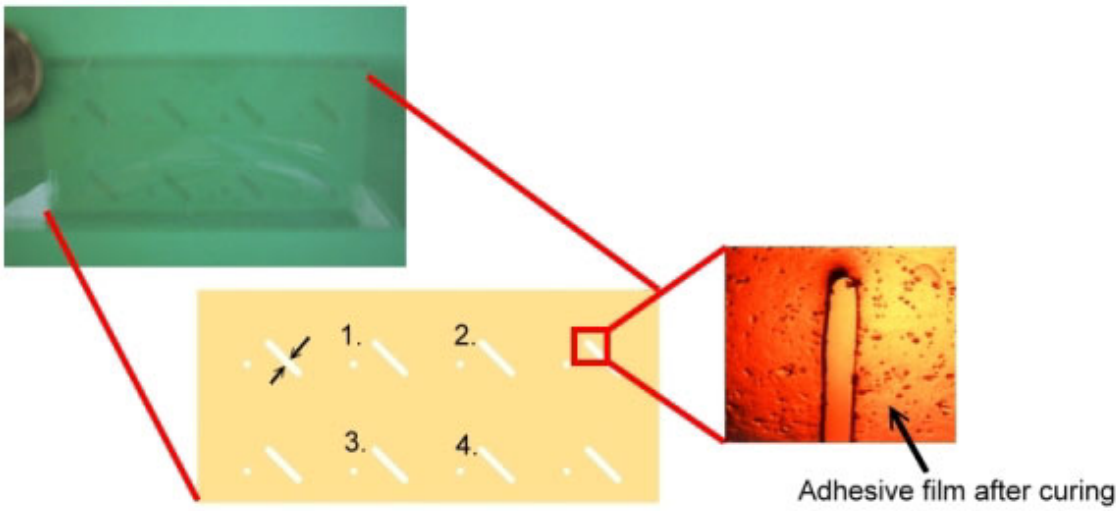


| | Channel No. | 1. | 2. | 3. | 4. |
|---|---|---|---|---|---|
| Sample I | Before curing (mm) | 1.496 | 1.573 | 1.500 | 1.522 |
| | After curing (mm) | 1.440 | 1.516 | 1.441 | 1.458 |
| | Deviation (mm) | 0.056 | 0.057 | 0.059 | 0.064 |

**Fig. 3.4.6** **The punched adhesive film flows toward inner side during the curing step. The channel dimension after curing is therefore smaller than that before the curing process. The deviations were computed by subtractions of the measured data after the process from the data before the process. Only inner four dimensions were used for the Taguchi analysis to avoid the imhomogeneity effects of the temperature distribution of the laboratory equipment.**

Table 3.4.1 shows the experimental results. In this case, the dimension deviation is a property of “Smaller is Better”. It means we would like to have a set of process parameters that lead to minimum deviation. The SN valve equation for a property of “Smaller is Better” in the Taguchi method is

$$SN = -10 * \log(\frac{1}{4} * (y_1^{\,2} + y_2^{\,2} + y_3^{\,2} + y_4^{\,2}))$$

(Equation 3.4.1)

To get a more concise and clear vision, the SN valve was subtracted by a number of 24. Assistant table was obtained by summation of the SN (-24) valves of the related factor levels. (Table 3.4.2)

Figure 3.4.7 shows the influence of the process parameter by the different factor levels. From the figure, we can understand that in contrast to the bonding strength, to minimize the deviation, lower press pressure, lower curing temperature and short process time are desired. Shortening the curing time and lowering the press pressure will have larger impact on the improvement of the curing deviation than lowering the temperature.

The microstructure deviation during curing using the process parameters of the maximum bonding strength, A3, B3, C3 was measured. The average valve was 0.0575 mm and the standard deviation was 0.0046 mm. (Figure 3.4.8) For application of the micro ball valves, the structures deviation of this scale is not critical (see the discussion), therefore, the process parameters for curing was chosen according to the maximum bonding strength. For future applications, when the microstructure deviation through curing step is very sensitive, the conclusions obtained above can be used as a reference rule for the curing process.

**Table 3.4.1. The experiment results**

| Experiments | **A** | **B** | **C** | E | **Structure deviation before and after curing process (mm)** | | | | **SN** | **SN (-24)** |
|---|---|---|---|---|---|---|---|---|---|---|
| | | | | | $y_1$ | $y_2$ | $y_3$ | $y_4$ | | |
| 1 | 1 | 1 | 1 | 1 | 0.001 | 0.002 | 0.001 | 0.001 | 56.80 | 32.80 |
| 2 | 1 | 2 | 2 | 2 | 0.006 | 0.006 | 0.004 | 0.004 | 45.61 | 21.61 |
| 3 | 1 | 3 | 3 | 3 | 0.023 | 0.024 | 0.030 | 0.032 | 31.21 | 7.21 |
| 4 | 2 | 1 | 2 | 3 | 0.007 | 0.007 | 0.009 | 0.006 | 42.96 | 18.96 |
| 5 | 2 | 2 | 3 | 2 | 0.029 | 0.027 | 0.031 | 0.030 | 30.75 | 6.75 |
| 6 | 2 | 3 | 1 | 1 | 0.001 | 0.005 | 0.006 | 0.006 | 46.14 | 22.14 |
| 7 | 3 | 1 | 3 | 2 | 0.051 | 0.059 | 0.056 | 0.059 | 24.98 | 0.98 |
| 8 | 3 | 2 | 1 | 3 | 0.005 | 0.002 | 0.010 | 0.009 | 43.20 | 19.20 |
| 9 | 3 | 3 | 2 | 1 | 0.031 | 0.024 | 0.027 | 0.030 | 31.02 | 7.02 |

**Table 3.4.2. Assistant table (SN (-24))**

| | | | | | |
|---|---|---|---|---|---|
| A1 | 61.61 | B1 | 52.75 | C1 | 74.14 |
| A2 | 47.86 | B2 | 47.56 | C2 | 47.59 |
| A3 | 27.20 | B3 | 36.36 | C3 | 14.95 |

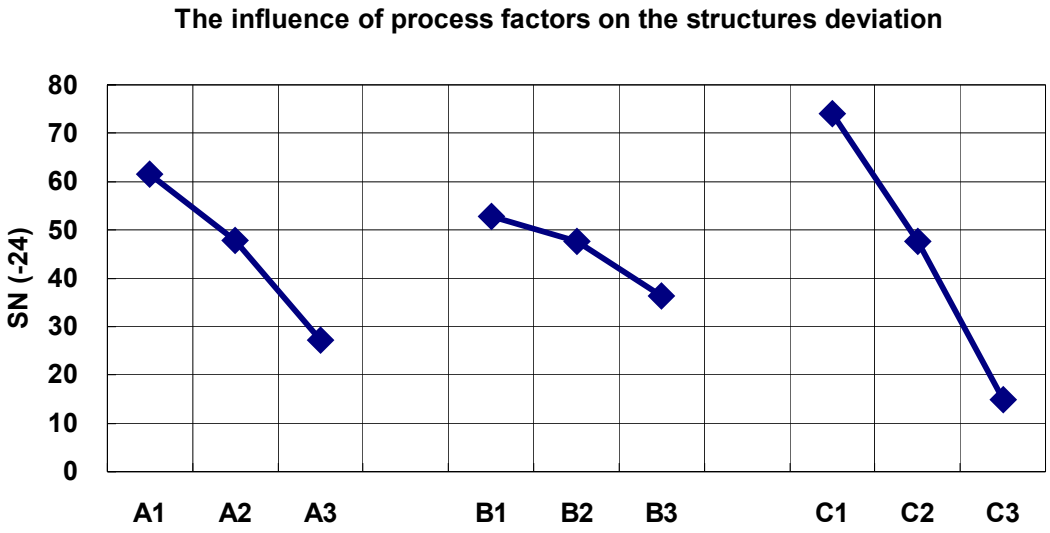


**Fig. 3.4.7.** **The influences on the punched microstructures deviation by the different levels of the process parameters. To minimize the deviation, lower press pressure, lower curing temperature and short process time are desired. Shortening the curing time and lowering the press pressure will have larger impact on the improvement of the curing deviation than lowering down the temperature. A presents the press pressure in the figure, B curing temperature and C process time.**

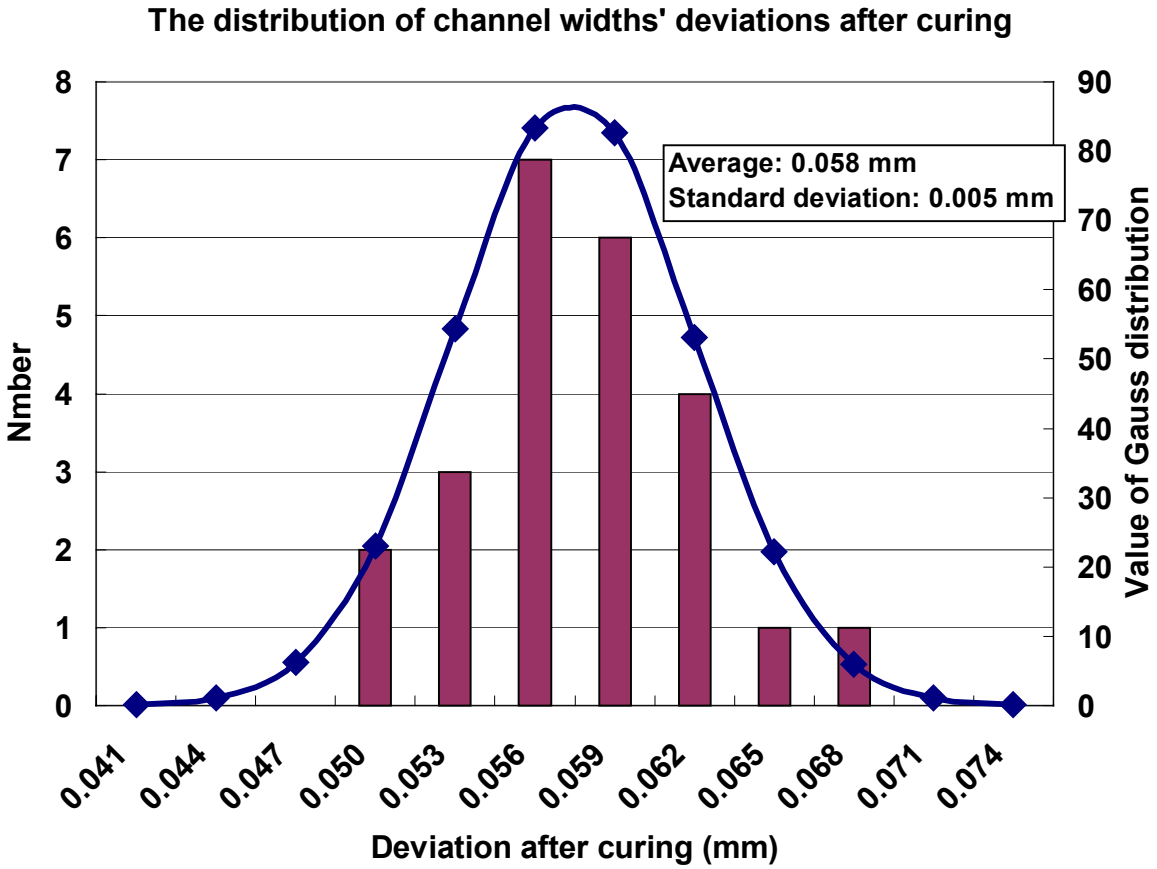


**Fig. 3.4.8** **The statistical result of measured 24 channels width deviations after curing. The standard deviation of the deviations was 0.005 mm. The blue line shows the corresponding Gauss distribution.**

### Discussion

The Gaussian distributions of the channels widths of the punched microstructures after different process steps are shown in figure 3.4.9. The green line is the width distribution after punching. It is a very narrow line with a small standard deviation of 0.006 mm. It represents the microstructures accuracy the punching process can achieve.

The blue line is the width distribution of the punched micro flow channel on the adhesive before curing. Because the adhesive film is somewhat visco-elastic under the room temperature, peeling off the protection papers and joining the adhesive film on the adherent will lead the microstructures to be expanded. The measured standard deviation of the expanded dimension is about 0.07 mm.

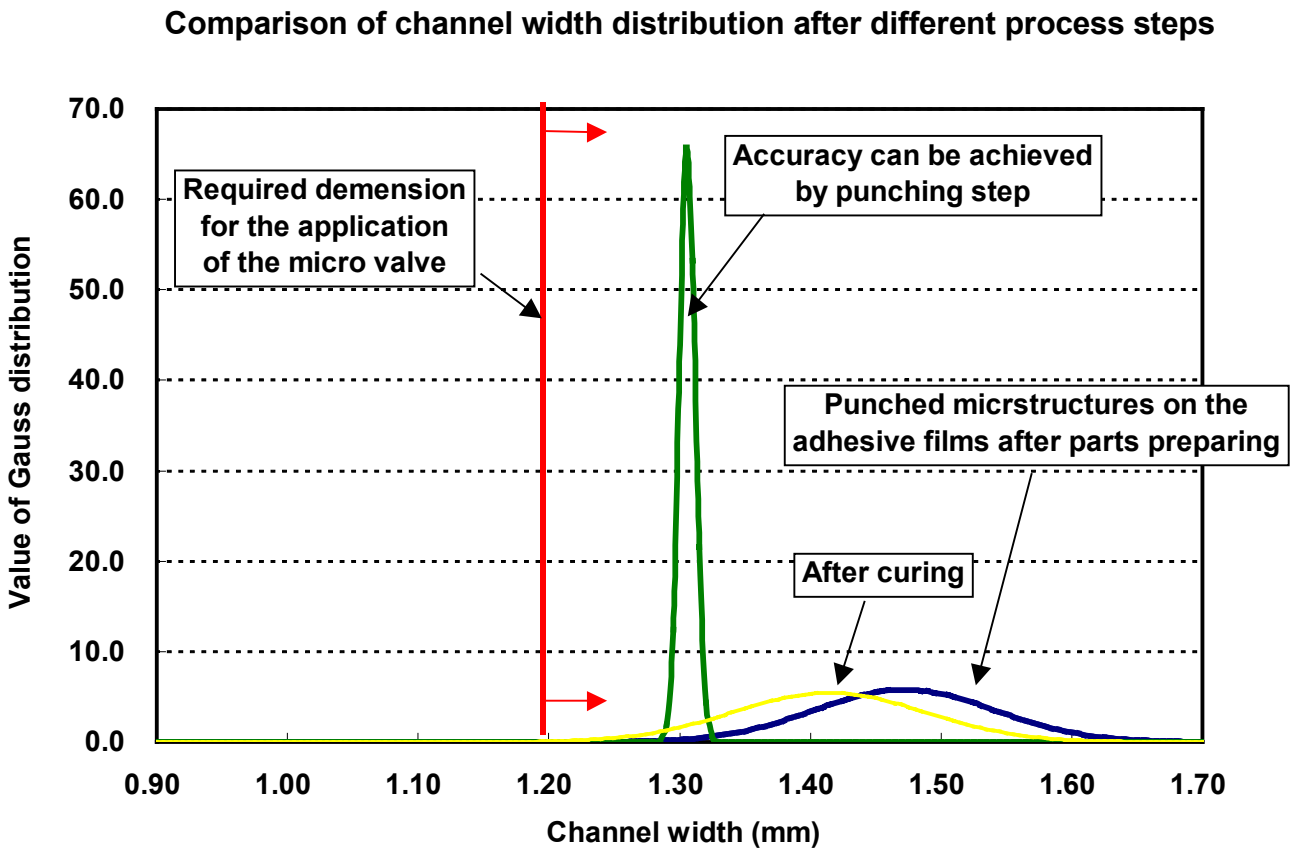


**Fig. 3.4.9 The Gauss distributions of the channels widths of the punched microstructures after different process steps**

After the curing process, the punched adhesive flows towards the inner side. The average deformation is 0.06 mm under the process parameters A3, B3, C3. The standard deviation is 0.005 mm. The yellow line was obtained by combining the values of the channel width distribution after parts preparing and the average deformation and its standard deviation through the curing process. Because the adhesive films flow toward the inner side without any exception, the average value was subtracted, while the standard deviations were added together.

The yellow line represents a typical final dimension distribution of the punched microstructures on the adhesive films after the deformation through the whole bonding process. For the application of the micro valves, the required dimension is larger than 1.20 mm that is needed to avoid the adhesive film affecting the micro channels formed by the metal layers. The micro channel was designed to be 1.0 mm wide.

With a compensation of the average deformation value, the variation of the microstructure dimension can be limited within a tolerance around the scale of the standard deviations. (See Fig. 3.4.9)

For future application, especially when the deformation of the punched microstructure is very critical to the function of the product, the improvement of the parts preparing specially in peeling off and joining steps should be more emphasized. A process environment with a temperature much lower than room temperature would let the adhesive film become more hard and solid [Sauer 00]. Therefore, the dimension can be controlled better, when the parts preparing can be processed at lower temperatures.

Besides, the exactly required dimensions for the function chambers / cavities of the micro components can be achieved by polymer housings that are equipped with a side wall around each cavity, as illustrated in figure 3.4.10. In this case, the adhesive film would not be a part of the microstructures of the product but only a bonding medium. The punched structure deformation on the adhesive film can be, therefore, not so critical and sensitive to the function of the components.

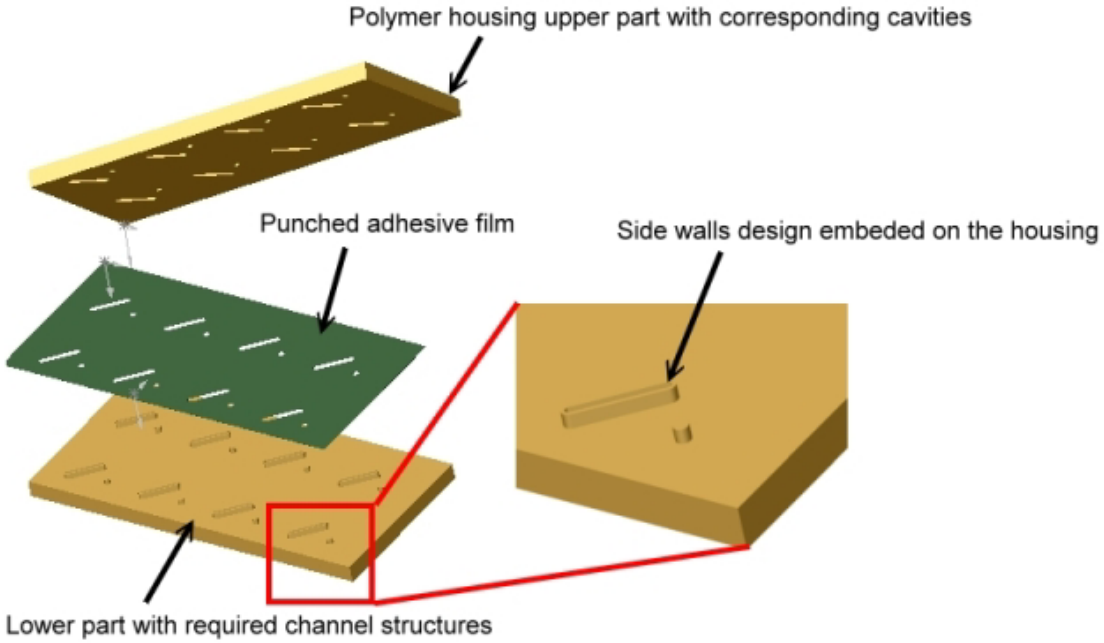


**Fig. 3.4.10 The exactly required dimensions for the function chambers / cavities of the micro components can be achieved by polymer housings that are equipped with a side wall around each cavity. In this case, the adhesive film would not be a part of the microstructures of the product but only a bonding medium. The punched structure deformation on the adhesive film can be, therefore, not so critical and sensitive to the function of the components.**

In addition, woven and fiber intensified adhesive films [3M] allow the films to be more solid at room temperature, further experiments using such adhesive films would be very interesting for structure sensitive applications.

### 3.5 Sealing test

**Water bath test (Nitrogen)**

To evaluate the sealing property of the bonded interface for nitrogen, a polymer plate with ball chamber structures was bonded with a cover plate using the punched adhesive film. (Fig 3.5.1) The cover has a hole in the center, which was connected with a standard fluidic connector. The whole test sample was merged in a water bath. Through the fluidic connector, nitrogen with a pressure of up to 300 kPa was injected. No air bubbles in the water bath were observed.

10 Pa vacuum was also connected with the sample in the water bath using the same way. No water drops were observed in the ball chamber.


**Fig 3.5.1 A polymer plate with a ball chamber structure was bonded with a cover plate using the punched adhesive film to evaluate the sealing property of the bonded interface. Nitrogen with a pressure of up to 300 kPa was supplied to the enclosed micro cavity; no air bubbles were observed in the water bath. A 10 Pa vacuum was also connected with the sample in the water bath in the same way; no water drops were observed in the ball chamber.**

**Methylene blue test (Water)**

The sealing properties of the bonded interface were tested with a solution of Methylene blue in water. The solution was injected into the flow channels cf. figure 3.5.2. When the blue colored medium stayed in the channel for less than one hour, the color could always be removed by injecting (flushing) cleaning water. However, when over 24 hours, the blue color residue was observed attaching to the punched edge of the adhesive film with a thickness of about 100 µm and was hard to be removed. Such contamination can be avoided by the sidewalls design illustrated in figure 3.3.10 for the future applications using such mediums for long time.

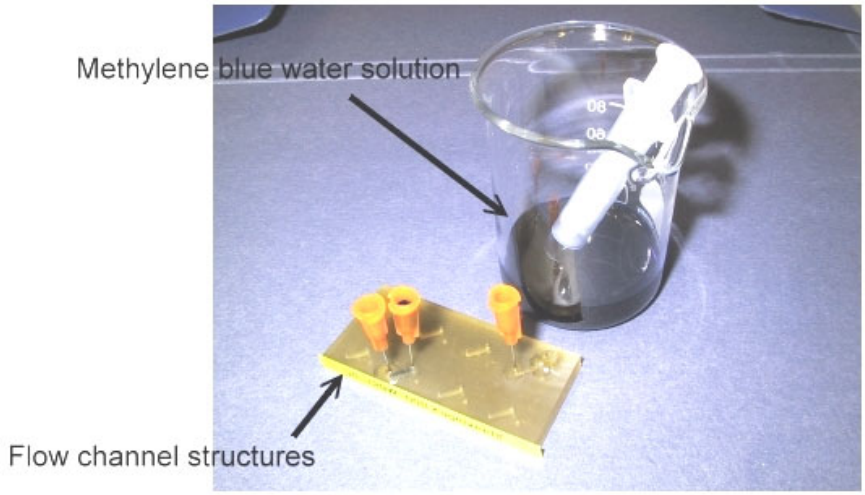


**Fig. 3.5.2 The sealing properties of the bonded interface for water solution was evaluated, a solution of Methylene blue in water was injected into the flow channel and stay for different long periods.**

## 3.6 Membrane bonding

For fabricating the AMANDA related products, a diaphragm has to be bonded with a polymer housing. To demonstrate the compatibility to the AMANDA process, the new bonding method was used to bond a 2 µm polyimide diaphragm by the membrane transfer technology (figure 3.6.1). For more information about the preparation of the membrane, please see section 1.1 in chapter 1.

Figure 3.6.2 shows an AMANDA pressure sensor membrane with strain gauge patterns made by photolithography bonded with a PSU housing. The PSU housing layer was not designed for patterns on the membrane, therefore, the strain gauge circuits didn't directly lie on the functional cavities.

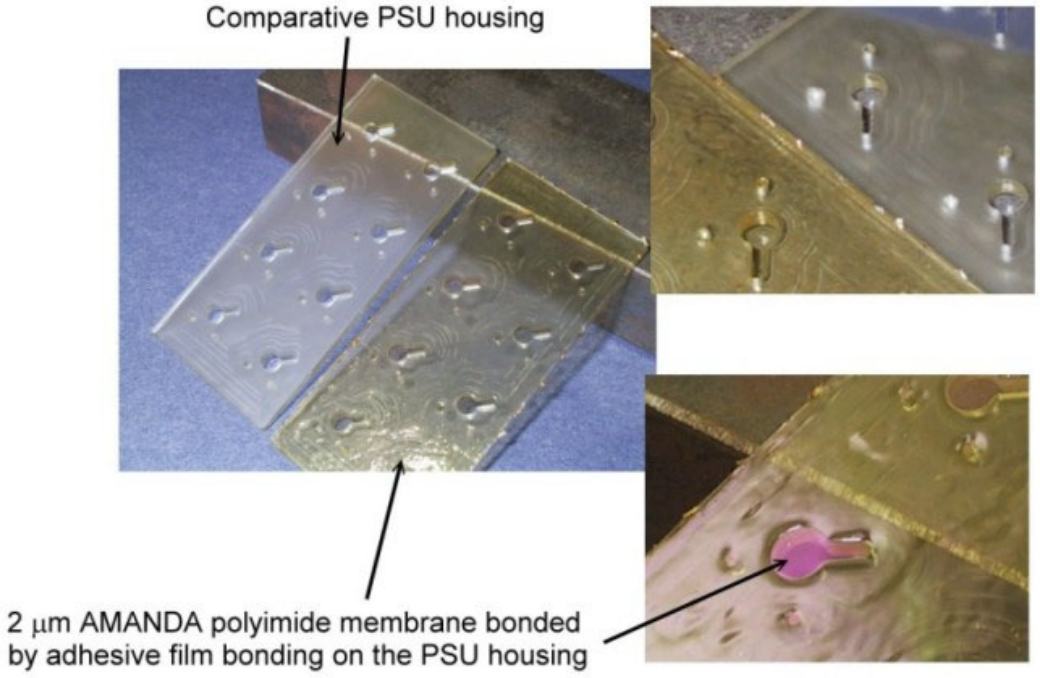


**Fig. 3.6.1 A 2 µm polyimide diaphragm made by the membrane transfer technology was bonded on the PSU housing by the new bonding method to demonstrate the compatibility with the AMANDA process.**

It is very easy and straightforward to bond such a membrane on the PSU housing be the new bonding method. The process steps are identical to the steps mentioned in section 3.2. The polyimide membranes can be separated directly from the silicon wafer before curing the adhesive films. The curing process can then be executed after the whole stack of different layers is assembled together, and therefore a multiple layer membrane module can be fabricated by this bonding method.

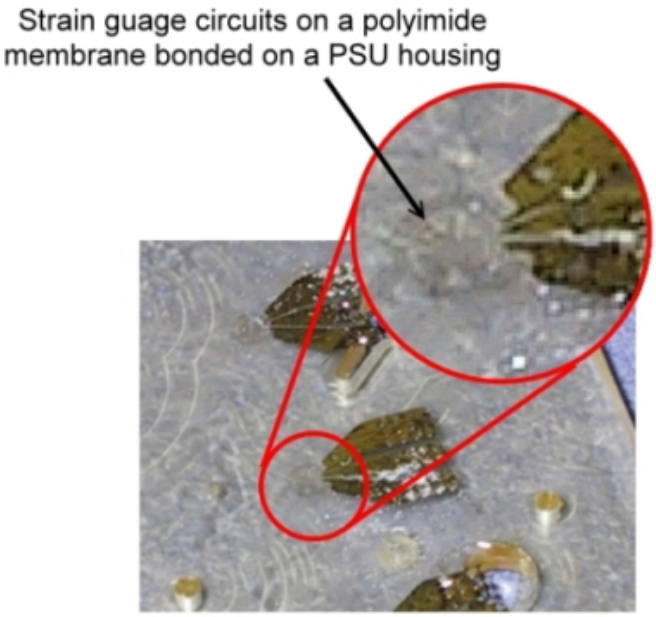


**Fig. 3.6.2 Pressure sensor strain gauge circuits on an AMANDA polyimide membrane bonded on a PSU housing by the adhesive film bonding process.**

## 3.7 Summary, discussion and conclusion

The adhesive film bonding was developed and demonstrated using the 3M VHB acrylate adhesive films with a thickness of 50 µm. The bonding strength was verified by tensile strength tests according to the standard process of DIN53288. The process parameters were optimized using the Taguchi method. With optimized process parameters, the bonding force can be larger than 600 kPa.

The achievable accuracy of the punching process was investigated by a statistical way using PSU films as punching medium. The standard deviation of the measured results on the punched microstructures was 6 µm. Larger deformation could occur during punching of the elastic adhesive films, however, this could not be investigated separately, because of the formation of burrs in the protection papers.

Microstructures deformation of the punched adhesive film through the whole parts preparing steps (punching, peeling off and joining) was investigated in a statistical way. A standard deviation of about 70 µm was measured.

Microstructures deformation of the punched adhesive film by curing was also analyzed using the Taguchi method under different process parameters. With the process parameters obtained for the maximum bonding strength, A3, B3, C3, a standard deviation of about 5 µm was measured.

For future applications, the design of microstructures could be corrected for the average deformation. The correction would be limited to the standard deviation. If a higher accuracy is required, the parts preparing steps should be improved, because these steps appear to show the most influence on dimensions.

The assembling and bonding process is usually the most costly process in microsystem field. Large manual expenditure and low efficiency in the packaging process are usually the crucial bottlenecks in production. The adhesive film bonding method is a straightforward process. It is very suitable for automation and mass production of microsystems in industry. This allows large reduction of cost, time and work.

The bonding process can be a good alternative to the existing adhesive bonding processes. Multiple layers with different materials can be bonded together in one step. Opaque material can also be applied by this bonding method. Three-dimensional structures can be easily built up by piling up multiple layers. More than 300 different kinds of adhesive films are available on the market for different kinds of application. Some adhesive films offer high bonding force, high temperature endurance or other properties in chemical or physical resistance.

### 3.8 SWOT* analysis of the adhesive film bonding process

| **Strengths** | **Weakness** |
|---|---|
| ● An easy and straightforward process.<br>● Easy automation.<br>● No optical alignment is necessary<br>● Multiple layers bonding possible<br>● Different materials can be bonded together.<br>● Opaque material is applicable.<br>● More than 300 different kinds of adhesive films are available on the market.<br>● AMANDA compatible. | ● Long time to design and fabricate a puncher with proper microstructure patterns.<br>● The minimum dimension of the microstructures on the adhesive films is limited by the fabrication method of the puncher. The minimum lateral dimension until now is 300 µm. |
| **Opportunities** | **Threats** |
| ● 3 dimensional microstructures can be easily built up. This allows expanding the micro system design possibilities.<br>● Expand usable material spectrum for micro systems.<br>● Mass production and automation.<br>● AMANDA products can be fabricated by this way in volume production in industry.<br>● Suitable for polymer microsystem bonding and packaging. | ● For some applications, adhesive is not desired. Some adhesives would contaminate the testing sample mediums. This can be improved by using extra preservation walls and properly selections of adhesive films. This threat is characteristic of any existing adhesive bonding processes. |

* SWOT is an abbreviation of **S**trength, **W**eakness, **O**pportunities and **T**hreats.

## 3.9 Remarks:

Some terminologies in the statistics and the Taguchi method used in this chapter are quoted and summarized here [Roy01]. More information can be found in the references [Tagu87].

**Normal Distribution / Gauss Distribution:** The normal distribution is a mathematical definition of a curve that simulates the shape of the bell-shaped histogram of a population of data. The normal distribution curve for a population can be completely defined and plotted by knowing the average and standard deviation of a representative sample of data from the population. Although the true nature of distribution is never known until an entire population is tested, the normal distribution allows a logical simulation of the distribution expected. The term *Distribution* refers to the normal distribution curve that is defined in terms of two quantities: standard deviation ($\sigma$) and average; often, the term refers to these two quantities: the location of the average, which shows the distribution curve is with respect to the target (when the target is present), and the standard deviation ($\sigma$), which indicates how narrow the distribution is. The property of the normal distribution is such that 99.7% of the area under the curve is bounded by the (average – 3$\sigma$) and (average + 3$\sigma$) lines.

**Mean-Squared Deviation (MSD):** The mean-squared deviation is a number (no unit) representing the average deviation of the results from the target (or the average, when the target is absent) and is strictly a function of average and the standard deviation. It is independent of the specification limits. *For comparison purposes, a set of data with a lower MSD is preferable.*

**MSD for a *"nominal is best"* property:** For this type of data, there is a nominal (i.e., target / desired) value. For a general definition of the MSD, assume that the sample readings are expressed by using $y_1$, $y_2$, …and so on, and that the target value is represented by T and the number of samples by n. Then

$$MSD = \frac{1}{n}[(y_1 - T)^2 + (y_2 - T)^2 + ... + (y_n - T)^2]$$

**MSD for a *"smaller is better"* property:** For this type of data, the smaller magnitude of data is considered preferable. It is equivalent to the target being zero. Therefore,

$$MSD = \frac{1}{n}[(y_1)^2 + (y_2)^2 + ... + (y_n)^2]$$

**MSD for a *"larger is better"* property:** For this type of data, larger values among the measured values are more desirable. As many measurements in science and technologies have well-established connotation, the word *deviation* has always been used for something we want as small as possible. In other words, the deviation or mean of deviation carries the sense of "smaller is better". To maintain this sense of desirability while using the MSD for this type of data, it is calculated by adding the squares of the inverse of the individual results. The expression for MSD in this case is:

$$MSD = \frac{1}{n}[(\frac{1}{y_1})^2 + (\frac{1}{y_2})^2 + ... + (\frac{1}{y_n})^2]$$

**Signal Noise Ratio (SN):** There are several expressions for SN ratios. The one used in the Taguchi method is a logarithmic transformation of MSD. In other words, the SN is the same as the MSD of the data set plotted in a log scale with a ***–10*** multiplier. The negative multiplier changes the desirability from "*smaller is better"* for MSD to "*larger is better"* for the SN ratio. Naturally, the SN ratio is independent of the specification limits.

**L9 Table:** Taguchi method uses specially arranged orthogonal array for designs of experiment method. L9 Table is one of the orthogonal arrays used in the Taguchi method. It can be used for up to 4 three-level experiments factors. Other commonly used orthogonal arrays for the Taguchi method is listed in the table 3.r.1. The arrangement of the L9 table was listed in the table 3.3.2. The arrangement of other arrays can be found in the reference [Tagu87].

**Table 3.r.1 Most commonly used orthogonal arrays for the Taguchi method**

| Arrays | Intended use (experiments with:) | Notation | Category |
|---|---|---|---|
| L4 | up to 3 two-level factors | $2^3$ | Two level arrays |
| L8 | up to 7 two-level factors | $2^7$ | |
| L12 | up to 11 two-level factors | $2^{11}$ | |
| L16 | up to 15 two-level factors | $2^{15}$ | |
| L32 | up to 31 two-level factors | $2^{31}$ | |
| L9 | up to 4 three-level factors | $3^4$ | Three level arrays |
| L18 | up to 1 two-level and 7 three-level factors | $(2^1, 3^7)$ | |
| L27 | up to 13 three-level factors | $3^{13}$ | |
| L16 (modified) | up to 5 four-level factors | $4^5$ | Four level arrays |
| L32 (modified) | up to1 two-level and 9 four level factors | $(2^1, 4^9)$ | |

# 4 The fabrication of the valves

The micro ball valves were fabricated in batch out of three polymer layers, three metal layers, and five punched adhesive film layers as illustrated in the figure 4.0.1. This chapter describes how each component was fabricated and/or selected.

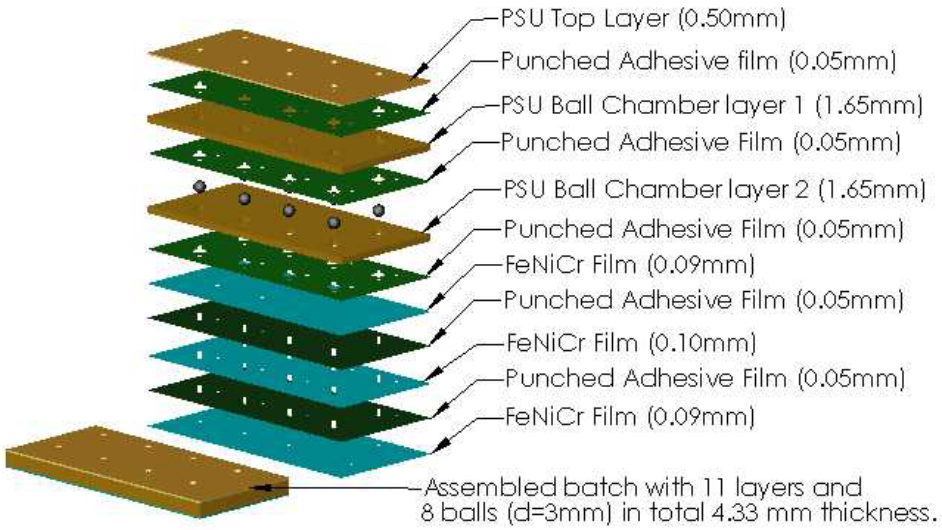


**Fig.4.0.1. The micro ball valves were fabricated in batch with three polymer layers, three metal layers, and five punched adhesive film layers. Eleven layers were bonded together using the adhesive film bonding process in one step.**

## 4.1 Overall considerations

### Alignment

To bond 11 layers together in one step, alignment is a crucial key point. Traditional alignment through an optical microscope would be too difficult in this case. Embedded alignment pins and holes have to be designed in each layer (figure 4.2.1 ~ 4.5.3). A tolerance of 25 μm was used for alignment in each layer. Combining with the consideration of shrinkage effect of polymer mentioned below, an easy assembly way was successfully realized.

### Shrinkage effect

The shrinkage effect of hot embossed polymers is another crucial point for multilayer alignment. Because demolding is performed at a higher temperature, the housings will shrink when they are cooled down to room temperature. The hot embossing mold has to be constructed larger than the dimension of the polymer housings needed for the micro valve design. The shrinkage correction factor is a function of the material used and the parameters of

the hot-embossing process. A factor of 0.9976 was selected in our PSU housings. It showed excellent results.

### Material

To withstand the heating up from the magnetic coil during operation, PSU was chosen for the polymer layers, which has a glass transition temperature of more than 190 °C and a long-term service temperature of 160°C [Lipp03]. The adhesive film was also selected based on this consideration. It resists temperatures of up to 150 °C for long time operation and up to 260 °C for a short time [3M96]. More information about the properties of the adhesive film used was given in chapter 3. The FeNiCr material was chosen for the three metal layers because of its soft ferromagnetic properties. It was attempted here to reduce the electric current needed during valve operation.

### Punching vs. Laser structuring

In this work, we demonstrated the mass production manufacturing method through a punching process for adhesive film as well as the rapid prototyping method through laser structuring of the metal layers.

Rapid-prototyping such as laser structuring, direct milling of the polymer housings...etc, are suitable to be applied in the phase of product development to shorten development time and to let the product design stay flexible. The patterns on the metal layers can also be fabricated massively by a punching process as it is done with the adhesive films.

Mass production processes such as molding, punching...etc, are more efficient and cost saving in the fabrication. However, it needs more time to fabricate proper tools or molds. These methods are, therefore, suitable to be applied when the constructions are verified and the products are planned to be fabricated in volume.

### Outsourcing

The iron balls and the magnetic coils were bought from a company. This means that we used the advantages and merits of the parts supply companies; used their mass production capabilities and their process optimizations to get low cost, mass producible, market standard elements to build up our high value-added products and minimize the unnecessary expensive production steps which will lead to the reduction of investment threshold of our potential industry partners.

## 4.2 Adhesive films and puncher

For the micro ball valves, two kinds of patterns of adhesive films were needed (Figure 4.2.1). The first one was used to bond the top layer, ball chamber layers and the first metal layer. The second was used to bond the metal layers that formed the three dimensional micro flow

channels. The total assembly of 11 layers was bonded together using the adhesive film bonding process described in the chapter 3 in a batch of 8 micro valves (Figure 4.0.1).

To demonstrate the mass production ability of the new bonding method, a puncher was designed and fabricated. The critical lateral dimensions were fabricated by wire electric discharge machining (EDM) by SISTA Werkzeugbau GmbH. To lower the cost and fabrication time, the punchers and the corresponding matrixes were designed to be exchangeable. Different kinds of microstructure patterns can be punched by one puncher system with the embedded alignment functions. Alignment accuracy between different cutters / matrixes by exchange is less than 10 µm (Figure 4.2.2).

Because the punching process can be easily executed within one second, mass production ability for adhesive films was successfully demonstrated in the laboratory.

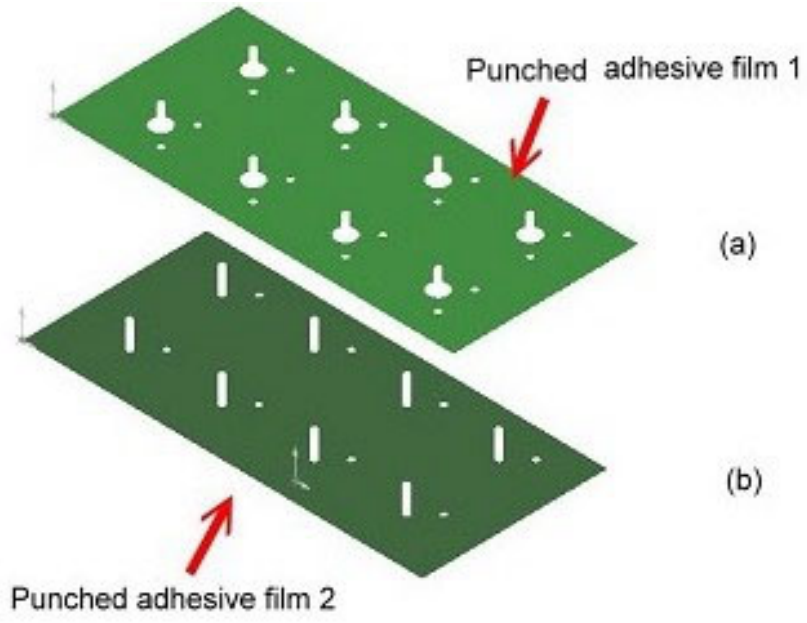


**Fig. 4.2.1: Two kinds of adhesive film patterns needed for the production of micro ball valves. Pattern (a) is for the ball chamber layers. Pattern (b) is for the micro flow channel layers. Alignment holes were embedded in each adhesive film layer. No optical alignment was needed during the assembly process.**

A proper compensation / correction of the patterns on the adhesive film has to be considered in the construction phase. In our case, because there were no design rules that could be used, an estimated value of 100 µm larger at each side than the corresponding pattern on the other layers (PSU and metal) was used. Pattern deformation through each process step was investigated in statistical way in chapter 3, after the puncher was developed.

Because long cycle time is needed to design and fabricate such a puncher, for future product developments, laser structuring should be used to pattern the required adhesive films at first during the products development and design phase as mentioned in section 4.4 for metal

layers. After the designs are verified, the punch process can then be applied to accelerate the production time and lower the production cost.

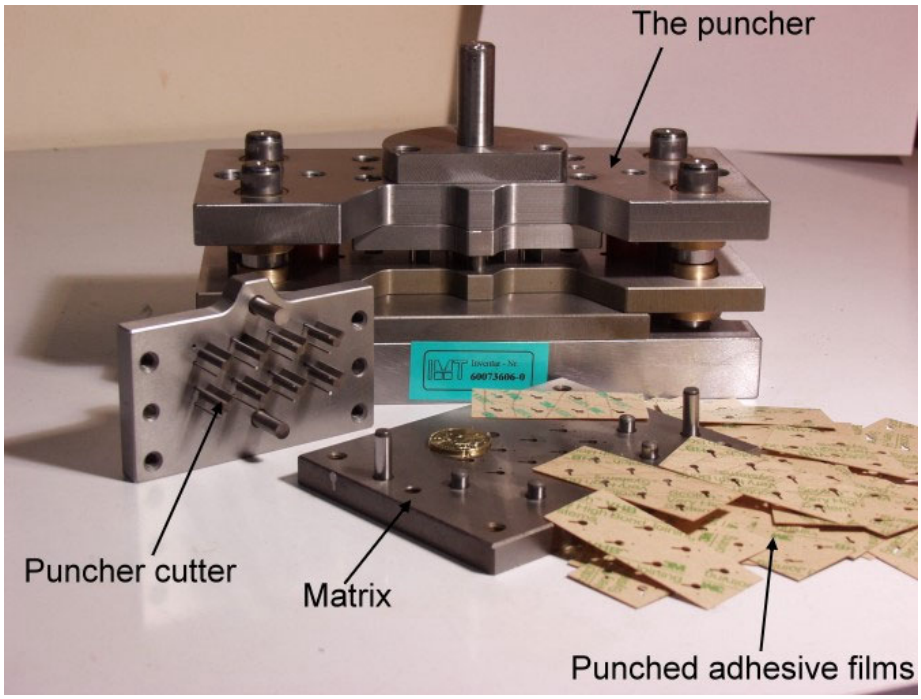


**Fig. 4.2.2: The puncher and the punched adhesive films. The critical dimensions were fabricated by WEDM (wire electric discharge machining). The smallest possible dimensions may reach up to 300 µm. Positioning pins were also embedded to facilitate both the punch process itself and the assembly process with other layers.**

## 4.3 The PSU housings

### 4.3.1 Fabrication of the molds

Mechanical milling process was selected to fabricate hot embossing molds for the three polymer layers of the micro ball valve.

**The top layer**

Miniaturized milling tools made from tungsten carbide with a diameter of 0.3 mm supplied by HAM Werkzeughandlung GmbH were used to fabricate the top layer mold by a CNC machine in our institute (Figure 4.3.1.1).

The most important dimension in this mold was the contour shape of the valve seat 2 pillars, because the valve seat holes in the top layer were produced by them. An un-rounded pillar would lead to a shape inconsistency between the balls and the valve seats resulting in leakage of the micro valves (Figure 4.3.1.2).

The diameter of the pillars was 300 µm. Tool diameter compensations and path modifications (TDCAPM) were used to improve the shape of the pillars. Figure 4.3.1.2 shows a comparison of the fabricated valve seat pillars before and after the TDCAPM. The tool paths near to the critical structures were modified in the CNC coding with fine multi-steps around the structures. The accuracy of the shape of the pillars was improved in this way. The leakage of the ball valve was much better after this modification.

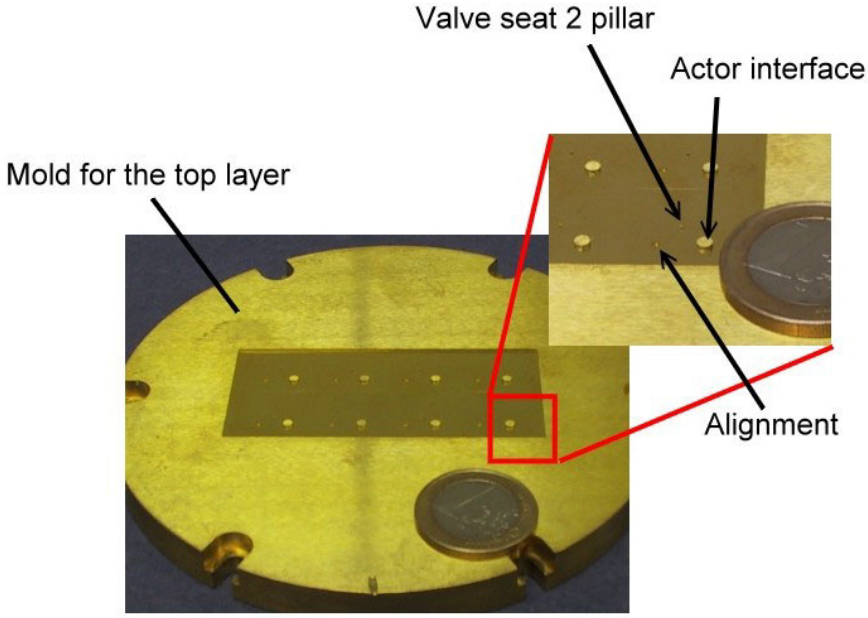


**Fig. 4.3.1.1 A hot embossing mold for the top layer of the micro ball valve was fabricated by CNC micro milling with tools made of tungsten carbide. The critical lateral dimensions were the valve seat 2 pillars with a diameter of 300 µm.**

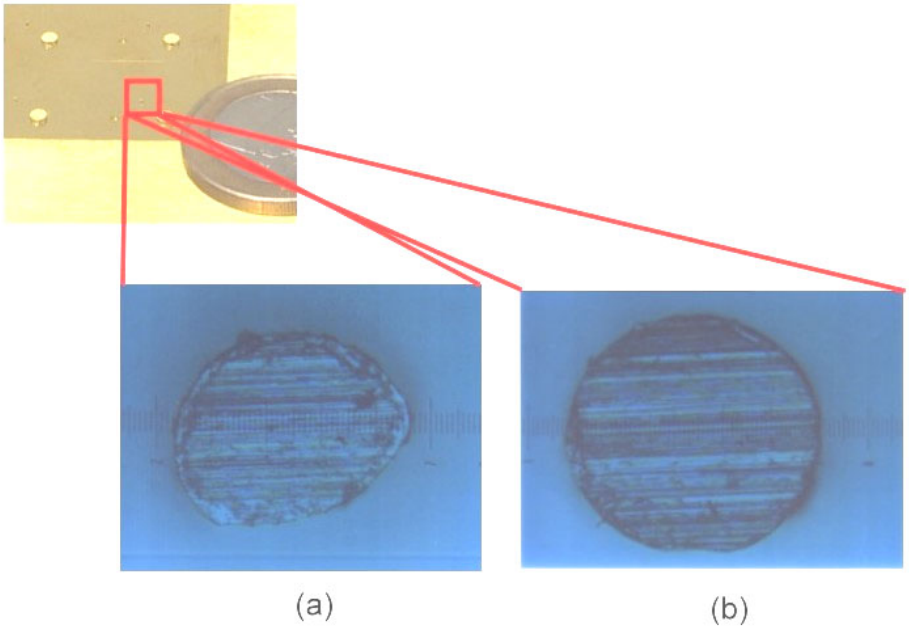


**Fig. 4.3.1.2 Pillars for the valve seat 2 with a diameter of 300 µm. Tool diameter compensations and path modifications (TDCAPM) were used to improve the contour accuracy of the pillars. (a) Before TDCAMP. (b) After TDCAMP.**

### The ball chamber layers

The technical critical point of this mold was the high thickness. The standard thickness of polymer layers processed in the institute is usually less than 1.0 mm. The required thickness of the ball chamber layer for the micro valves was 3.20 mm. The thicker the layer thickness is, the larger is the de-molding force of the hot-embossing process. To reduce the de-molding force induced from the mold, the ball chamber layer was separated into two parts with a thickness of 1.60 mm each (figure 4.3.1.3 and 4.3.1.4).

CNC milling using tools made from tungsten carbide in the institute were used at first to fabricate the mold. The surface roughness obtained was $R_a$ = 350 nm. The experiments showed that such surface roughness led to extremely large demolding forces and the polymer samples were torn through the large shearing forces between the mold and the polymer (figure 4.3.2.3).

Ultra diamond milling was then used to fabricate the mold of the ball chamber layers by I-sys GmbH. The tools used were made from diamond with a diameter of 300 µm, 2 ° cone angle, and 1.35 mm in length, which were supplied by the company Medidia GmbH. The obtained surface roughness of $R_a$ = 200 nm was measured. With this mold, smaller demolding forces were achieved. The housings were successfully demolded without any damage (Figure 4.3.1.4).

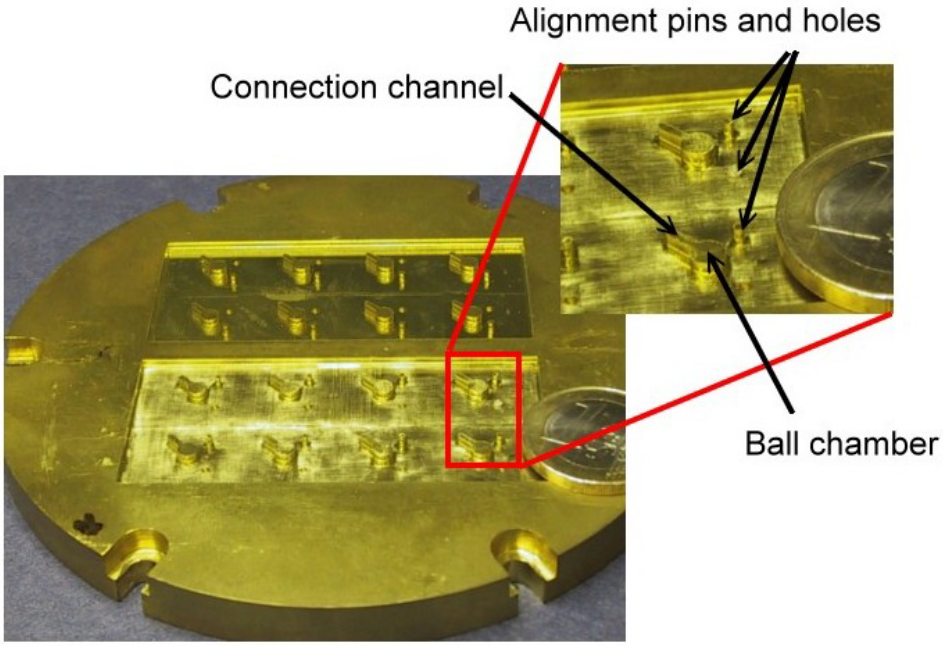


**Fig. 4.3.1.3 A mold for the ball chamber layers fabricated by a precision CNC machine using miniature-milling tools from tungsten carbide. The layer was separated into two parts with a thickness of 1.60 mm each. The obtained surface roughness of this mold was about $R_a$ = 350nm.**

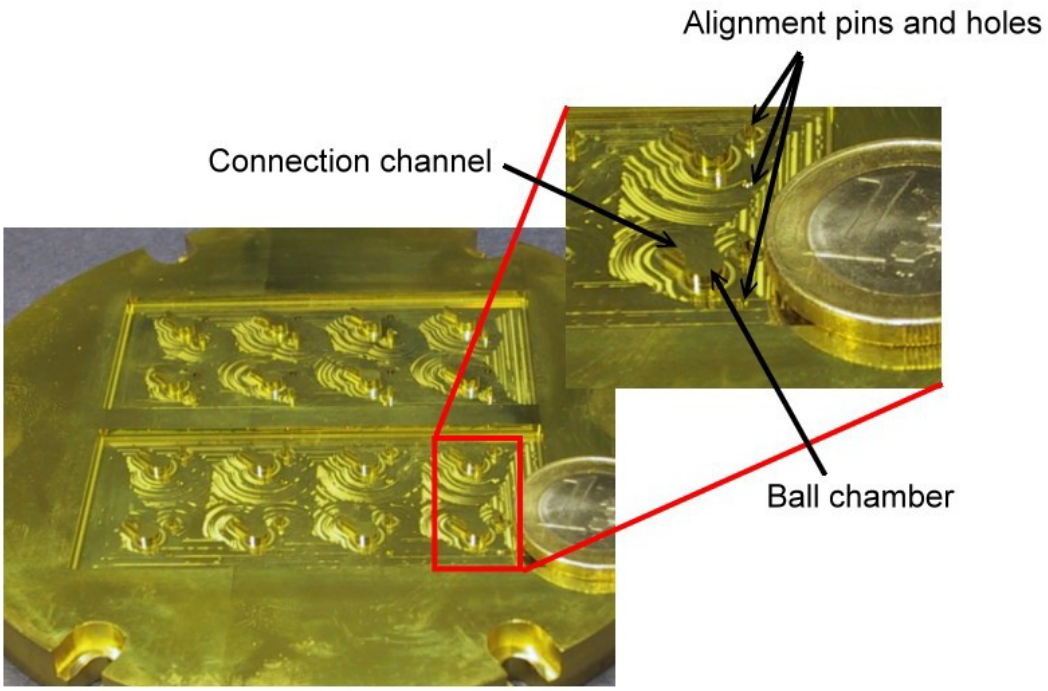


**Fig. 4.3.1.4 A mold for the ball chamber layers fabricated by ultra diamond milling (I-sys GmbH). The obtained surface roughness is $R_a$ = 200 nm.**

### 4.3.2 Hot embossing

**The top layer**

A stack of two PSU films with a thickness of 380 µm was used as the raw material for the top layer in the hot-embossing process. The process took about 25 minutes using the hot-embossing machine WUM1. Figure 4.3.2.1 shows the molded PSU top layer. The minimum lateral dimensions were the valve seats with a diameter of 300 µm.

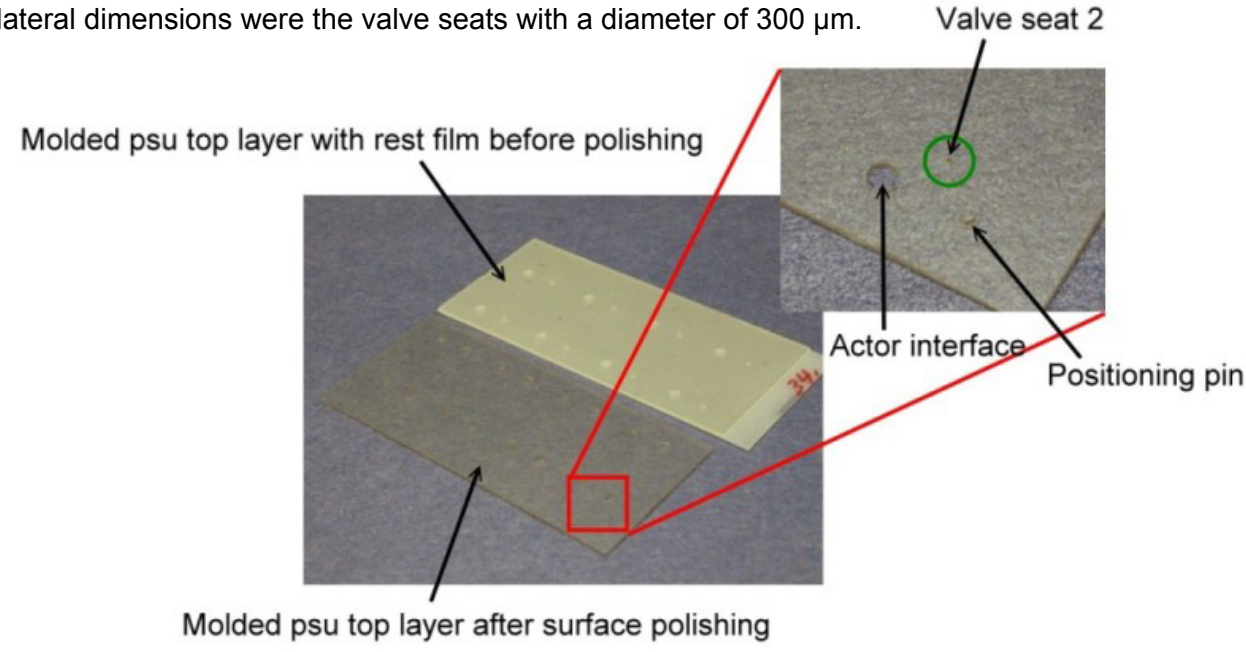


**Fig. 4.3.2.1 Molded PSU top layers with a thickness of 0.5mm (after the molding process). The picture shows one before surface polishing and one after.**

**The ball chamber layers & thick layer demolding**

Although the ball chamber layers were separated into two parts with a thickness of 1.6 mm each, the demolding was still the most critical step. Extremely high frictions between the molded polymer housing and the brass mold were observed. Molded polymer housings were torn very easily during the demolding step (Figure 4.3.2.2).

The thermal expansion coefficient of PSU is much larger than that of brass, the mold material. Lower demolding temperature will result in larger demolding force, because the shrinkage of the polymer will be larger and hold the mold. Higher demolding temperatures, however, would let the polymer remain still too soft to withstand the mechanical tearing forces during the demolding. Demolding temperatures of 180 ℃ were evaluated to be suitable in this case.

In order to avoid damaging on the subtle housing structures, multiple steps demolding was used. Several individual steps with smaller forces *gently and gradually* pulled the molded polymer housing from the brass mold (Figure 4.3.2.3).

In addition, in order to ensure that the molded housings always stay on the counter plate during the demolding phase, a very high adhesion between the polymer and the counter plate was required. The counter plate was lapped at first and trenched with four line-shaped small structures by wire EDM process (Figure 4.3.2.4). During hot embossing, the melted polymer flowed into the trenches, after re-solidification, the resulted burrs induced a very large adhesion force during the demolding phase. The housings were then successfully de-molded (Figure 4.2.3.5).

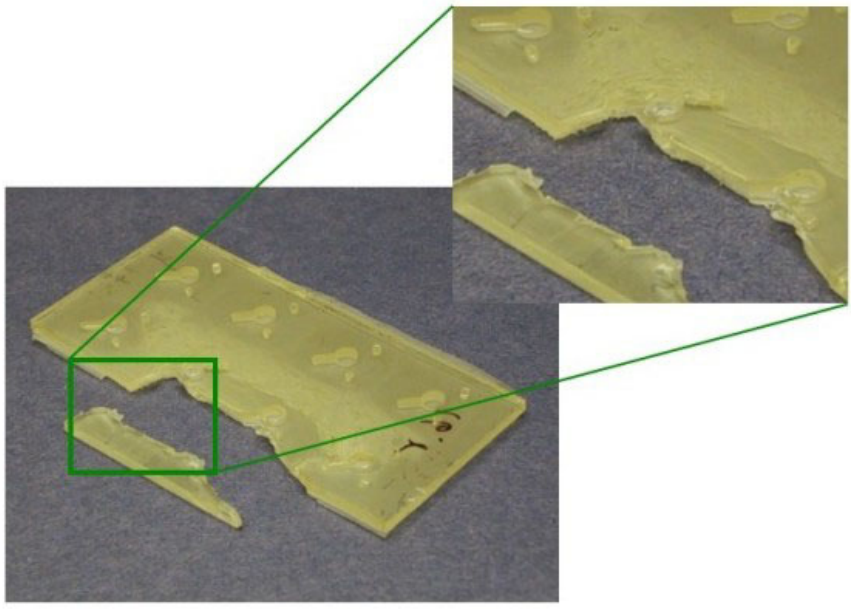

**Fig. 4.3.2.2 Damaged hot-embossed ball chamber layer due to large demolding / tearing forces.**

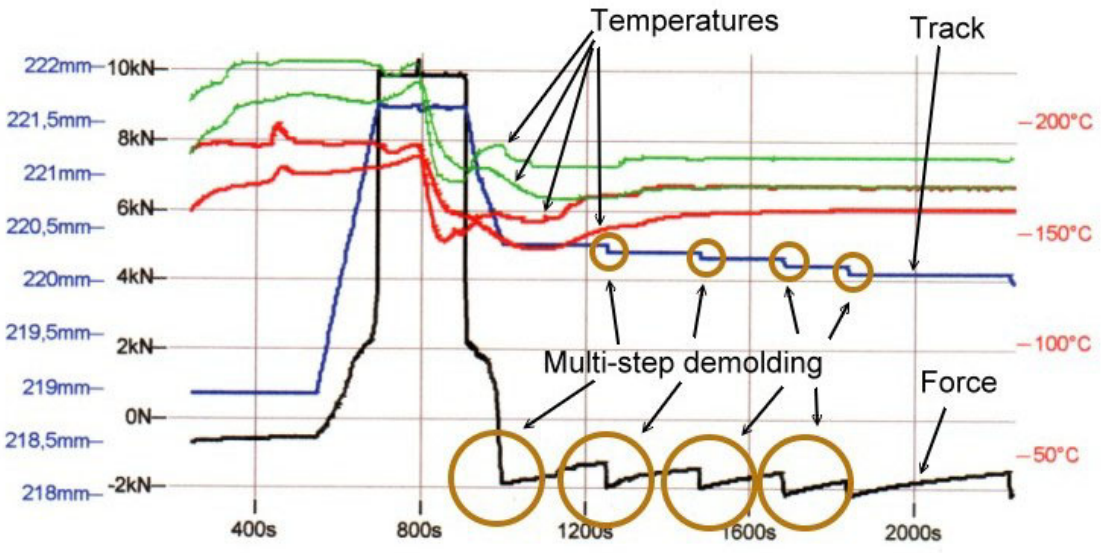


**Fig. 4.3.2.3 The process profiles for molding and de-molding of the ball chamber layers. Multiple steps demolding method was applied to pull the molded polymer housing from the mold *gently and gradually*. The force used in each step was 700N.**

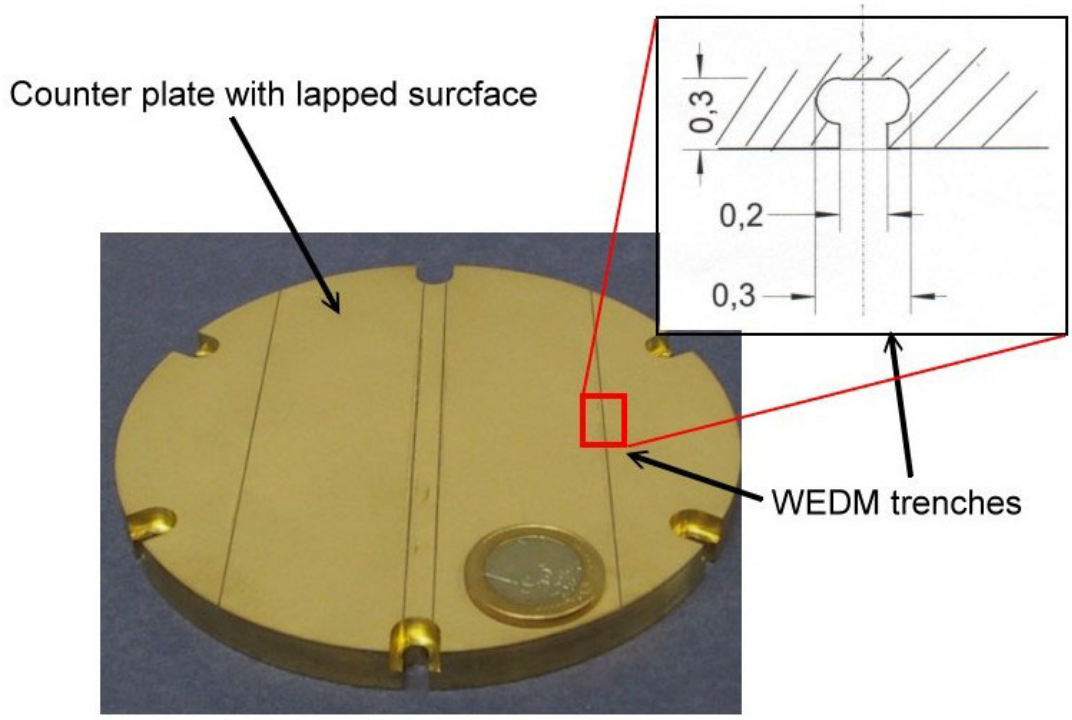


**Fig. 4.3.2.4 The lapped counter plate with wire EDM trenches used in the hot-embossing process for the ball chamber layers.**

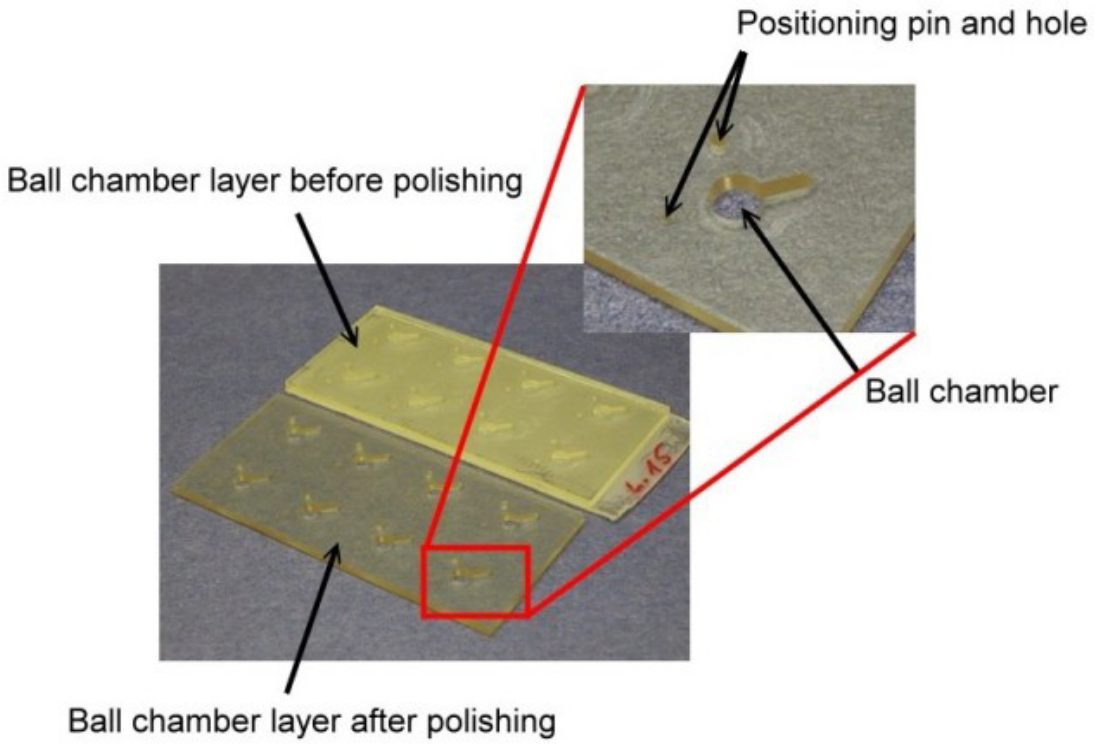


**Fig. 4.3.2.5 Molded PSU ball chamber layers with a thickness of 1.60 mm. The picture shows one before surface polishing and one after.**

### 4.3.3 Chamber height modification

Because the induced magnetic force is inverse square proportional to the distance between the iron ball and the coil, the function of the micro ball valves is very sensitive to the height of the ball chamber layers. A diamond tool, as shown in the figure 4.3.3.1, was needed to remove and trim the rest layer and to obtain the accurate height of the molded polymer housings. The machine comprises a diamond tool holder that is fixed on a rotational axis. A z-directional axis can move very accurately. Combining with a y- directional table, the molded polymer housing can be polished and trimmed step by step. The achievable accuracy in the z-direction is 5 μm. A vacuum fixture gadget was designed on the y-directional table, which can hold polymer housing during the polishing / trimming process.

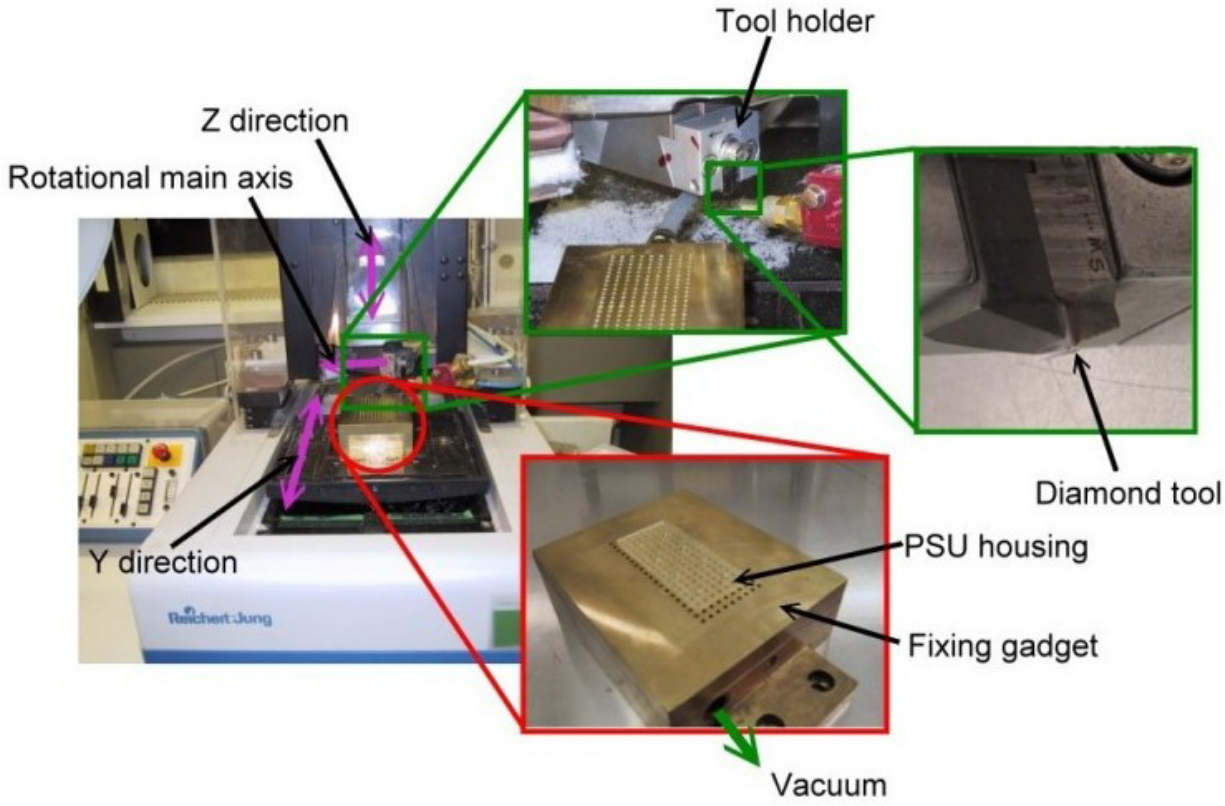


**Fig. 4.3.3.1 Polymer housing trimming and polishing machine using diamond tools.**

## 4.4 The metal layers

Metal layers were fabricated by a 20-Watt Nd: YAG Laser with wavelength 1067 nm (figure 4.4.1). Microstructure patterns were structured by moving the X-Y table through the laser beam with a cone shape. The achievable microstructures accuracy depended on the resolutions of the axes on the X-Y table and the thickness of the working samples. The tracking resolution of each axis on this machine was ±10 μm. In our case, ± 20 μm accuracy for the three metal layers with a thickness of 100 μm was achieved. The critical lateral dimensions required of the metal layers were the valve seats 1 with a diameter of 300 μm. An accuracy of ± 20 μm was, therefore, sufficient.

The 3-dimensional micro flow channel was built by the three differently patterned metal layers. As mentioned before, alignment holes were also embedded in each metal layer. Combining with the alignment functions on the polymer housings and the punched adhesive films, the easy assembly way has been realized. (Figure 4.4.2)

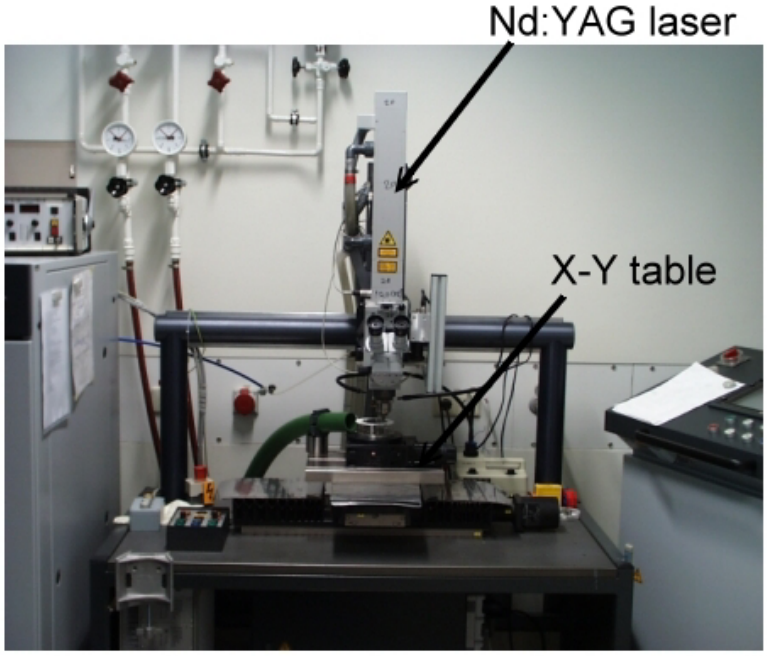


**Fig. 4.4.1** **The 20-W Nd-YAG laser with a wavelength of 1067 nm was used to fabricate the three micro ball valve metal layers. The achievable microstructure accuracy depends on the tracking resolution of the X-Y table and the thickness of the working samples. Here, the resolution of each axis was ±10 um. In our case, the accuracy of ±20 µm for FeNiCr layers with a thickness of 100 µm was achieved.**

### 4.5 The bought components

Iron balls were bought from the company Britannia Waelzlager & Industrietechnik GmbH for 1.56 € per 100 pieces (Figure 4.6.1). The magnetic coils were supplied by the company Era Electronik GmbH as test samples provided without any charge.

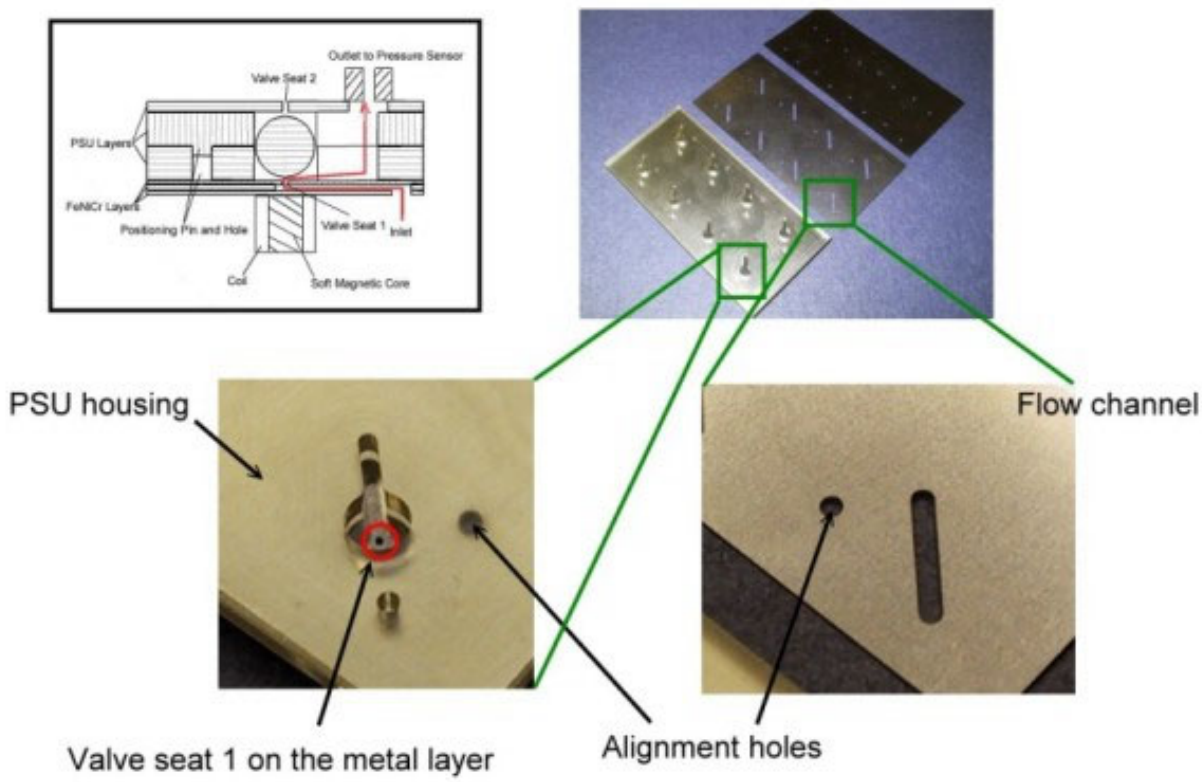


**Fig. 4.4.2** **Three laser-structured FeNiCr layers forms the 3-D flow channels. The critical dimensions of these layers were the valve seats 1 with a diameter of 300 µm. All layers were assembled using alignment holes. Figure 2.4.4 is repeated here to show the 3-D flow channel structures.**

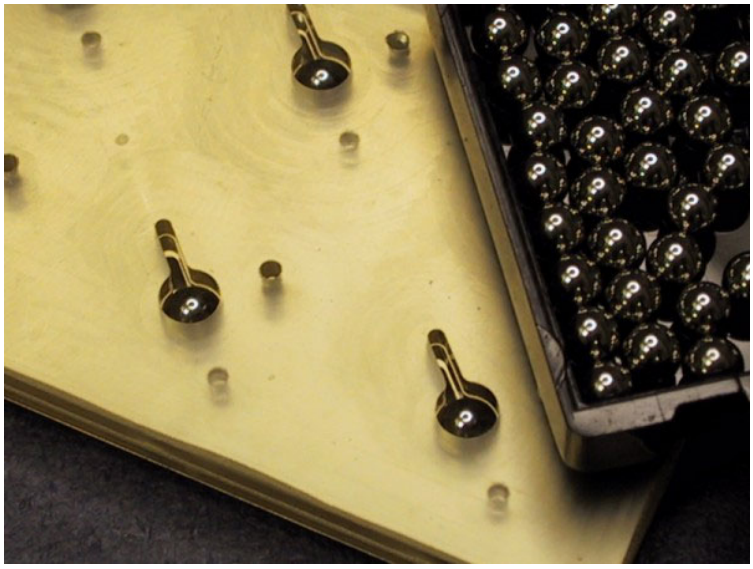

**Fig. 4.5.1** **Iron balls with a diameter of 3 mm on the assembled PSU ball chamber layers, which were bought from the company Britannia Waelzlager & Industrietechnik GmbH.**

### 4.6 The fabricated valves

Eleven layers, three PSU housings, three FeNiCr, and five punched adhesive films, and the iron balls were put together and bonded using the bonding process described in chapter 3 in one step in one hour. The production process appears to be suitable for a series production. After dicing, micro ball valves with a dimension of 10*10*4.33 $mm^3$ were produced (Figure 4.6.1). The characteristics of the micro ball valves are described in the next chapter.

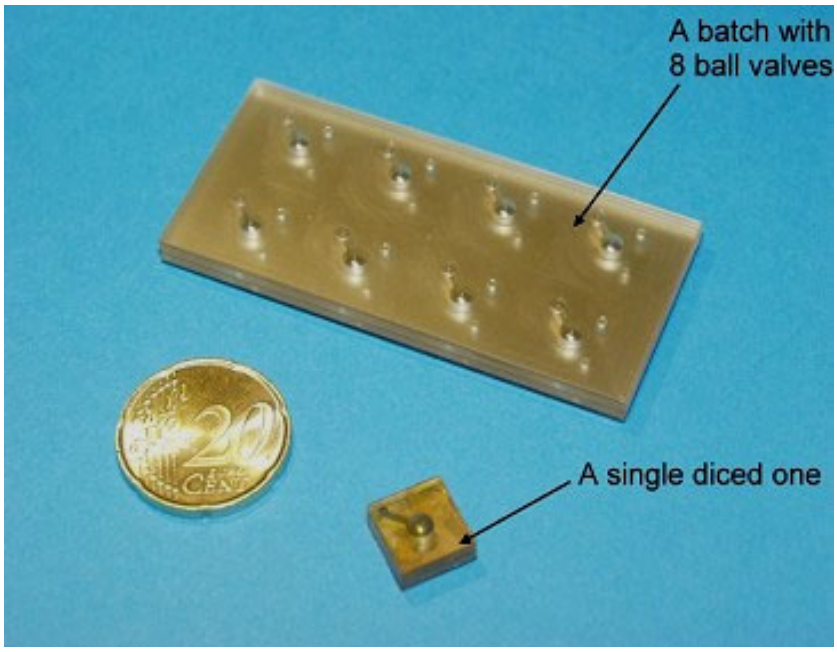


**Fig. 4.6.1: A fabricated batch of eight micro ball valves and a single diced one (outer dimensions are 10*10*4.33 $mm^3$) compared with a European 20 cent coin. (The coin diameter is 22 mm.)**

### 4.7 Summary

The multilayer adhesive film bonding process was successfully used to fabricate the micro valves in batch. Three PSU housings and three FeNiCr layers were bonded together to construct the necessary valve seats, ball chambers and 3-D flow channels of the valve.

Alignment pins and holes system was embedded in each layer. A tolerance of 25 µm at each side was proven to be suitable.

Micro mechanical milling was successfully employed to produce the molds needed as usual for AMANDA products.

The brass mold for the ball chamber layer was separated into two parts to reduce the demolding force during the hot-embossing process.

For molding of the 1.6 mm thick housings ultra diamond milling of the mold turned out to be necessary to get a better surface roughness and to reduce the induced demolding force.

With the aids of a lapped counter plate and a multi-step demolding process the thick ball chamber layers were successfully demolded.

Laser cutting technology was selected to pattern FeNiCr layers demonstrating the rapid prototyping production. The achievable accuracy was ±20 µm for the metal layers with a thickness of around 100 µm.

The following chapter describes the detailed characteristics of the fabricated micro ball valves.

# 5 Characteristics of the Valve

This chapter reports the characteristics of the valve. The valve can operate in two modes. One is the on-off switching mode and the other is the proportional mode. In the on-off switching mode, the valve switches the outlet pressure at two different levels. The maximum switchable differential pressure of this valve is 200 kPa. The switch frequency was up to 30 Hz. In the proportional mode, the outlet pressure can be regulated by controlling the ball position. The magnetic force of the coil balances the forces of the flow and the weight of the ball. In this mode, the valve can operate continuously in a range between 0 to 110 kPa, when the input pressure is 200 kPa. Inclination effects are also investigated in this chapter. The valve was found to be suitable for use at the different inclination angles. The average ratio of leakage to the flow through the open valve was measured. It was approximately 0.27%. The measurement results were also published in the reference [Fu03].

## 5.1 On-Off switching mode

### Mechanism

The magnetic coil with a soft magnetic core drives the micro ball valve. When no power is supplied to the coil, the fluid enters the three-dimensional flow channel formed by the metal layers from the inlet, then passes valve seat 1 and flows into the ball chamber (cf. Fig. 5.1.1). The pressure difference between the inlet and valve seat 2 lifts the ball up to seal valve seat 2. The inlet pressure is then transmitted through the outlet to the pressure sensor. When a sufficient current is applied to the coil, the magnetic force pulls the ball down sealing valve seat 1. The outlet pressure is then reduced to the surrounding pressure by ventilation through valve seat 2.

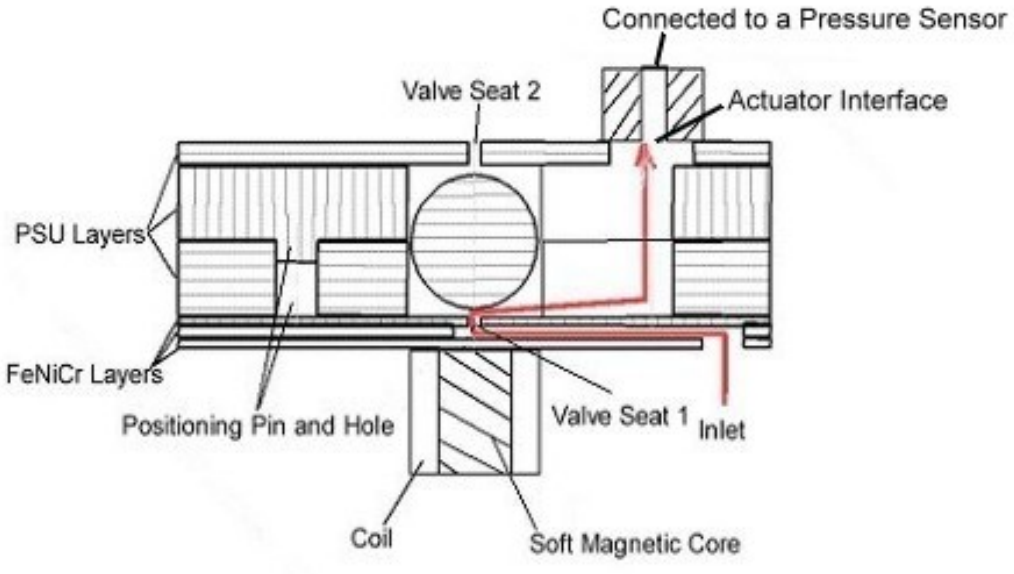


**Fig. 5.1.1: Mechanisms of the valve. The gas flows from the inlet through the three-dimensional flow channel formed by FeNiCr layers to the ball chamber. The ball has 350 µm stroke. It can be pulled and controlled by the coil. Outlet is connected to a pressure sensor to obtain the pressure signal.**

### Minimum inlet pressure

The valve operates with an inlet pressure ranging between 50 and 200 kPa. A minimum inlet pressure of 50 kPa is needed to ensure the flow to overcome the weight of the ball and the stiction effects to lift up the ball.

### Minimum initial current

Figure 5.1.2 shows the measured minimum initial current that is needed to pull the ball down from the valve seat 2 at different inlet pressures. At a minimum inlet pressure of 50 kPa, a coil current of about 130 mA is needed, which is corresponding to a power consumption of about 1.18 Watt. At 200 kPa, a current of 300 mA is necessary, which is corresponding to a power consumption of about 6.30 Watt.

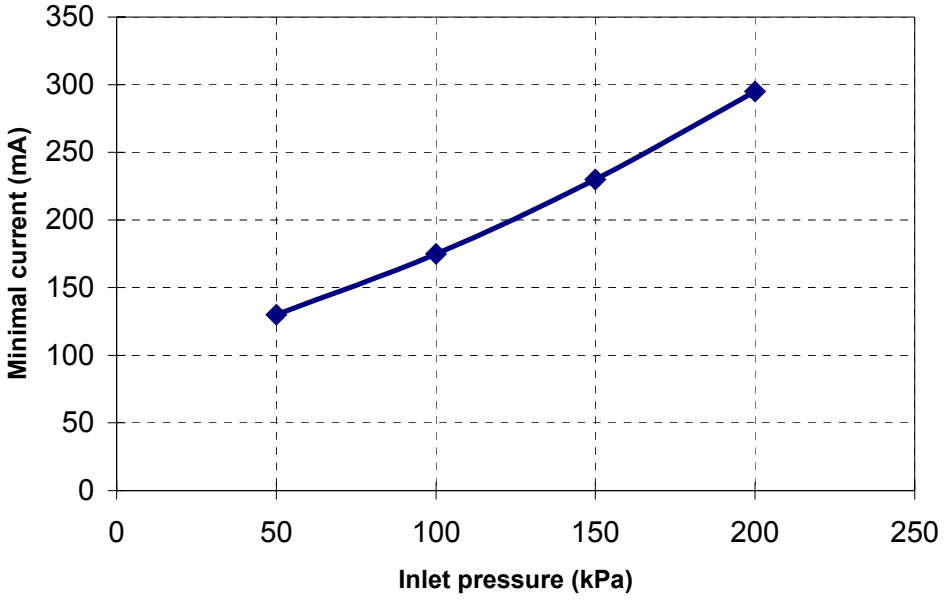


**Fig. 5.1.2: The minimum initial current needed to pull the ball down as a function of the inlet pressure. The valve worked at an inlet pressure range between 50 and 200 kPa with a minimum initial current between 130 and 300 mA.**

### Dynamic Behavior

Figure 5.1.3 shows the results of the dynamic behavior of the valve in the on-off switching mode. The driving voltage was increased until the ball was pulled down onto valve seat 1. After the ball had been pulled down, the coil needed only about 30 % of the minimum initial current to hold the ball and seal the valve seat 1 (Figure. 5.1.1). The average power consumption in the real actuation is then reduced to 0.39 ~ 2.10 Watt corresponding to the input pressure of 50kPa ~200 kPa respectively.

The outlet of the valve was connected to a pressure sensor. The pressure signal was connected to an oscilloscope. Figure 5.1.3 shows the result of a test at an inlet pressure of 100 kPa. The micro valve was switched for more than three hours in this test and no change of the switching parameters was observed. The maximum frequency tested so far has been up to 30 Hz.

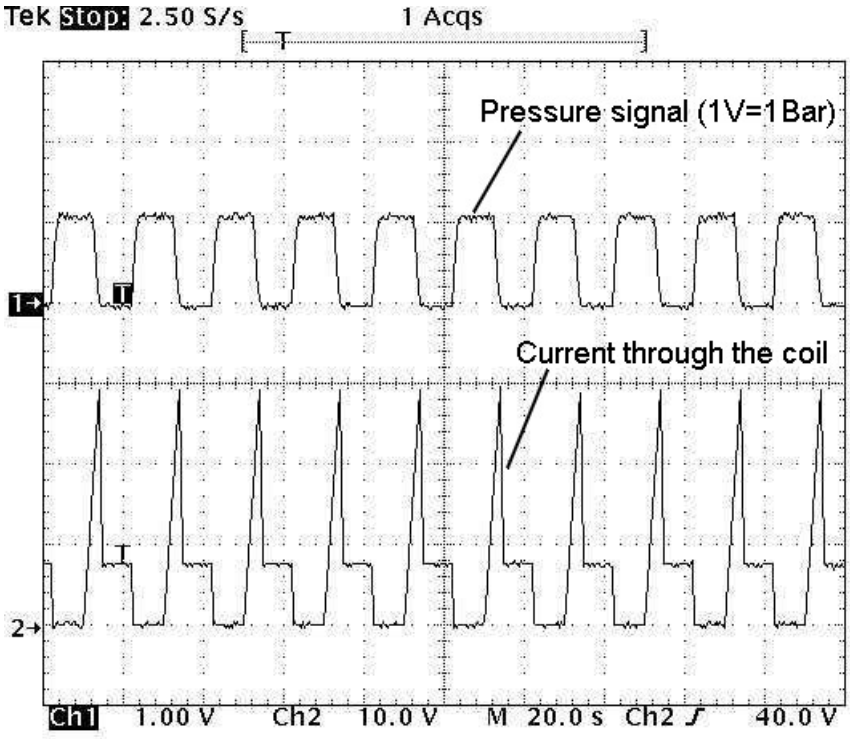


**Fig. 5.1.3: Dynamic behavior of the valve in on-off switching mode. Outlet pressure signal and the driving current in the magnetic coil showed as a function of time. The inlet pressure in this test is at 100kPa.**

## 5.2 Proportional mode

### Mechanism

After the ball is pulled down to the valve seat 1 by the minimum initial current, tuning the input current in the magnetic core can control the ball position because the magnetic force balances the friction with the flow and the weight of the ball. Figure 5.2.1 shows the change of the outlet pressure measured with a sensor as indicated in Fig. 5.1.1, when the input current is decreased continuously. The inlet pressure was set to 200 kPa. When the current was dropped below 100 mA, the outlet pressure started to rise. When the current was further reduced, the outlet pressure continued to rise up to nearly 112.5 kPa at about 40 mA. Beyond that point, the ball was instantaneously lifted up to valve seat 2. The pressure at the outlet then increased to the pressure at the inlet (200 kPa).

### Dynamic behavior

With a proper input signal, the distance between the ball and valve seat 1 can be controlled. In this mode, the valve operates continuously as a proportional valve which regulates the outlet pressure. In figure 5.2.2, the current through the coil was continuously driven up and down between 18 and 130 mA. As a result, the pressure at the outlet was changing in the range between 0 and 35 kPa. The inlet pressure in this test was set to 100 kPa.

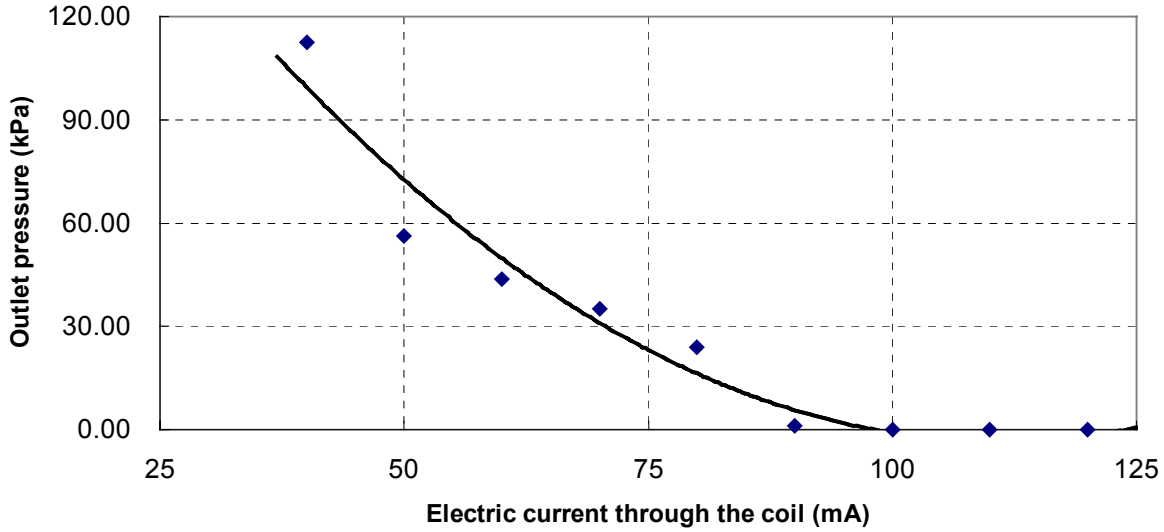


**Fig. 5.2.1: Outlet pressure behavior as a function of the electric current through the driving coil at a pressure difference of 200 kPa. The current is continuously decreased after the initial current pulls the ball down.**

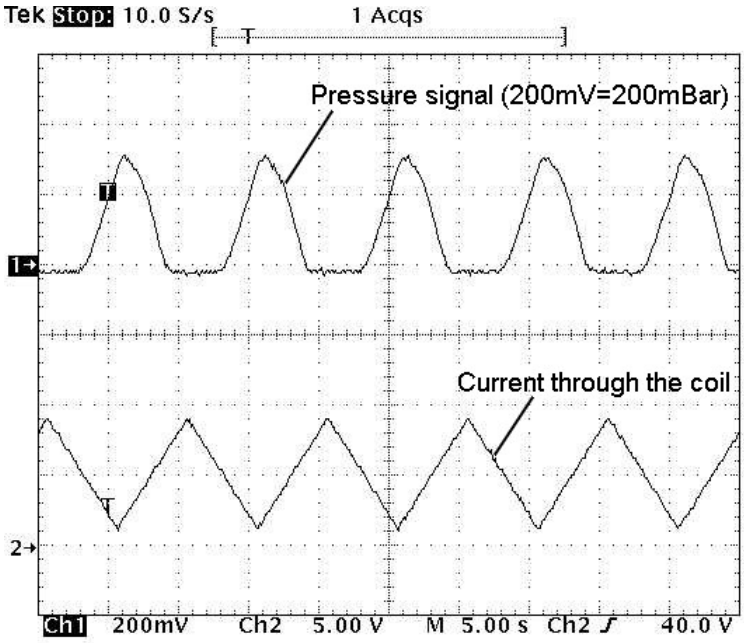


**Fig. 5.2.2: Dynamic behavior when the valve operates as a proportional valve. The outlet pressure was changed between 0 and 35 kPa when the current through the coil was driven between 18 and 130 mA. The inlet pressure in this test was 100 kPa.**

### Hysteresis phenomenon

The voltage level to seal the valve in the ramp-up stage (Fig. 5.2.3 voltage level A, point A) was larger than the voltage in the ramp-down stage (Fig. 5.2.3, voltage level B, point B), when the valve starts to open again. This is owing to the hysteresis phenomenon of the magnetic material. This phenomenon needs to be taken accounted for, when a close-looped pressure or flow control unit is to be constructed.

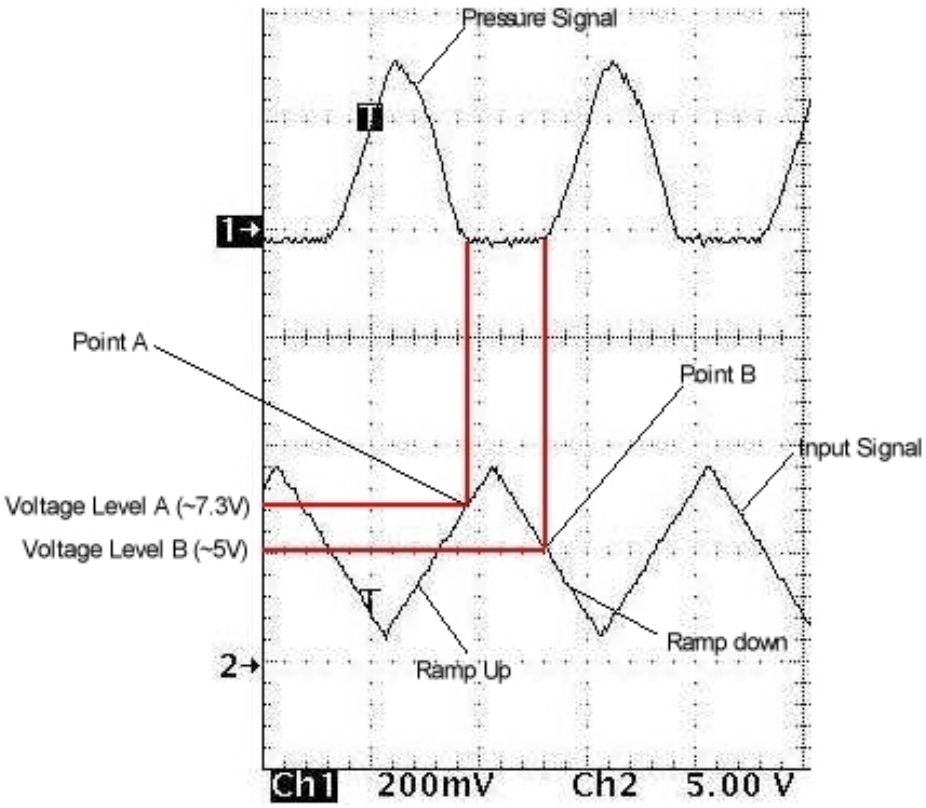


**Fig. 5.2.3: Hysteresis phenomenon. The voltage level to seal the valve in the ramp-up stage (voltage level A at point A) was larger than the voltage in the ramp-down stage (voltage level B at point B), when the valve starts to open again.**

### 5.3 Response time

In Fig. 5.3.1, the measurement of the response time of the ball valve is shown. The valve was connected to a pressure sensor with a dead volume of 15 µl by means of a tube that was approx. 50 mm long and had an inner diameter of 900 µm. The inlet pressure was set to 200 kPa and the pressure signal was recorded while the current through the coil was switched off. The response time of the valve is defined as the time during the rise of the pressure signal between 10 and 90 % of the maximum output signal. This results in a response time of approximately 10 ms (Figure 5.3.1). Since the dead volume of the pressure sensor and the connecting tube delay the pressure rise, the true response time of the valve will be less than 10 ms. Fig. 5.3.2 shows the dynamic behavior when the current through the coil is switched on. The valve was closed in this case. The estimated time response time was approximately 8 ms.

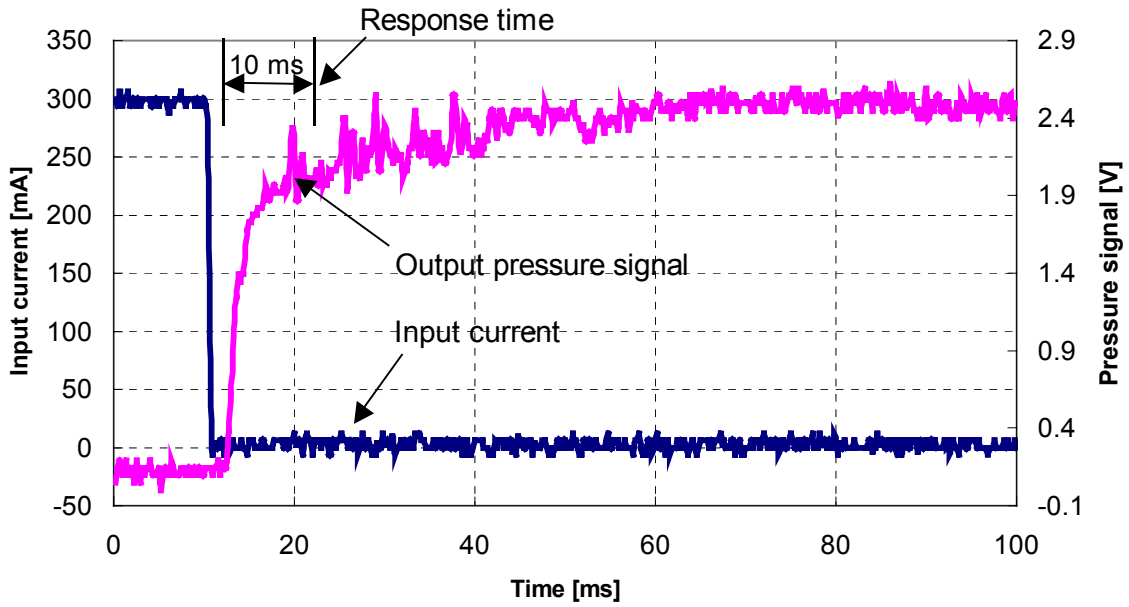


**Fig. 5.3.1: Input current of the driving coil and output signal of the pressure sensor when the valve is opened at a differential pressure of 200kPa.**

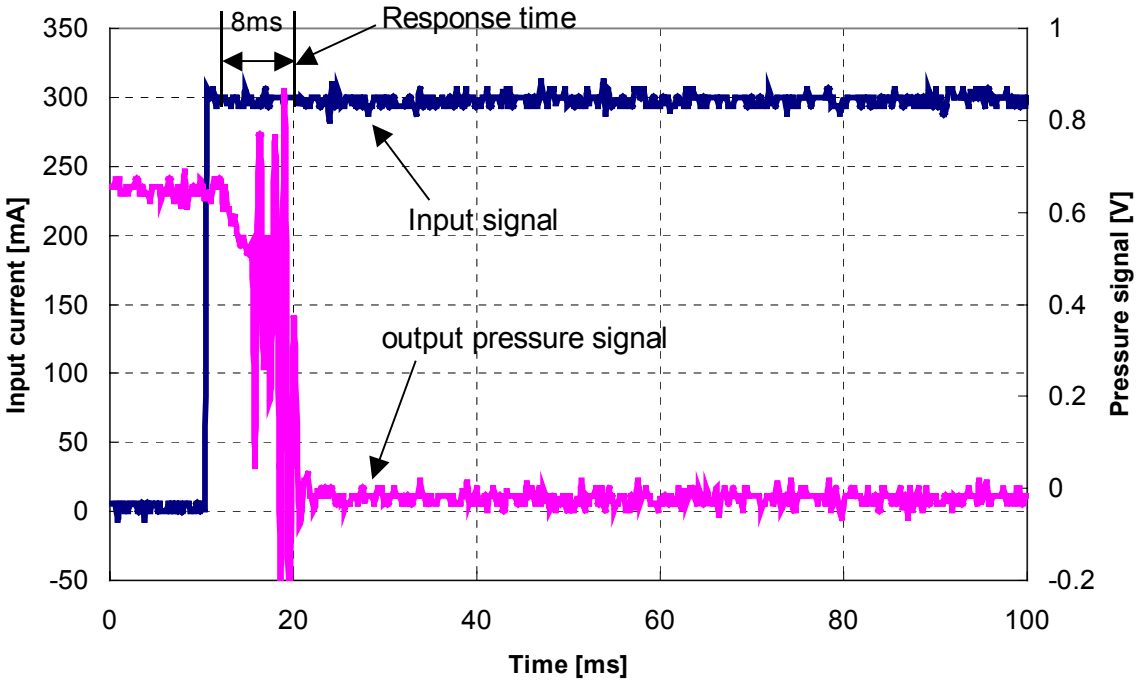


**Fig. 5.3.2: Input current of the driving coil and the output signal of the pressure sensor when the valve is closed at a differential pressure of 200 kPa.**

### 5.4 Inclination effects

In real applications, the valve may be used at different tilting angles. For the application reliability, we investigated the valve properties in four extreme cases 45°, 90°, 135° and 180° (Figure 5.4.1). The theoretical initial force needed to pull the ball down in normal position (0 °) was

$$F = \pi r^2 P - W_{ball}$$

(Equation 5.4.1)

Where the r is the radius of valve seat 2, P denotes the pressure difference between inlet and outlet, and $W_{ball}$ is the weight of the ball. In our case, the radius of valve seat 2 was 150 μm. The initial force needed at normal position (0 °) was computed to be about $1.30X10^{-2}$ N. The weight of the ball is $1.10X10^{-3}$ N, which is about 10 % of the total force needed.

Figure 5.4.2 shows the experimental results of the initial currents needed to close the valve as a function of the input pressure and the inclination angle. The valve can operate even upside down. The initial driving current was about 20 % larger than in the normal position. That is in agreement with the theoretical estimation.

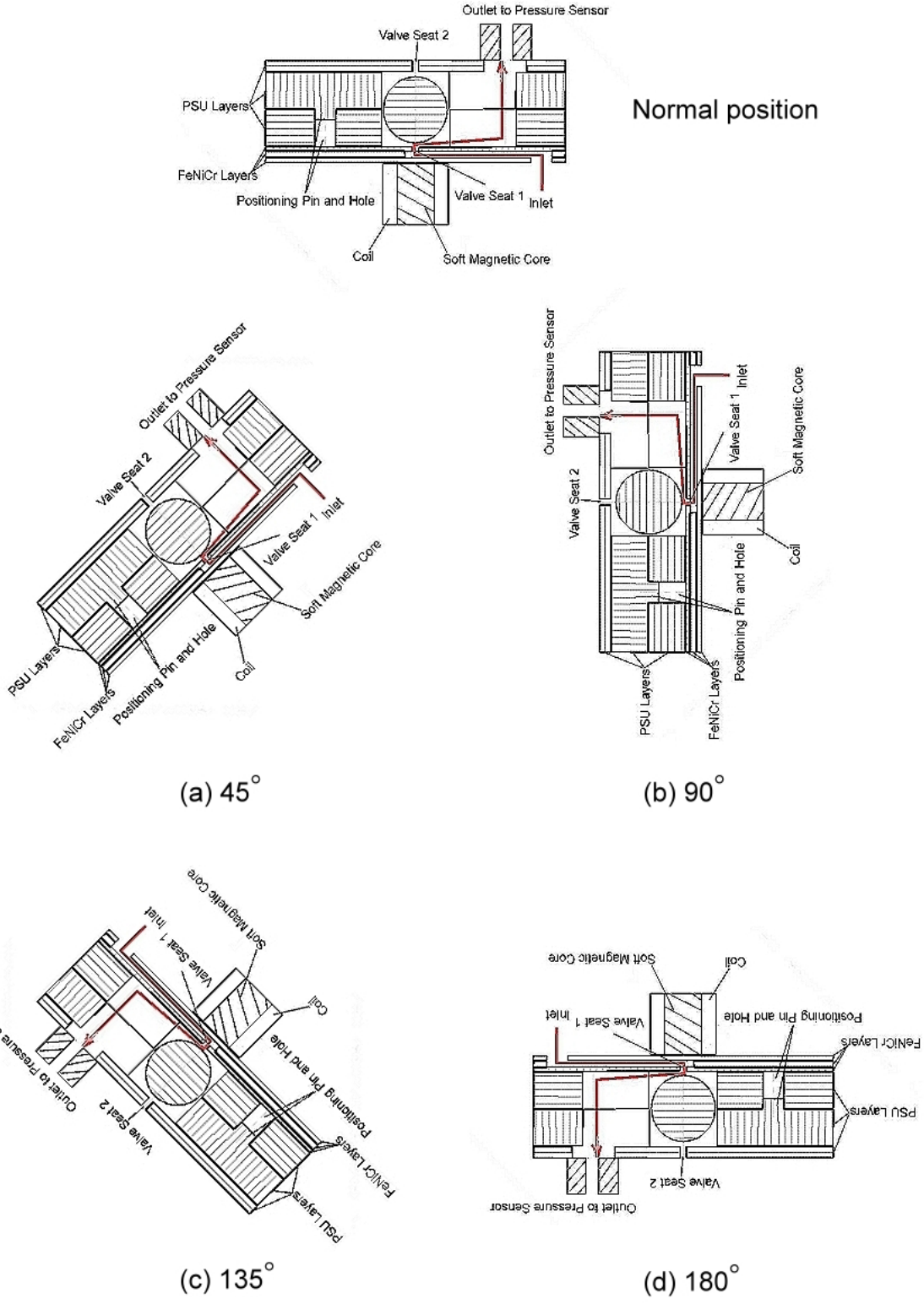


**Fig. 5.4.1: The inclination effects influenced by the gravitational forces were investigated using four tilting angles 45˚, 90˚, 135˚ and 180˚ of the valve.**

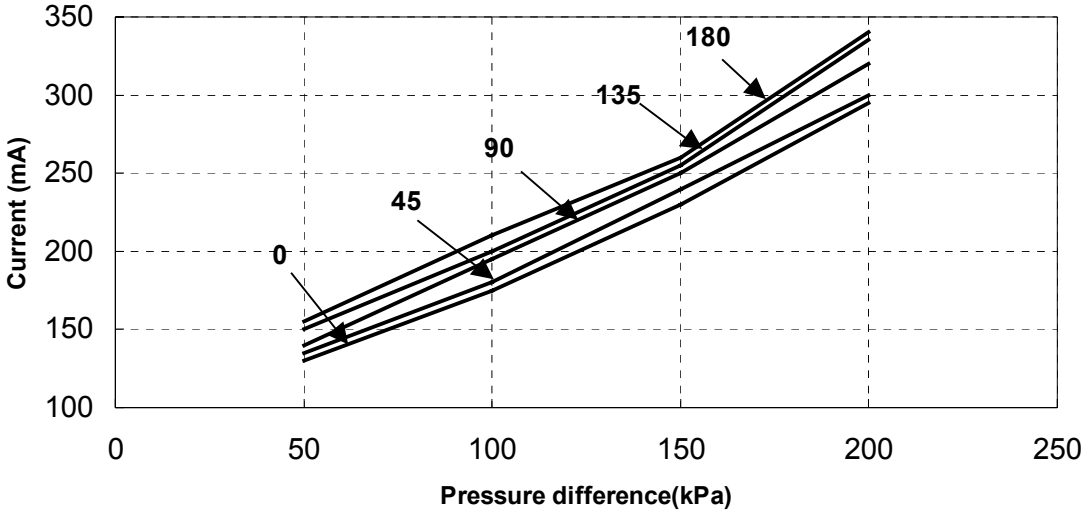


**Fig. 5.4.2: Electrical current needed to close the valve as a function of the pressure differences and the inclination angles in the on-off switching mode.**

Figure 5.4.3 shows the proportional case. The current through the coil at which the ball started to be released from valve seat 1 is a function of the inclination angle of the valve. The controllable pressure range was higher at larger inclination angles. Combining with a pressure or flow sensor, the valve can be used as a control valve for dosing purposes to accurately regulating output the pressure or flow.

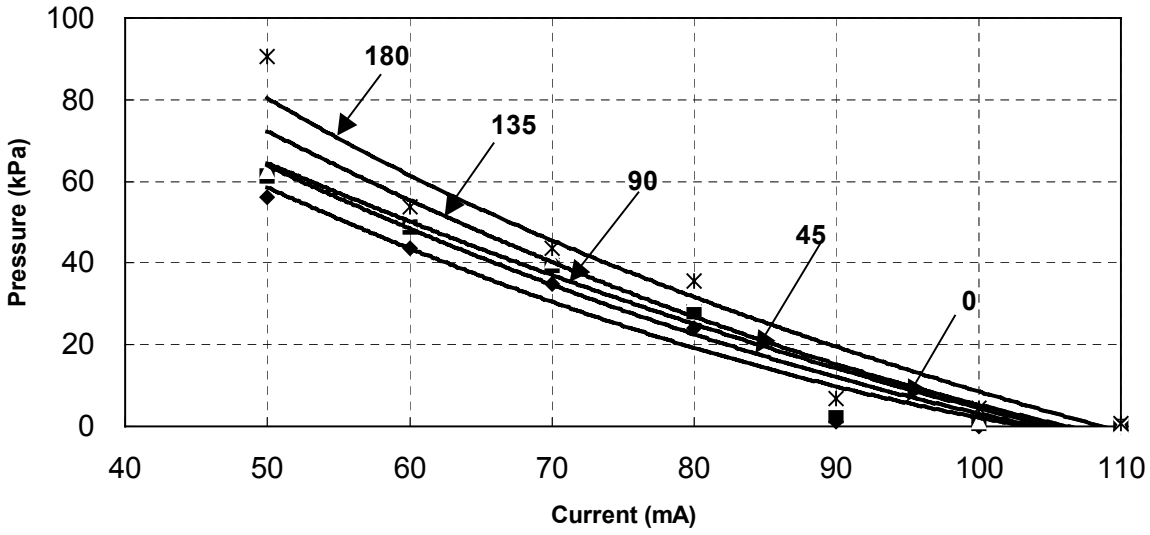


**Fig. 5.4.3: Outlet pressure as a function of the driving current at 200kPa for different inclination angles of the valve in the proportional mode.**

## 5.5 Open flow rate and leakage

The flow rate through the opened valve is shown in the Figure 5.5.1 as a function of the pressure difference over the valve. The flow rate ranged from 590 sccm to about 2000sccm, when the inlet pressure was set between 50 and 200 kPa. Fig. 5.5.1 shows the leakage flow through the closed valve at an input current through the coil of 200 mA at different pressure differences. The leakage to open flow rate ratio of this valve is shown in the figure 5.5.2 as a function of the pressure difference. The average leakage to open flow rate is approximately 0.3%.

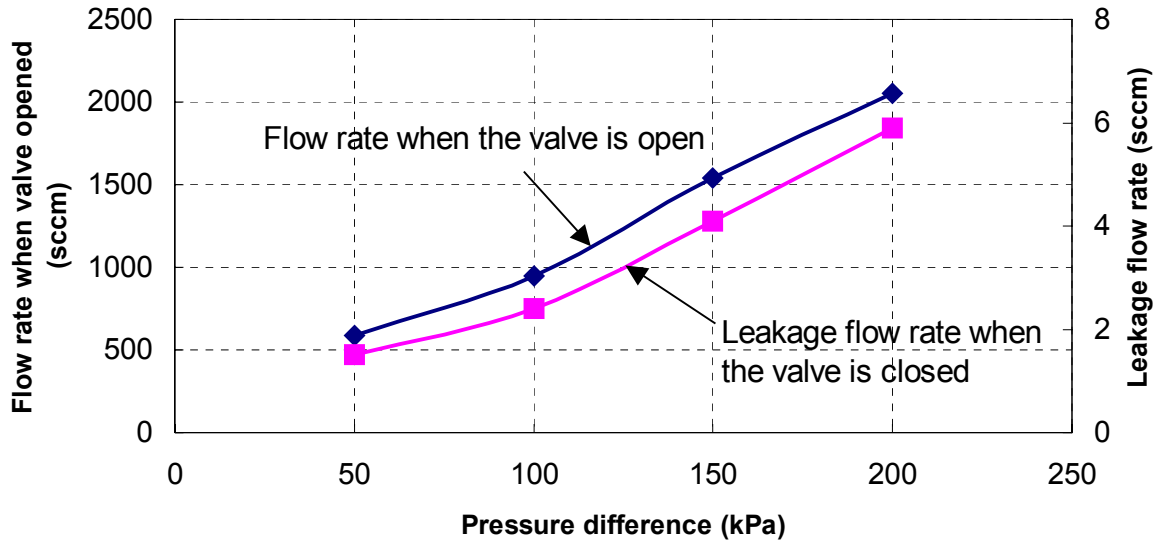


**Fig. 5.5.1: Flow through the outlet when the valve is open and leakage when the valve is closed with 200mA as a function of the pressure difference over the valve.**

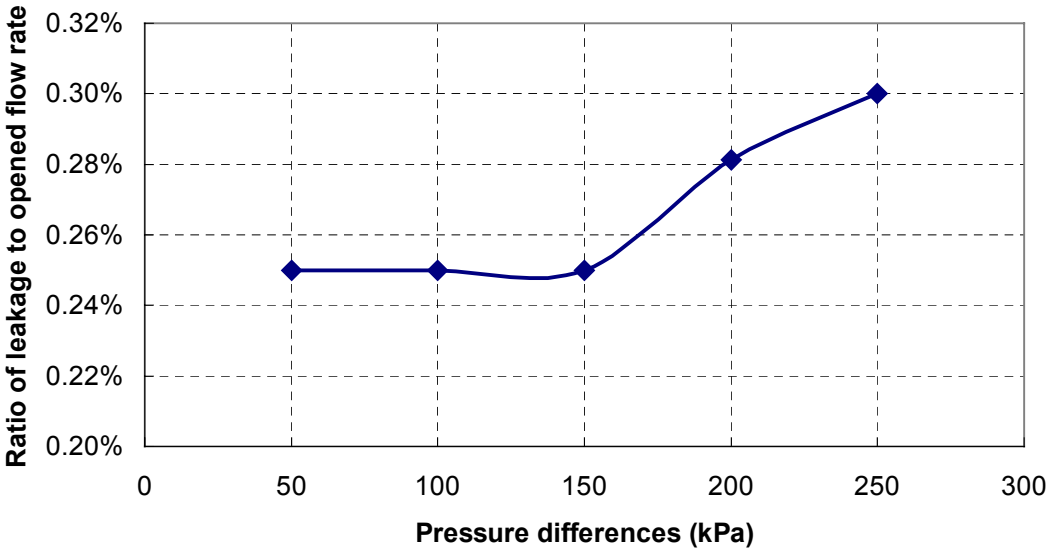


**Fig. 5.5.2: The leakage to open flow rate ratio of this valve as a function of different pressure differences.**

## 5.6 Discussion and conclusion

The valve can be operated in both the on-off switching mode and the proportional mode at different inclination angles. As an on-off switching valve, it switched up to 200kPa differential pressure. The switch frequency was up to 30 Hz. As a proportional valve, it operated in a range from 0 to 110 kPa with an input pressure of 200 kPa.

In the proportional mode, the stroke of the ball should be further reduced to avoid loss of the ball in case of a small current being applied. This can be achieved by modifying the height of the ball chamber layer. In the experiment, a warm-up phenomenon at the coil during operations was observed, it can be very interesting to use different modern magnetic materials to further reduce the power consumption, enhance the performance of the valve and minimize the warm-up temperature.

Reliable switching at all inclination angles is achieved if the applied input current is 20% larger than the minimum input current. The performance of the valve in the proportional mode is affected by the inclination angle, but if the micro valve is combined with a flow or pressure sensor. It can be used as a control valve for dosing purpose.

The average ratio of leakage to the flow through the open valve was approximately 0.3%. It is believed that the leakage is due to deviations of the valve seats from the ideal form. If necessary, setting o-rings onto the valve seats may further improve the flow leakage, but will increase the difficulty of the assembling process in the mass production.

# 6 Summary and Outlook

Objective

The objective of this work was to develop a fabrication process that allows producing micro components at low cost and reasonable investment. Such a process should enable small and medium companies to earn their money even with small-scale production series in the field of micro system technologies.

Guidelines

To achieve this strategic task, two main guidelines were followed through out the whole work. One is *"Process Simplification "*. The second is *"Outsourcing".*

A new bonding process using 3M VHB acrylate adhesive films was, therefore, developed in this dissertation. A magnetically driven micro ball valve was developed and fabricated by this method as a demonstrator. Alignment pins and holes were used throughout the entire fabrication. The valve can be fabricated and assembled without any difficult optical alignments. The moving element and the driving part of the valve were outsourced. By this way the advantages and merits of the parts supply companies was employed. Their mass production abilities and their process optimizations to get low cost, mass producible, market standard elements was used to minimize unnecessary expensive production steps and reduce the investment threshold of small companies.

The bonding method

The properties of the adhesive films and the process steps of the bonding method were described. The bonding strength was verified by tensile strength tests according to the standard process of DIN53288. The process parameters were optimized using the Taguchi method. With optimized process parameters, the bonding strength can be larger than 600 kPa.

The deformation of punched microstructures through each process step was analyzed separately in a statistical way. The achievable accuracy of the punching process was evaluated using PSU films as punching medium. The standard deviation of 6 µm was measured from 56 flow channel structures with an average dimension of 1.306mm. Deformation of the punched adhesive film through the part preparing steps (punching, peeling off and joining) was analyzed in a statistical way as well. A standard deviation of 70 µm was measured from 56 valid data with an average value of 1.472 mm. Deformation of the punched adhesive film during curing was analyzed using the Taguchi method under different process parameters. With the process parameters obtained for the maximum bonding strength, an average deformation of 0.056 mm was measured from 56 samples with a standard deviation of 5 µm.

The sealing properties were tested with nitrogen and water solution. The compatibility to the AMANDA process was demonstrated by bonding separated polyimide membranes on PSU housings using this new bonding method.

The bonding method can be applied to bond polymer housings, membranes and other different materials. Multiple layers with different materials can be bonded together in one step. Opaque material can also be applied by this bonding method. Three-dimensional structures can be easily built up by piling up multiple layers. The bonding process can be a good alternative to the existing adhesive bonding processes.

Valve fabrication

The micro ball valve was made from three PSU and three FeNiCr layers. They were bonded together in one step using five punched adhesive films. To fabricate the hot-embossing molds for PSU housings, micro mechanical milling was employed. To obtain different surface roughness requirements, two kinds of fabrication methods, diamond ultra milling and tungsten carbide micro milling, were used. Critical microstructure contours were improved by tool diameter compensations and path modifications. The ball chamber layer was separated into two parts in the mold to reduce the demolding force. With the aid of a multi step demolding method and a high adhesive counter plate, the ball chamber layers with a thickness of 1.6 mm each were successfully demolded. Laser cutting technology was selected to pattern FeNiCr layers. In the mass production, these layers could be fabricated by punching as well. A small series production of approximately 50 micro ball valves was successfully realized in the laboratory.

Characteristics of the valve

The valve can be operated in two modes. One is on-off switching mode and the other is a proportional mode. In the on-off switching mode, the valve switches the outlet pressure at two distinguished levels. The maximum switchable differential pressure of this valve is 200 kPa. The switch frequency was up to 30 Hz. In the proportional mode, controlling the ball position can regulate the outlet pressure. The magnetic force of the coil balances the lifting force of the flow and the weight of the ball. In this mode, the valve can steer the outlet pressure continuously in a range between 0 to 110 kPa, when the input pressure is 200 kPa. Inclination effects caused by gravitational force were also investigated in this work. The valve was found to be suitable for use at all inclination angles. The average rate of leakage of the closed valve to flow through the open valve was measured to be approximately 0.3%.

Future

In a next generation of micro ball valves, the stroke of the ball should be further reduced. On one side, this can avoid the loss of the ball in case of a small current being applied to the driving coil. On the other side, it can reduce the amount of electric current needed. This can be achieved by modifying the height of the ball chamber layer. Modern magnetic materials can be applied to the metal layers to further enhance the performance of the valve and reduce the power consumption.

The value of this work

The assembling and bonding process is usually the most costly process in the field of micro systems. Large cost for manual labor and low efficiency in the packaging process are usually

the crucial bottlenecks in production. The adhesive film bonding method is an easy and straightforward process. It is very suitable for automation and mass production of micro systems in industry. This allows large reduction of cost, time and work. The working micro valves show that the process developed in this thesis is suitable to produce micro components in batches, with little investments, and at low cost.

More than 300 adhesive films are available on the market. Some of them even claim higher bonding strength, higher temperature endurance or other important chemical and physical properties. They can be employed by the bonding method for developing different kinds of application products in the future.

# Appendix 1

## 1.1 The measured results of channel widths on the punched PSU films through the punching process.

### 1.1.1 The measured data

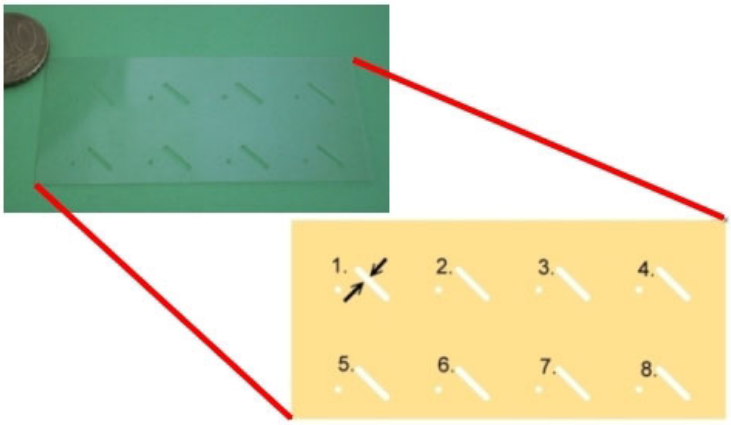


| Channel No. / Width (mm) | 1. | 2. | 3. | 4. | 5. | 6. | 7. | 8. |
|---|---|---|---|---|---|---|---|---|
| **PSU Sample I** | 1.300 | 1.308 | 1.296 | 1.315 | 1.307 | 1.317 | 1.317 | 1.297 |
| **PSU Sample II** | 1.313 | 1.307 | 1.303 | 1.318 | 1.313 | 1.308 | 1.306 | 1.303 |
| **PSU Sample III** | 1.309 | 1.313 | 1.299 | 1.302 | 1.298 | 1.302 | 1.300 | 1.307 |
| **PSU Sample IV** | 1.305 | 1.305 | 1.302 | 1.306 | 1.313 | 1.316 | 1.303 | 1.305 |
| **PSU Sample V** | 1.316 | 1.304 | 1.301 | 1.313 | 1.304 | 1.305 | 1.301 | 1.307 |
| **PSU Sample VI** | 1.308 | 1.306 | 1.307 | 1.307 | 1.306 | 1.318 | 1.302 | 1.305 |
| **PSU Sample VII** | 1.304 | 1.302 | 1.299 | 1.308 | 1.303 | 1.312 | 1.310 | 1.302 |

*Average: 1.306 mm.*
*Stand deviation: 0.006 mm*

### 1.1.2 Grouping

| **Range** | 1.2950 ~ 1.3003 | 1.3003 ~ 1.3056 | 1.3056 ~ 1.3109 | 1.3109 ~ 1.3162 | 1.3162 ~ 1.3215 | 1.3215 ~ 1.3268 | Total |
|---|---|---|---|---|---|---|---|
| **Number** | 7 | 20 | 16 | 9 | 4 | 0 | 56 |

## 1.2 The measurement results of channel widths on the punched adhesive films after peeling off and joining.

### 1.2.1 The measured data

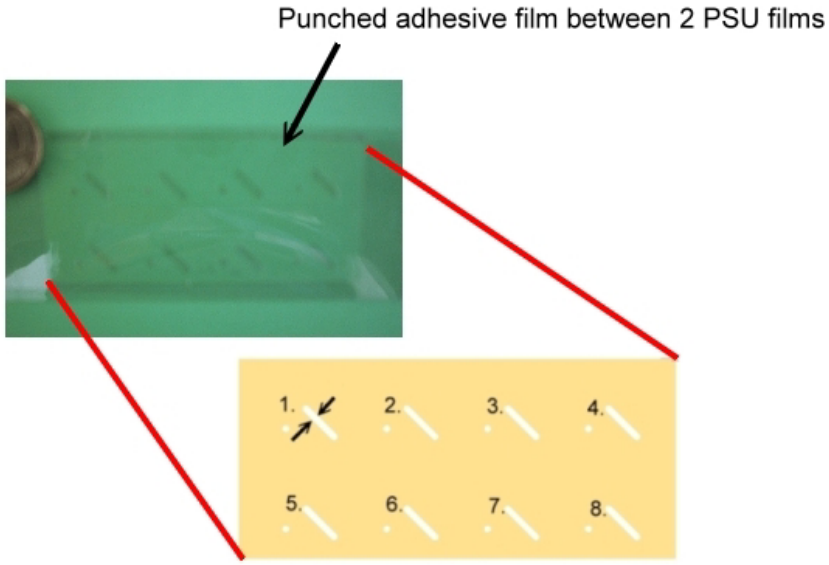


| Channel No. / Width (mm) | 1. | 2. | 3. | 4. | 5. | 6. | 7. | 8. |
|---|---|---|---|---|---|---|---|---|
| **Sample I** | 1.442 | 1.496 | 1.573 | 1.514 | 1.354 | 1.500 | 1.522 | 1.469 |
| **Sample II** | 1.506 | 1.396 | 1.491 | 1.312 | 1.574 | 1.440 | 1.416 | 1.425 |
| **Sample III** | 1.527 | 1.374 | 1.385 | 1.419 | 1.462 | 1.447 | 1.487 | 1.567 |
| **Sample IV** | 1.403 | 1.520 | 1.472 | 1.495 | 1.399 | 1.581 | 1.467 | 1.543 |
| **Sample V** | 1.447 | 1.561 | 1.543 | 1.521 | 1.590 | 1.356 | 1.547 | 1.422 |
| **Sample VI** | 1.391 | 1.465 | 1.437 | 1.421 | 1.523 | 1.478 | 1.300 | 1.546 |
| **Sample VII** | 1.527 | 1.398 | 1.529 | 1.497 | 1.453 | 1.502 | 1.474 | 1.549 |

*Average: 1.472 mm.*
*Stand deviation:0.069 mm*

### 1.2.2 Grouping

| **Range** | 1.30 ~ 1.34 | 1.34 ~ 1.38 | 1.38 ~1.42 | 1.42 ~ 1.46 | 1.46 ~ 1.50 | 1.50 ~ 1.54 | 1.54 ~1.58 | 1.58 ~1.62 | 1.62 ~1.66 | Total |
|---|---|---|---|---|---|---|---|---|---|---|
| **Number** | 2 | 3 | 8 | 9 | 13 | 10 | 9 | 2 | 0 | 56 |

## 1.3 The measured results of the deviations of channel widths on the punched adhesive films through curing process under the process parameter A3, B3, C3.

### 1.3.1 The measured data

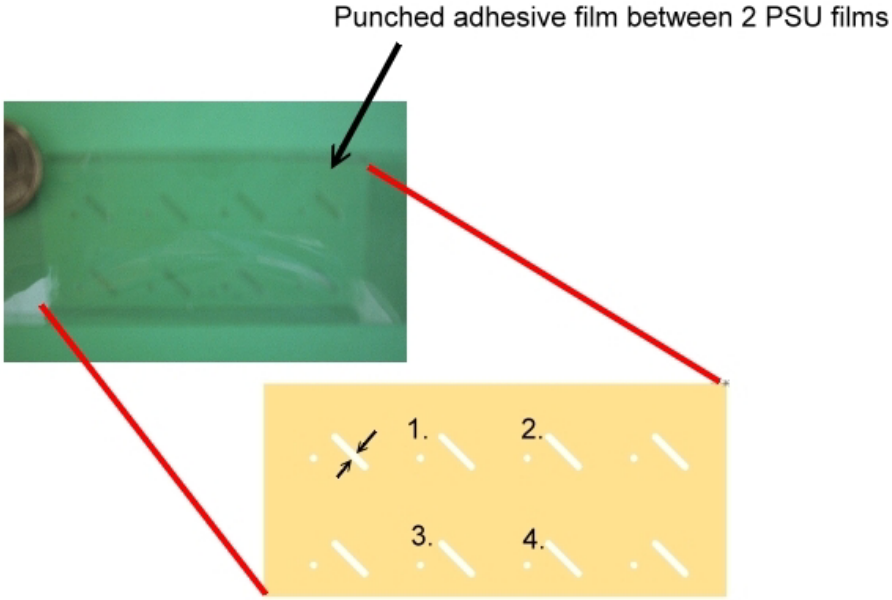


| | Channel No. | 1. | 2. | 3. | 4. |
|---|---|---|---|---|---|
| **Sample I** | **Before curing (mm)** | 1.496 | 1.573 | 1.500 | 1.522 |
| | **After curing (mm)** | 1.440 | 1.516 | 1.441 | 1.458 |
| | **Deviation (mm)** | 0.056 | 0.057 | 0.059 | 0.064 |
| **Sample II** | **Before curing (mm)** | 1.396 | 1.491 | 1.440 | 1.416 |
| | **After curing (mm)** | 1.340 | 1.432 | 1.383 | 1.358 |
| | **Deviation (mm)** | 0.056 | 0.059 | 0.057 | 0.058 |
| **Sample III** | **Before curing (mm)** | 1.520 | 1.472 | 1.581 | 1.467 |
| | **After curing (mm)** | 1.470 | 1.411 | 1.521 | 1.398 |
| | **Deviation (mm)** | 0.050 | 0.061 | 0.060 | 0.069 |
| **Sample IV** | **Before curing (mm)** | 1.561 | 1.543 | 1.356 | 1.547 |
| | **After curing (mm)** | 1.498 | 1.488 | 1.294 | 1.492 |
| | **Deviation (mm)** | 0.063 | 0.055 | 0.062 | 0.055 |
| **Sample V** | **Before curing (mm)** | 1.465 | 1.437 | 1.478 | 1.300 |
| | **After curing (mm)** | 1.411 | 1.377 | 1.426 | 1.238 |
| | **Deviation (mm)** | 0.054 | 0.060 | 0.052 | 0.062 |
| **Sample VI** | **Before curing (mm)** | 1.398 | 1.529 | 1.502 | 1.474 |
| | **After curing (mm)** | 1.340 | 1.472 | 1.453 | 1.418 |
| | **Deviation (mm)** | 0.058 | 0.054 | 0.049 | 0.056 |

*Average: 0.0575 mm*

*Standard deviation: 0.0046 mm*

### 1.3.2 Grouping

| **Range** | 0.045 ~0.048 | 0.048 ~ 0.051 | 0.051 ~ 0.054 | 0.054 ~0.057 | 0.057 ~ 0.060 | 0.060 ~0.063 | 0.063 ~0.066 | 0.066 ~0.069 | Total |
|---|---|---|---|---|---|---|---|---|---|
| **Number** | 0 | 2 | 3 | 7 | 6 | 4 | 1 | 1 | 24 |

# Reference

[3M96] 3M VHB/VHB+ Product Information, 3M Deutschland GmbH, 1996

[3M01] 3M, ”Das Kleben von Kunststoffen in Industrie und Handwerk“, 3M Deutschland GmbH, 2001.

[Bosc93] D. Bosch, B. Heimhoefer, G. Mueck, H. Seidel, U. Thumser, W. Welser, “A Silicon Microvalve with Combined Electromagnetic/Electrostatic Actuation”, Sensors and Actuators A, 37-38 (1993), pp684 – 692.

[Bran92] J. Branjeberg, P. Gravesen, “A New Electrostatic Actuator Providing Improved Stroke Length and Forth“, Proc. MEMS 92, Travemuende, pp 6-11.

[Büst94] B. Buestgens, W. Bacher, W. Bier, R. Ehnes, D. Mass, R. Ruprecht, W. K. Schomburg, L. Keydel, “Micro Membrane Pump Manufactured by Molding”, Proceedings der 4th International Conference on New Actuators, Actuators’94, Bremen, Juni 15-17, 1994, pp86 – 90.

[Ditt98] D. Dittmann, “Mikroventile mit Formgedaechtnis-Duennschichten”, Diplomarbeit, Forschungszentrum Karlsruhe und Universitaet Karlsruhe (TH), 1998.

[Ditt02] D. Dittmann, “Durchflusssensoren aus Kunststoff fuer sehr kleine Volumen-stroeme auf der Basis des AMANDA-Verfahrens”, Dissertation, Diplomarbeit, Forschungszentrum Karlsruhe und Universitaet Karlsruhe (TH), 2002.

[Esah89] M. Esashi, S. Shoji, A. Nakano, “Normally Closed Microvalve and Micropump Fabricated on a Silicon Wafer”, Sensors and Actuators 20, 1998, pp163 - 169.

[Fu02] C. Fu, T. Koller, R. Ahrens, Z. Rummler, W. K. Schomburg, “Optimization of Chamber Adhesive Bonding for Packaging of Micro Components,“ Proc. of Eu-rosensors XVI, 2002, pp. 149-150.

[Fu03] C. Fu, Z. Rummler and W. K. Schomburg, “Magnetic Driven Micro Ball Valve Fabricated by Multilayer Adhesive Film Bonding”, Journal of Micromechanics and Microengineering13, 2003, pp. 96 – 102.

[Fahr94] J. Fahrenberg, W. Bier, D. Mass, W. Menz, R. Rupprecht, W. K. Schomburg, “Microvalve System Fabricated by Thermoplastic Molding”, Proc. MME’94, Pisa, pp. 178 –181.

[Fahr95] J. Fahrenberg, D. Mass, W. K. Schomburg: Entwicklung eines aktiven Ventilsystems in LIGA-Technik fuer minimalinvasive Therapie; Wissenschaftliche Berichte FZKA 5504, Forschungszentrum Karlsruhe GmbH,1995.

[Goebe99] J. Goebes, M. Kohl, V. Saile, " Entwicklung von Normally Closed Mikroventile mit Formgedaechtnis-Dickfilmen", Diplomarbeit, Forschungszentrum Karlsruhe und Universitaet Karlsruhe (TH), 1999.

[Goll96] C. Goll et al: Microvalves with bi-stable buckled polymer diaphragms, Journal of Micro mechanical and Micro Engineering. 6, 1996, pp.77 - 79.

[Goll97] C. Goll, W. Bacher, W. Menz, W. K. Schomburg: Entwicklung, Herstellung und Test von aktiven Mikroventilen fuer pneumatische Anwendungen. Wissenschaftliche Berichte FZKA 5902, Forschungszentrum Karlsruhe GmbH, 1997.

[Hamm01] M. Hammer: The Agenda: What Every Business Must Do to Dominate the Decade, Crown Business, October 2001.

[Hane00] T. Hanemann, M. Heckele, V. Piotter. "Current Status of Micro molding Technology", Polymer News 25, 2000, pp.224 – 229.

[Heck98] M. Heckele, W. Bacher, K. D. Müller: Hot embossing – The molding technique for plastic microstructures. Microsystem Technologies 4, 1998, pp.122-124.

[Heck99] M. Heckele, K. D. Müller, W. Bacher: Microstructured Plastic Foils Produced by Hot Embossing. HARMST, Kisarazu, 1999, pp. 84 – 85.

[Heck00] M. Heckele, H. Dittrich: Prägen von Mikrobauteilen ohne Restschicht. 4. Status Kolloquium PMT, FZKA 6423, Forschungszentrum Karlsruhe, 2000, pp. 195.

[Huff93] M. A. Huff, J. R. Gilbert, M. A. Schmidt, "Flow Characteristics of a Pressure-Balanced Microvalve", Proc. Transducer '93, Yokohama, Japan, 1993, pp 98-101

[Kais00] S. C. Kaiser: Entwicklung eines magnetisch-induktiven Mikroventils nach dem AMANDA-Verfahren. Dissertation, Universität Karlsruhe, 2000.

[Kohl00] M. Kohl, I. Hürst, B. Krevet: Time response of shape memory micro valves, Actuator Conference Proceeding 2000, pp. 212 – 215.

[Kotl99] P. Kotler, S. H. Ang, C. T. Tan, S. M. Leong: Marketing Management: An Asian Perspective, Prentice Hall, November 1999.

[Kotl02] P. Kotler, D. C. Jain, S. Maesincee: Marketing Moves --- A New Approach to Profits, Growth and Renewal, McGraw Hill, April, 2002.

[Krus99] O. Krusemark, K. Pfeiffer, J. Mueller, An Optimized Electromagnetically Activated Micro Ball Valve, Sensor 99, pp. 405- 408.

[Maas96] D. Maas, B. Büstgens, J. Fahrenberg, W. Keller, P. Ruther, W. K. Schomburg. D. Seidel: Fabrication of Micro components using Adhesive Bonding Techniques.

Proceedings des International Workshop on Micro Electro Mechanical Systems MEMS`96, San Diego, USA ,1996, pp. 331-336.

[Mart98] J. Martin, W. Bacher, O. F. Hagena, W. K. Schomburg: Strain gauge pressure and volume-flow transducer made by thermoplastic molding and membrane transfer, MEMS1998, Heidelberg, pp. 361-366.

[Robe94] J. K. Robertson, K. D. Wise: A nested Electrostatically actuated microvalve for an integrated micro flow controller, IEEE Micro Electro Mechanical Systems, 1/1994, pp. 7-12.

[Rogg01] T. Rogge: Entwicklung eines Piezogetriebenen Mikroventils von der Idee bis zur Vorserienfertigung. Dissertation, Universität Karlsruhe, 2001.

[Ross95] R. Rossberg, B. Schmidt, S. Buettgenbach, “Micro liquid dosing system”, Microsystem Technologies 2, Srpinger Verlag, 1995, pp 11 – 16.

[Roy01] R. K. Roy, Design of experiments using the Taguchi approach, J. Wiley & Sons Inc, 2001.

[Rumm00] Z. Rummler, M. Berndt, H. G. Härtl, M. Hempel, R. Peters, W. K. Schomburg: Micro Degasser Made of Inert Polymers for HPLC Devices. ASME Winter Annual Meeting, November 2000, in Orlando, Florida, USA , 2000.

[Sauer00] I. Sauer, persoenliche Mitteilung, Industrie-Klebebaender, Klebstoffe und Spezialprodukte, 3M Deustchland GmbH, 2000.

[Scho96] W. K. Schomburg, R. Ahrens, W. Bacher, C. Goll, J. Martin, V. Saile: AMANDA – Surface Micromachining, Molding and Diaphragm Transfer, Sensor and Actuator A 76, 1996, pp.173-178.

[Shoj91] S. Shoji, B. van der Schoot, N. De Rooji, M Esashi, “Smallest Dead Volume Microvalve for Integrated Chamical Anlyzing Systems”, Proc. Transducer ’91, San Francisco, 1991, pp 1052 –1055.

[Skro97] K. D. Skrobanek, M. Kohl, S. Miyazaki, “Stress Optimized Shape Memory Micro Valves”, MEMS 97, Nagoya, Japan, 1997, pp. 256 –261.

[Tagu87] G. Taguchi, S. Konishi, “Taguchi Methods Orthogonal Arrays and Linear Graphs: Tools for Quality Engineering”, American Supplier Institute, 1987.

[Vacu98] Vacuumschmelze, “Soft magnetic material and semi-finished products”, Vacuumschmelze GmbH, 1998.

[Wagn90] B. Wagner, W. Benecke, “Magnetically Driven Microactuator: Design Considerations”, Microsystem Technologies 90.

[Wagn91] B. Wagner, W. Benecke, " Microfabricated actuator with moving perment magnet", MEMS 91, Nara, Japan, pp. 27- 32.

[Wagn96] B. Wagner, H. J. Quenzer. S. Hoerschelmann, T. Lisec, M. Juerss, " Bistable Microvalve with Pneumatically Coupled Membranes", MEMS 96, San Diego, pp. 384 – 388.

[Whit86] F. M. White, "Fluid Mechanics", McGraw-Hill Books Corp., International Second Edition, 1986.

[Wulff01] K. Wulff: Hybride Drucksensoren aus Kunststoff und Glas nach dem AMANDA Verfahren. Dissertation, Universität Karlsruhe, 2001.

[Zdeb94] M. J. Zdeblick, R. Anderson, J. Jankowski, B. Kline-Schoder, L. Christel, R. Miles, W. Weber, "Thermopneumatically Actuated Microvalves and Integrated Electro-Fluidic Circuits", Proc. Actuator 94, 4th Int. Conf. On new Actuators, Bremen, 1994, pp. 56-60.